This work is protected by copyright and other intellectual property rights and duplication or sale of all or part is not permitted, except that material may be duplicated by you for research, private study, criticism/review or educational purposes. Electronic or print copies are for your own personal, non-commercial use and shall not be passed to any other individual. No quotation may be published without proper acknowledgement. For any other use, or to quote extensively from the work, permission must be obtained from the copyright holder/s.

CONSTRUCTION AND INVESTIGATION OF AN ATOMIC HYDROGEN BEAM MASER

Thesis submitted to the
University of Keele for
the Degree of Doctor of Philosophy
by

Howard William Lightfoot B.Sc. M.Inst.P.

Department of Physics,
University of Keele.

February, 1975.

BRITISH LIBRARY

IMAGING SERVICES NORTH

Boston Spa, Wetherby
West Yorkshire, LS23 7BQ
www.bl.uk

TEXT IS CLOSE TO EDGE OF PAGE IN ORIGINAL.

SOME TEXT IS CUT OFF.

ACKNOWLEDGEMENTS

The Author would like to thank

Professors D.J.E. Ingram and W. Fuller for the provision of experimental facilities.

Dr. D.C. Lainé for his guidance and enthusiastic encouragement.

Mr. Alf Smallman for his invaluable help and friendship.

The Technical staff of the Department for their help.

The S.R.C. and the University for personal finance.

His wife, Dawn, who typed this thesis and gave continual support and encouragement.

Mr. M. Daniels for the photographic work.

ABSTRACT

Details are given of the design and construction of an atomic hydrogen beam maser. The static and dynamic properties of the maser are investigated and discussed. In particular, various methods of oscillation amplitude transient production are studied and compared with those in other beam maser systems based on hydrogen and ammonia. The analogue between hydrogen and ammonia (magnetic and electric dipole systems respectively) is discussed in some detail.

The future use of the hydrogen maser constructed as a frequency standard is considered.

CONTENTS

CHAPTER ONE

INTRODUCTION

Although frequency standards work is not of prime concern with the hydrogen maser described in this thesis, it is useful to consider the background to the maser and its application as an atomic frequency standard. The use of the hydrogen maser as a research tool is also considered.

Atomic and molecular frequency standards depend on the observation of electromagnetic radiation absorbed or emitted by atoms or molecules when a transition is stimulated from one energy level to another. In a maser standard, emitted radiation is stored in a resonant cavity and stimulates further coherent radiative emissions. The first maser was produced in 1954 by Gordon et al (1) in the U.S. and Basov and Prokhorov (2) in the U.S.S.R. This worked on an electric dipole transition of the J=3 K=3 lines in the inversion spectrum of ammonia, $^{14}NH_3$. The accuracy of this, then new, frequency standard, suffered from the complicated structure of the inversion line and that its frequency stability, although very good, was limited by the short interaction time of the molecules with the high frequency fields. The time flight of the molecules through the resonator, 100 μsec approximately, is their useful lifetime, and by the uncertainty principle, the width of the line is rather large, usually several kilohertz. As far as the short term frequency stability is concerned, this drawback is partly compensated by the comparitively high power of the ammonia maser, about 10^{-10} W, as shown by the general formula due to Bernstein (3) and Blaquière (4), for a classical oscillator and to Townes (5) for quantum oscillators.

$$\frac{\langle \Delta f^2 \rangle^{1/2}}{f_o} = \left(\frac{kT}{P\tau}\right)^{1/2} 2Q_l$$

where $\langle \Delta f^2 \rangle^{1/2} / f_0$ is the fractional frequency fluctuation, Q_ℓ is the atomic line Q-factor, P is the emitted power and τ the averaging time. After intensive effort with this device, the limiting frequency stability achieved is of the order 1 part in 10^{11} long term (ie averaged over days).

To overcome the drawbacks encountered with $^{14}NH_3$, Ramsey proposed the hydrogen maser and demonstrated its success (Goldenberg et al. 1960) (6) at Harvard University. The idea was to use a simpler atomic spectrum and to achieve a new optimization based on a trade off between power and line width, for the overall benefit of its properties as a frequency standard. The unprecedented high stability of the microwave oscillation from the atomic hydrogen maser arises from four desirable features, all of which contribute to increased stability. These features are :

(i) The atoms are stored in a vessel placed in the microwave cavity, for much longer times than in a normal molecular beam apparatus. Consequently the resonance line is much narrower and the maser oscillation output signal more stable since it is easier to locate the peak of a narrow line than a broader one. The width of the line is that to be expected from the application of the Heisenberg Uncertainty Principle. The narrowness of the line produces frequency pulling due to cavity mistuning. In addition the cavity can be accurately tuned by ensuring that the output frequency is independent of the flux of hydrogen atoms entering the cavity (7).

(ii) Unlike resonance experiments using liquids, an hydrogen atom in the maser is relatively free and unperturbed while radiating. Consequently all atoms have essentially the same radiating frequency and the resultant resonance line will not be broadened as it would be if it consisted of a superposition of a number of resonances at slightly different frequencies.

The hydrogen atoms are not entirely free and collide with the Teflon coated walls of the storage vessel. This produces a shift in the maser frequency, the wall shift, which may be corrected for by observing the frequency output with bulbs of different diameter and extrapolating the results to an infinite diameter bulb size (8).

(iii) A further advantage of the hydrogen maser is that the first order Doppler Shift is greatly reduced. Since atoms observed in most resonance experiments are moving in random directions and at random velocities, the resonance frequencies for different atoms are shifted different amounts and the net effect is a marked broadening of the observed resonance curve. On the other hand, with the very narrow line characteristic of the atomic hydrogen maser, the relevant quantity for the Doppler Shift is the ratio of the average velocity of the hydrogen atom to the velocity of light. Since the hydrogen atoms enter the storage bulb through a small hole, and then stay in the vessel for about one second before finally emerging from the same hole, the average velocity is zero or close to zero. Consequently the first order Doppler Shift is completely negligible. There is a small second order Doppler shift due to the relativistic slowing down of any moving clock or oscillator. Since the second order shift depends on the velocity squared, it is not averaged to zero while the atoms are in the bulb. However, the second order Doppler shift is a correction which can be exactly calculated if the temperature and hence mean square velocity of the atoms is accurately known.

(iv) A final advantage, contributing to the high precision of the atomic hydrogen maser is low noise characteristics of maser amplification. Since the amplifying element is an isolated atom, there is little opportunity for any extra noise to develop beyond the theoretical minimum noise. As a result, the maser is a very low noise amplifier, the only

sources of noise being thermal noise and the noise due to spontaneous emissions.

For these above reasons the hydrogen maser frequency should be very stable. This has been confirmed experimentally as shown in fig.(1.1).

In addition to its obvious qualities as a frequency standard, the hydrogen maser is also useful as a research tool. Its high stability and narrow line width, make it a powerful spectrometer for studies of frequency deviations or level variations arising in the interaction of hydrogen atoms with magnetic and electric fields or with atomic particles introduced into the bulb. Experiments carried out include measurement of the hyperfine separations of deuterium and tritium (9) (10), the value of the proton magnetic moment (11) and spin exchange and surface relaxation in the storage vessel with added gases (12).

Relativistic experiments are also possible with the hydrogen maser and may be used to check, with greater accuracy than previously feasible, the dependance of the rate of a clock upon its gravitational potential. The predicted frequency emitted from a source at an altitude of a few miles (eg. in an orbiting satellite), differs from that on the surface of the earth by about 500 parts in 10^6. This difference is large in comparison to the stability of a hydrogen maser. The maser can, therefore, be used to check this predicted frequency shift to a greater accuracy than was previously possible.

A vast amount of fundamental physics has been carried out in experiments with hydrogen masers. This thesis is intended to contribute by comparison with other hydrogen maser studies and ammonia maser results, to the general area of maser physics and also produce the starting point for the development of a useful frequency standard for

FREQUENCY COMPARISONS
BETWEEN TWO HYDROGEN MASERS

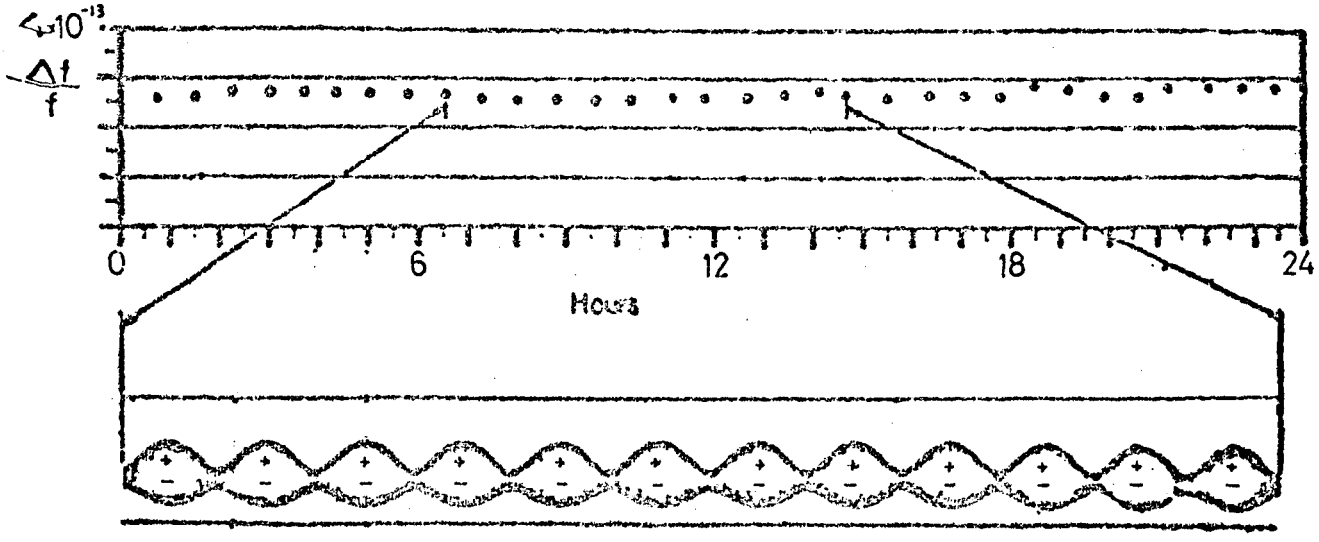

Relative frequency stability of two hydrogen masers.

(After Ramsey)

FIG(1-1)

application in spectroscopic studies and other experiments with ammonia masers in the laboratory.

CHAPTER TWO

INTERACTION OF RADIATION WITH MATTER: THE MASER PRINCIPLE

Introduction

An atom can exist with various internal arrangements which give considerable variation in its energy. The energies of such a system are quantized, that is, it exists only in certain discrete energy states. An atom consists of an assembly of electrons and nuclei. The energy of such an assembly can change only if the electrons or nucleons change their motion, or orientation, or both, corresponding to one permitted energy state to yield another permitted energy or quantum state of the system. For an isolated atom to alter its internal energy, the energy difference between the two states involved must either be absorbed from an electromagnetic field, or be emitted in order to conserve energy and momentum. The process is therefore one of absorption or emission of radiation accordingly as the final state is higher or lower in energy.

The radiation field is also quantized in energy so that it can only exchange a discrete amount of energy in the form of a photon (quantum of energy) with the interacting atom. If the two states have energies W_1 and W_2 ($W_2 > W_1$) then the frequency of the radiation involved in an upward transition $1 \rightarrow 2$ (absorption) or a downward transition $2 \rightarrow 1$ (emission) between the two states is given by

$$h\nu = W_2 - W_1 \qquad (2.1)$$

where h is Planck's constant. The observed emission or absorption line is however not monochromatic, the most fundamental source of broadening being given by the uncertainty relation $\Delta W . \Delta t \sim \hbar$

Stimulated Emission and Absorption.

In considering an atomic system, there are two distinct types of

transition occuring which involve the energy levels plus photons. These are spontaneous and induced transitions. The spontaneous are always in the form of emission of radiation due to the zero point fluctuations in the electromagnetic field and result in the falling of an atom from a higher energy level to a lower one, with the emission of a photon of energy given by equation (2.1). This photon mayhave apolarization vector σ and any frequency in the range ν to $\nu+\delta\nu$. If an atom in the upper energy state is in the presence of a radiation field at a frequency ν close to W_2-W_1/h , there exists a finite probability that the presence of this radiation field may induce transitions from state 2 to state 1, with the corresponding emission of a photon of energy. This is known as stimulated emission. If the presence of the field caused the upward transition $1\rightarrow 2$ this process is absorption since a photon of energy is absorbed from the field in the process.

The concept of stimulated emission was introduced by Einstein in order to be able to describe adequately the interaction of radiation and matter. The Einstein description is based on thermodynamic and phenomenological considerations. A complete and rigorous theory has been given by Dirac, based on quantum electrodynamics. Both stimulated and spontaneous emissions are naturally accounted for in Dirac's theory as a consequence of quantizing the radiation field. The spontaneous emission acts as a damping term in the theory and leads to an explanation of the natural width of spectral lines (13).

A one-photon absorption process is schematically represented in fig. (2.1(a)). The initial state of the two level system is the ground state 1 and a radiation field is incident on the atom with $n_{\ell\sigma}$ quanta of frequency $\omega_\ell (=2\pi\nu_\ell)$, where ℓ and σ specify the direction and polarization of the quanta respectively. The absorption of one quantum of energy causes

(a)

Schematic representation of a one-photon absorption by an atom.

(b)

Schematic representation of a one-photon emission by an atom.

FIG. (2-1)

the atom to jump to excited state 2. The atom and radiation field constitute a single closed system. Thus, since energy must be conserved, the initial energy W_i of the system must be equal to the final energy W_f. Therefore

$$W_2 - W_1 = \hbar\omega_\ell = h\nu_\ell$$

The emission of a single photon of an atom initially in an excited state is shown in fig. (2.1(b)). The matrix element of the interaction Hamiltonian between the two states for absorption and stimulated emission processes respectively are given by (13).

$$\left|\langle f|H_1|i\rangle\right|^2_{abs.} = \frac{n_{\ell\delta}\hbar\omega_\ell}{2V}\left|\bar{e}_{\ell\delta}\cdot\bar{\mu}_{12}\right|^2 \qquad (2.2)$$

$$\left|\langle f|H_1|i\rangle\right|^2_{emiss.} = \frac{(n_{\ell\delta}+1)\hbar\omega_\ell}{2V}\left|\bar{e}_{\ell\delta}\cdot\bar{\mu}_{12}\right|^2 \qquad (2.3)$$

where H_1 is the interaction between atom and radiation field, $|i\rangle$ is the initial state function, $|f\rangle$ the final state function, V the volume of the cavity containing the atoms and radiation field, $\bar{e}_{\ell\delta}$ the polarization vector and $\bar{\mu}_{12}$ the dipole matrix elements between the two atomic states. The matrix element of the interaction Hamiltonian for the emission process consists of two parts. The term containing $n_{\ell\delta}$ arises from the interaction of the atom and the radiation field and therefore represents stimulated emission. This term is identical with the matrix element for absorption and can be calculated without quantizing the radiation field as is done classically. The term containing 1 in equation (2.3) arises fromthe zero point energy of the radiation field which is $\frac{1}{2}\hbar\omega_\ell$ rather than zero. This term does not come out of the theory automatically, unless the radiation field is quantized. The consequence is that when $n_{\ell\delta}=0$, i.e. in the absence of any radiation field, there may be emissive transitions between the initial and final states of the system. This is spontaneous emission.

The total transition probabilities for the processes described are obtained after multiplying the interaction matrix elements by the radiation density and suitably averaging. These appear as the familiar Einstein coefficients

$$A = \frac{64\pi^4\nu^3}{3hc^3} \left| \bar{\mu}_{12} \right|^2 \qquad (2.4)$$

for spontaneous emission and

$$B = \frac{8\pi^3}{3h^2} \left| \bar{\mu}_{12} \right|^2 \qquad (2.5)$$

for absorption and stimulated emission probabilities which are identical.

An important point to note here is that the stimulated emissions are in phase at the centre of the atomic resonance, with the incident stimulating radiation and are therefore coherent.

Remembering that in thermal equilibrium the emission (stimulated and spontaneous) and absorption must be balanced and using Boltzman's distribution together with the above equations, one directly obtains Planck's law of radiation

$$U(\nu) = \frac{8\pi h\nu^3}{c^3} \frac{1}{\exp\left(\frac{h\nu}{kT}\right) - 1} \qquad (2.6)$$

and

$$\frac{A}{BU(\nu)} = \exp.\left(\frac{h\nu}{kT}\right) - 1 \qquad (2.7)$$

The relative importance of stimulated and spontaneous emissions at various frequencies can be seen from this equation. Thus, at microwave frequencies, spontaneous emissions will be negligible and hence not a serious source of noise in a maser system.

The Maser Principle

When a system of atoms is placed in a radiation field which is stronger than the thermal radiation of equation (2.6), a fraction of the incident power is absorbed by the atoms. The radiation density of a monochromatic incident power flow P through unit area is $U=P/c$. Thus for the two level system with populations N_2, N_1, and energies W_2, W_1 where $W_2>W_1$ and $N_2+N_1=N$, the power of induced absorption is $N_1 h\nu BP/c$ while that of induced emission is $N_2 h\nu BP/c$. The net power absorption per unit path length is

$$P_{abs.} = (N_1 - N_2) h\nu BP/c \qquad (2.8)$$

From the normal Boltzmann distribution, the excess population taking part in the process is

$$N_1 - N_2 \simeq \frac{N}{2} \cdot \frac{h\nu}{kT}$$

and therefore

$$P_{abs.} = \frac{4\pi^3 N \nu^2}{2ckT} \left|\bar{\mu}_{12}\right|^2 P \qquad (2.9)$$

When $N_2>N_1$ equation (2.8) shows negative absorption, that is the emission of power. This is the principle of maser action. The actual achievement of maser action is dependent on the production of suitable levels of population inversion in the atomic system.

CHAPTER THREE

GENERAL HYDROGEN MASER THEORY

The ground state of the neutral hydrogen atom is an S state having zero orbital angular momentum and a spherically symetrical electron distribution. The electron can be considered as oscillating from side to side of the nucleus. Both particles have intrinsic angular momentum, or spin, designated $h\underline{I}$ and $h\underline{J}$ for the proton and electron respectively and have magnetic moments $\underline{\mu}_I$ and $\underline{\mu}_J$ where $\underline{\mu}_I = g_I \mu_o \underline{I}$, $\underline{\mu}_J = g_J \mu_o \underline{J}$ and g_I, g_J are the proton and electron gyromagnetic ratios respectively and μ_o is the Bohr magneton $eh/2mc$. g_J is very nearly equal to -2 and g_I is positive and much smaller.

The Hamiltonian describing this system in a magnetic field $\underline{H}$ is given by

$$\mathcal{H} = A\underline{I}\cdot\underline{J} - g_J \mu_o \underline{J}\cdot\underline{H} - g_I \mu_o \underline{I}\cdot\underline{H}$$

in the presence of a magnetic field along the z-axis of quantization ie. $\underline{H} = (H_o + H_z \cos\omega t)\underline{k}$ this becomes

$$\mathcal{H} = A\underline{I}\cdot\underline{J} - g_J \mu_o \underline{J}\cdot(H_o + H_z \cos\omega t)\underline{k} - g_I \mu_o \underline{I}\cdot(H_o + H_z \cos\omega t)\underline{k}$$

The corresponding energy level diagram is shown in fig. (3.1). The states $(F=1, m_F=0)$ and $(F=0, m_F=0)$ are connected by matrix elements

$$\langle F', m_{F'} | \mathcal{H} | F, m_F \rangle = \langle 1,0 | \mathcal{H} | 0,0 \rangle = \langle 0,0 | \mathcal{H} | 1,0 \rangle$$

Consider an aton in the state $(F, m_F) = (1,0)$ and subject to a field in the z-direction with both static and alternating components such that $\underline{H} = (H_o + H_z \cos\omega t)\underline{k}$. $H_o\underline{k}$ is assumed small and we can ignore the distortion of states produced by it. If the alternating part induces transitions from the $(1,0)$ state to the $(0,0)$ state, then at some time t the atom will be in a mixed state

$$\Psi(t) = a_1(t)\Psi(0,0) + a_2(t)\Psi(1,0)$$

where $a_1(t), a_2(t)$ are in general complex quantities and assuming perfect state selection $a_1(0)=0$, $a_2(0)=1$

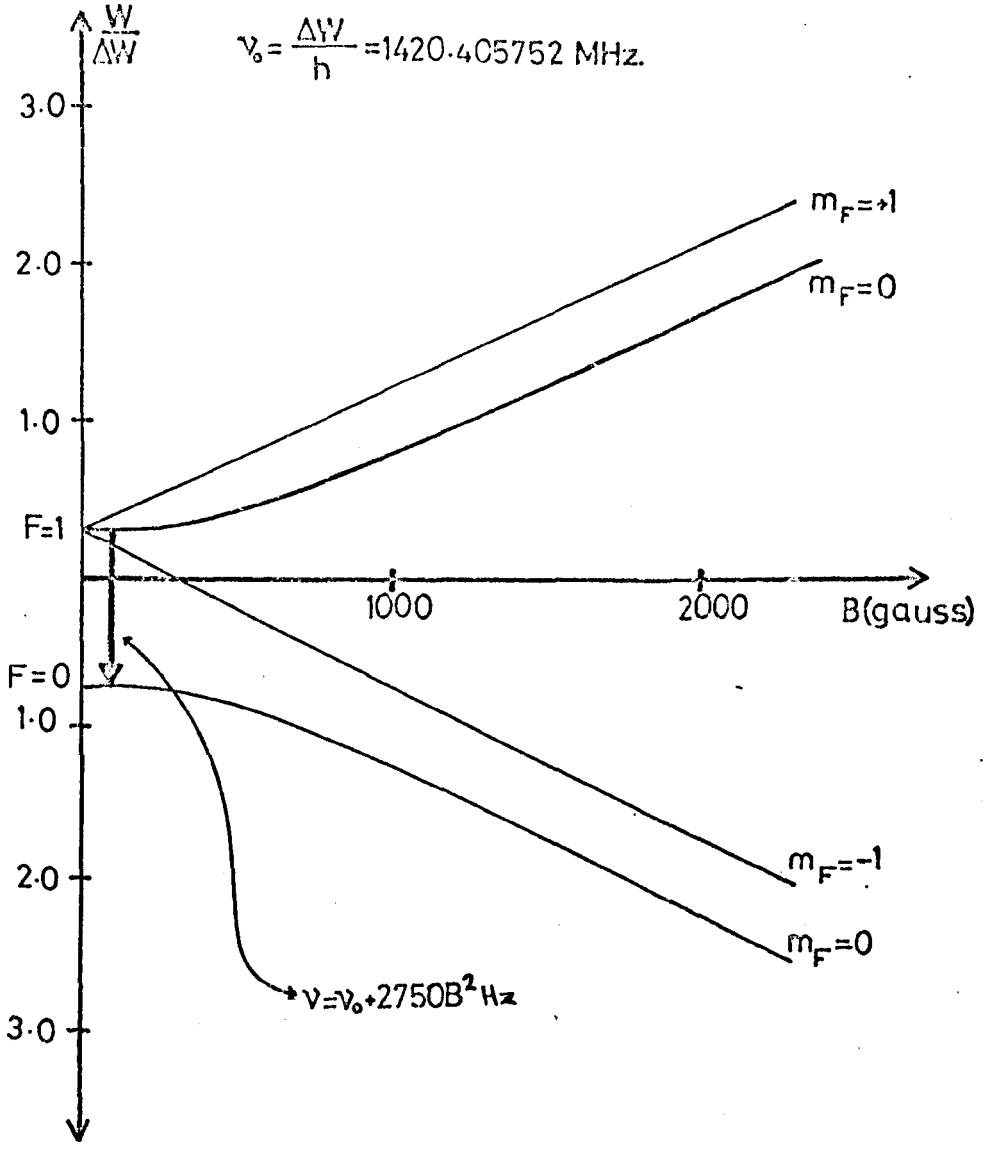

Energy diagram for atomic hydrogen in the ground electronic state $1^2S_{1/2}$. Heavy arrow indicates transition used in stable atomic oscillators.

FIG. (3·1)

Expressions for $|a_1(t)|^2$ and $|a_2(t)|^2$ can be derived using time dependent perturbation theory involving the matrix element $\langle 1,0|H|0,0\rangle$ The values of the expression are plotted against time in fig. (3.2) and as is expected

$$|a_1(t)|^2 + |a_2(t)|^2 = 1$$

Both these functions vary sinusoidally in time with the same period and amplitude. The period is given by $\frac{2\pi}{\Omega}$ where

$$\Omega = \sqrt{X^2 + (\omega - \omega_0)^2}$$
$$X^2 = \left(\frac{\mu_e H_z}{\hbar}\right)^2$$

If H_z is non-uniform throughout the bulb, X^2 is replaced by

$$\langle X\rangle^2 = \left(\frac{\mu_e}{\hbar}\right)^2 \langle H_z\rangle_b^2$$

where $\langle H_z\rangle_b$ indicates averaging over the volume of the storage bulb.

$$\frac{\omega_0}{2\pi} = \frac{W(1,0) - W(0,0)}{h} = \nu$$

ν is the frequency of the hyperfine transition. The peak value of $|a_1(t)|^2$ is $\left(\frac{X}{\Omega}\right)^2 = \frac{X^2}{X^2 + (\omega-\omega_0)^2}$

If $\omega - \omega_0 \ll X$ as in the case of the maser this becomes unity and the period is

$$\frac{2\pi}{X} = \frac{h}{\mu_e H_z}$$

By suitable timing of its entrance and exit, an atom, could be made to deliver up its full energy $h\nu$. In general if long and random times were spent in the radiation field, atoms would be re-emitting and re-absorbing energy and the mean value of $|a_1(t)|^2$ would be $\frac{1}{2}$ i.e. a beam of I atoms/sec. could be made to radiate an average power $P = \frac{1}{2} I h\nu$. If atoms delivered to the bulb escape with a time constant $1/\gamma$, the probability per unit time of leaving at a time t is $f(t) = \gamma e^{-\gamma t}$ and $|a_1(t)|^2$ must be averaged allowing for this fact. In this case

$$P = \tfrac{1}{2} I h\nu \left(\frac{X^2}{\gamma^2 + X^2 + (\omega - \omega_0)^2}\right)$$

This is a typical Lorentzian line shape with full bandwidth at half power of $2\sqrt{(\gamma^2 + X^2)}$. The frequency accuracy obtainable with the maser is due firstly to the natural reproducibility of atoms in a suitable environment

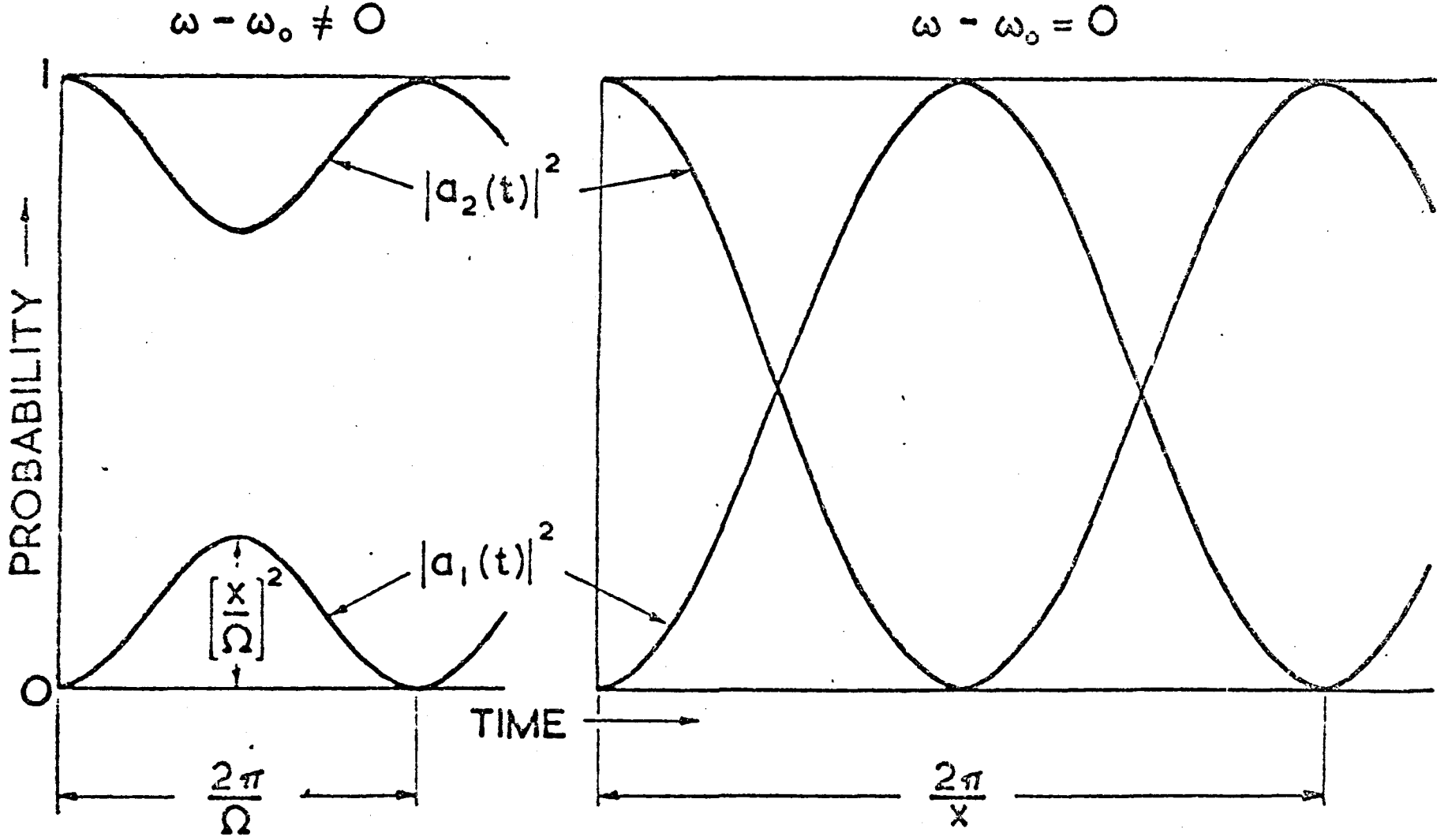

$$\Omega^2 = x^2 + (\omega - \omega_0)^2$$

FIG.(32)

$$x = \frac{\mu_0 H_z'}{\hbar}$$

and secondly to the narrowness of this bandwidth. This is one reason for keeping the stimulating field H_z small and hence x small. If $x \ll \gamma$ the linewidth becomes 2γ and the atomic response has an effective Q - factor $Q = \omega_c/2\gamma$

Threshold Flux:

For oscillation to occur the power delivered to the cavity by the beam must equal the power dissipated in the cavity. As above, when $\omega - \omega_o < x < \gamma$ the power delivered is

$$P = \tfrac{1}{2} I \hbar \omega_c \frac{x^2}{\gamma^2}$$

This must equal the power dissipated which is $W\omega_c/Q_c$ where W is the electromagnetic energy stored in the cavity and Q_c is the cavity Q. W and x involve averages of $(H)^2$ and H_z over the cavity volume and atom path respectively, and depend on cavity and bulb geometry. Thus the expression for threshold flux arrived at is

$$I_{th.} = \frac{\hbar \gamma^2 V}{4\pi Q_c \mu_c^2 \eta}$$

where V is the bulb volume and η is a factor depending on magnetic field averages. This factor is not dependent on the level of cavity excitation, so the condition for oscillation build up exists even at the level of thermal noise excitation of the cavity.

When the oscillation level is such that the condition $x \ll \gamma$ is not satisfied, then $P \propto x^2/x^2+\gamma^2$ instead of x^2/γ^2 and the oscillation level stabilizes at a value of x determined by this. If the input beam is increased beyond I_{th}, the level of storged energy is proportional to

$$I - I_{th.} / I_{th.}$$

Owing to the low probability of a magnetic dipole transition (~1/100 of the electric dipole in the case of $^{14}NH_3$) in the atomic hydrogen, maser oscillation requires a long radiative lifetime for atoms in the storage bulb inside the resonant cavity. This lifetime is affected by various relaxation processes which will now be discussed.

RELAXATION PROCESSES

The radiative lifetime of atoms in the storage bulb is limited by a variety of random processes leading to time independent relaxation rates which may be added to give the total relaxation rate.

The time constants T_1 and T_2 are used to describe the return of magnetization, in a given direction, to its equilibrium value and the decay of the oscillating dipole moment respectively. It must be remembered that a given perturbation frequently causes relaxation by both changing the magnetization along the axis of quantization and by causing a loss of coherence between the oscillating dipole moment and the radio frequency field. These processes may be considerably different and hence subscripts 1 and 2 are used to identify them.

The relaxation processes under consideration are due to escape from the bulb, atomic collisions at the walls of the storage vessel, magnetic field inhomogeneities, spin exchange and second order Doppler broadening and pressure broadening.

Escape from the storage vessel:

The escape rate from the bulb, γ_0, is determined by equating the incident beam flux I with the emergent flux $N\bar{v}A_e/4k$, where N is the density of the atoms in the bulb, $\bar{v}$ the mean atomic velocity, A_e the total escape area and k a numerical factor depending on the geometry of the exit apperture. If the volume of the bulb is V_b then $N = I/\gamma_0 V_b$

$$\gamma_0 = \bar{v}A_e/(4kV_b)$$

For a 15cm diameter vessel with an exit apperture plug having a duct a few millimeters in diameter and a length/diameter ratio approximately 10/1, then assuming $\bar{v}=3\times10^5$ cm/sec. with atomic hydrogen at room temp., the figure for the relaxation parameter is $\gamma_0 \sim 0.5\,\text{sec.}^{-1}$

Wall Collisions

These may be conveniently placed into two categories: adiabatic and non-adiabatic collisions. In the former, the atom colliding with the wall of the vessel does not undergo any transition between states but a small change in the spacing of the energy levels is produced and this shift eventually causes loss of coherence of the radiating atom with the oscillating magnetic field. Following a non-adiabatic collision, the atom is lost as far as any further contribution to the radiation field is concerned. Relaxation here occurs during a single collision, hence the mean number of collisions an atom undergoes is inversely proportional to the probability that a single collision is adiabatic. Consider the above processes in more detail.

An adiabatic collision is described by a phase shift parameter ϕ, the phase shift per collision, where

$$\phi = \int \frac{\delta W(1,0) - \delta W(0,0)}{\hbar} dt$$

δW is the difference in energy of a given state between free space value and that when surface forces are present. The integration is over the time of one collision. It is shown (14) that an atom loses coherence after a number of collisions $\sim \frac{2}{\phi^2}$. The situation in the maser is different in that unlike the above reference, a radio frequency field is present and also the adsorption energy is large compared with kT so that adsorption time is described by an exponential distribution function. Since the result is fundamentally due to the random nature of the perturbation it is quite general and can be applied to the case of the maser. If the collision rate is $\frac{\bar{v}}{l}$, then the relaxation rate γ_s is equal to $\frac{1}{2}\left(\frac{\bar{v}}{l}\right)\phi^2$. A reasonable value for γ_s would be $<10^{-4}\,sec^{-1}$.

In a non-adiabatic chemical reaction with the surface where no strong adsorption forces are present, then physical adsorption does not by itself

limit radiative lifetime. Chemical reaction between an atom and the surface can occur, leading to the decay rate γ_r which is the probability per unit time that an atom under-goes such a reaction. In order for a reaction to take place the incident atom must possess kinetic energy eaual to E_a, the activation energy for that reaction. From thermodynamics (15) an expression for the rate r, at which atoms hit the surface, with an energy greater than E_a, is arrived at, which gives

$$r = \left(\frac{2\bar{v}}{\pi^{1/2}\ell}\right)\exp\left(\frac{-E_a}{KT}\right)$$

where $\bar{v}$ is the r.m.s. velocity of the atom $\left(\frac{3kT}{m}\right)^{1/2}$, the mean distance between collisions and T the temp. of the storage bulb. The actual reaction rate differs from r by a stearic factor P (16), because not every collision satisfying the energy requirements leads to a reaction. The relaxation rate is thus

$$\gamma_r = \left(\frac{2\bar{v}P}{\pi^{1/2}\ell}\right)\exp\left(\frac{-E_a}{KT}\right)$$

For a flurocarbon surface on a 15cm diameter bulb at room temperature, a typical value for γ_r would be approximately $10^{-1}\,sec^{-1}$. Fortunately this type of reaction has a low probability of occurrence.

Magnetic Field Inhomogeneities

A non-uniform magnetic field in the storage bulb can cause relaxation in two ways. By virtue of their motion in the bulb, the atoms experience a time varying magnetic field and thus Zeeman transitions can be induced similar to Marjorana transitions of atomic beams. In addition, since the resonant atomic frequency is slightly field dependent and because different atoms have different histories in the bulb due to the random nature of their paths, there is eventually a loss of coherence of the oscillating moment. These relaxation rates are designated γ_{H_1} and γ_{H_2} respectively.

In the case of the relaxation rate γ_{H_1}, the effect of the inhomogeneities on the Zeeman states ($F=1; m_F=0,\pm1$) is analysed by neglecting the F=0 state and considering a spin-one system in the presence of a random perturbation.

Transitions are induced between the states at a rate W, and the decay rate for an atom from the state of interest $(F=1, m_F=0)$ is $=W_{1,0}+W_{0,0}$, the W-subscripts denoting m_F values. γ_{H_1} does not correspond to T_1^{-1} since the quantity of interest is the rate of decay of an atom from a given state, not the decay rate of magnetization. The relaxation rate for the simplest type of symmetrical field inhomogeneity is shown to be (17)

$$\gamma_{H_1} = \tfrac{1}{2}\gamma_F^2 h^2 \frac{t_0}{1+\left(\frac{\omega t_0}{2}\right)^4}$$

A typical value for this relaxation rate is $\gamma_{H_1} \sim 0.3 \text{sec.}^{-1}$.

A simple method with which to obtain an estimate of γ_{H_2} is to assume that the field has a separate value on either half of the storage vessel of $H_0 \pm \frac{\Delta H}{2}$. The field dependence of the $(F=1, m_F=0) \rightarrow (F=0, m_F=0)$ transition is given by $\nu = \nu_c + \alpha H_0^2$ where $\alpha = 275 \text{CH}_z/\text{gauss}^2$. The resonant frequencies on either side of the bulb differ by $2\alpha H_0 \Delta H$, assuming $\Delta H \ll H_0$. If the mean number of collisions an atom makes before leaving the bulb is n, then the mean time an atom spends in one half of the bulb in excess of the other is $2n^{1/2}t_0$ and for coherence it is necessary to have

$$2n^{1/2}t_0(2\alpha H_0 \Delta H) < 1$$

Therefore

$$\gamma_{H_2} = \frac{1}{nt_0} = t_0(16\alpha^2 H_0^2 \Delta H^2)$$

and for $H_0 = 10^{-2}$ gauss, $\Delta H = 10^{-3}$ gauss parallel to H_0, then with $t_0 = 3\times10^{-5}$ sec. the value of the relaxation rate γ_{H_2} is approximately 10^{-6}sec.^{-1}

If the transitions of interest are $(F=1, m_F=\pm1)$ to $(F=0, m_F=0)$ the π-transitions, then there is a first order field dependence $\nu = \nu_0 + \beta H_0$ where $\beta = 1.4\times10^6$ Hz/gauss and it follows that

$$\gamma_{H_1}(\pi) = 4\beta^2 \Delta H^2 t_0$$

and with the same fields as above $\gamma_{H_1}(\pi)$ is approximately 240sec.^{-1}. On the other hand, if the field varies due to inhomogeneities which are only

perpendicular to the axis then an inhomogeneity of 10^{-3} gauss in the same field as above, yields $\gamma_{H_i}(\pi)$ approximately equal to $0.6 sec^{-1}$.

Spin Exchange

At sufficiently high densities of atomic hydrogen, the dominating relaxation process is due to hydrogen-hydrogen collisions. The mechanism which leads to relaxation is chiefly spin exchange in which the electron spins of the colliding atoms exchange state, leaving the atoms in states different from their initial ones. The decay rate for spin exchange γ_{se} is related to the number of hydrogen atoms per cm^3, N, by

$$\gamma_{se} \simeq 5 \times 10^{10} N sec^{-1}$$

This expression, which is valid for electron spin resonance systems, should be slightly modified for the hydrogen maser since there is initially a non-equilibrium distribution of states. On the other hand, this introduces only a minor change in γ_{se} and the above equation is still correct.

Pressure Broadening

At easily obtainable pressures, collisions with inert atoms or molecules have no effect on the line width of the resonant transition. Relaxation due to the presence of an impurity gas at elevated pressure has been observed by Berg (12). For example the relaxation rate due to O_2 was found to be approximately $2 \times 10^{-7} sec^{-1}$/torr. This effect is accounted for by spin exchange between atomic hydrogen and the oxygen impurity. Berg has also made measurements using other gases such as N_2O, CO and D_2.

Doppler Broadening

First and second order Doppler broadening have negligible effects in the hydrogen maser as far as line broadening is concerned.

FREQUENCY SHIFTS IN THE HYDROGEN MASER

Ideally the oscillation frequency of the maser is identical with the

hyperfine transition frequency between the levels of the atomic system as measured with the atoms at rest in free space. The atoms are not free and they interact with the surrounding electromagnetic system and with the walls of the storage vessel. The important effects leading to a shift in frequency are, wall shift, first and second order Doppler shift, cavity pulling, Zeeman effect and the effect of neighbouring atomic states.

Wall Shift

The phase shift, ϕ, introduced into the wave function of an atom during a wall collision causes a shift $\delta\omega$ in the resonant frequency given by

$$\frac{\delta\omega}{\omega} = \phi/(\omega t_0)$$

where t_0 is the mean time between collisions. The value for ϕ is difficult to predict theoretically because of the uncertainty of the exact interaction potential and lack of knowledge of microscopic wall structure. Upper limits for hydrocarbon surfaces are quoted (17) as $\delta\omega/\omega < 10^{-9}$ and lower limits as $\delta\omega/\omega > 1.3\times10^{-13}$. The shift with saturated flurocarbon surfaces such as Teflon is probably better than the above value due to its relatively tight binding and small polarizability.

Essen et.al. (8) have measured the frequency of the Hydrogen maser by including an independant measurement of the wall shift, their results being accurate to $\pm$ 0.001Hz.

First and Second Order Doppler Shift

With the storage bulb arrangement for the containment of atoms, the first order Doppler effect can be completely neglected as a source of frequency shift. The second order effect does not average in the same manner because of its dependance on the square of the atomic velocity. The fractional shift introduced is

$$\frac{\omega - \omega_0}{\omega_0} = \frac{\delta\omega}{\omega_0} = -\frac{1}{2}\frac{\bar{v}^2}{c^2} = -\frac{3}{2}\frac{kT}{mc^2}$$

where m is the atomic mass, k Boltzman's constant and T the absolute temperature.

This can be seen to be the ratio of the thermal energy to the rest energy of the atom. For hydrogen this gives

$$\frac{\delta\omega}{\omega_o} = -3\times10^{-13}/^{\circ}K$$

Cavity Pulling

If the cavity is mistuned from resonance by an amount $\delta\omega_c$, then the oscillator frequency will be displaced by an amount

$$\delta\omega = \delta\omega_c\,(Q_c/Q_l)$$

Q_c is the cavity Q.

Q_l is the atomic line Q.

Since the shift decreases with increasing Q_l it does not become relatively more significant as lifetime increases. This expression is not exact for a conventional beam maser, but must be multiplied by a slowly varying function of power level. In the case of an exponential distribution for lifetime, however, the pulling effect is independant of power level. For a ratio Q_c/Q_l of 10^{-6}, giving a shift $\delta\omega/\omega_c$ no larger than 10^{-13}, the cavity must be tuned to approximately 100Hz. Hence for frequency standard work, the cavity must be accurately tuned and either temperature controlled or thermally compensated to a high level.

Zeeman Effect

The second-order magnetic field dependance of the $(F=1, m_F=0)$ $(F=0, m_F=0)$ transition is

$$\nu = \nu_o + 2750H^2 \quad \text{Hz.}$$

where H is in gauss. The shift due to a change ΔH in the magnetic field is

$$\frac{\omega-\omega_o}{\omega_c} = 3.9\times10^{-6}\Delta H.H$$

A fractional shift of no more than 10^{-13} requires $\Delta H.H \simeq 3\times10^{-8}$ or for example a field of 1mgauss held constant to 3%.

Effect of Neighbouring States

The presence of atoms in other states than $(F=1, m_F=0)$ can cause a change

in the permeability of the cavity and hence shift the resonant frequency. The only states which make appreciable contributions to this are $(F=1, m_F=\pm 1)$. The pulling effect of these states is very small however for the following reasons. Normally these states do not couple to the resonant mode because the static magnetic field is parallel rather than perpendicular to the oscillating field. In addition the two states have effects of opposite sign so that if care is taken to populate them equally they have negligible net effect, even if the static magnetic field is not precisely parallel to the oscillating field.

CHAPTER FOUR

CONSTRUCTION OF THE MASER

The Vacuum System

The system comprises a lower or source chamber, which houses the atomic hydrogen effuser and state separating magnet, and an upper or storage bulb chamber, where at one end is mounted the quartz storage bulb and cavity fig.(4.1). All parts of this main vacuum envelope are made from welded, non-magnetic, thin walled stainless steel. The upper and lower vacuum chambers are separated by a stainless steel sheet flange in which a 3mm. diameter hole is drilled on the beam axis. Although this constriction obviously decreases the pumping speed by the diffusion pump on the upper chamber, the aperture acts as an alignment point and collimator along the beam path from the source to the storage bulb entrance. Irrespective of this, the upper chamber is pumped by a vac-ion pump. At the very bottom of the system the atomic hydrogen source and state selecting magnet are housed in an adjustable stainless-steel bellows.

The lower vacuum chamber is pumped on using an Edwards Speedivac oil diffusion pump, operated using Midland Silicone oil type 705. This unit is water cooled and separated from the 6in. inside diameter stainless-steel elbow, which connects it to the lower chamber, by a 6in. water cooled stainless-steel chevron baffle. The speed for this type of pump is 600litres/sec. for air. The use of such an oil diffusion pump does give rise to the possibility of contamination in the system by oil vapour. However, any effect due to this would only manifest itself in a measurable amount as a frequency pulling and since frequency standard work is not of prime importance here, this poses no severe restrictions on the system.

The upper vacuum chamber is pumped by a Ferranti getter-ion pump, type FJ145, the pumping speed being 145 litres/sec at 10^{-4} torr for air. The main

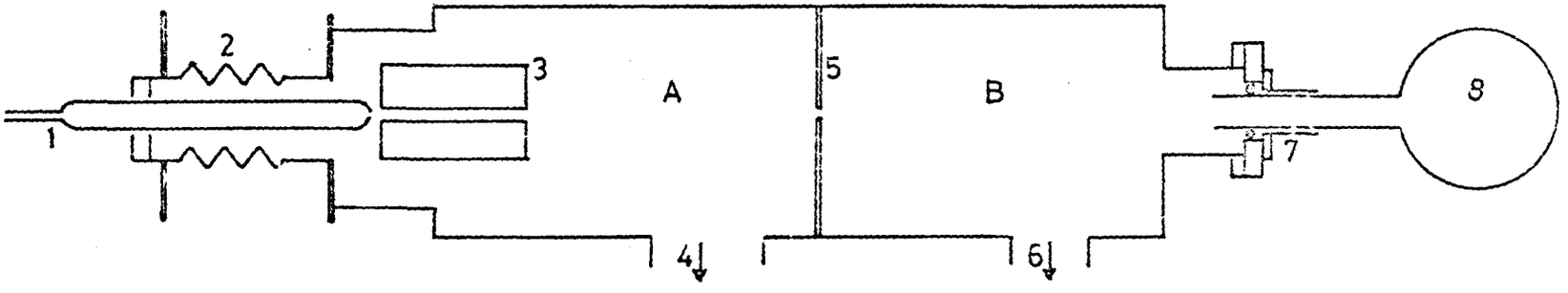

A. Lower Vacuum Chamber
1. Discharge Tube
2. Adjustable Bellows
3. State Separator
4. Oil Diffusion Pump
B. Upper Vacuum Chamber
5. Dividing Flange
6. Vacion Pump
7. Viton Seal Assembly
8. Storage Bulb

VACUUM SYSTEM

FIG.(4.1)

advantage of this pump over a radial electric field pump which was initially used, is the much shorter 'pumping-down' time after opening the system to the atmosphere (5 hours as opposed to 48 hours for the electric field pump). The big disadvantage of a getter-ion pump on the maser is the stray magnetic field produced due to the presence of the large permanent magnet on the unit, which is essential for its operation.

The lower chamber pressure is approximately 10^{-6} torr, whilst the upper chamber with no hydrogen gas flow is 1×10^{-7} torr. With gas flowing at normal operational background effuser pressures, the upper chamber pressure rises to $2\text{-}3 \times 10^{-7}$ torr. Baking the system should allow the ultimate pressures to be reached between 5×10^{-8} torr and the pressures already achieved.

Atomic Hydrogen Source

Molecular hydrogen is dissociated by using radio frequency (r.f.) discharge arrangement which has so far proven the most convenient dissociation process in hydrogen maser applications. Of the other possibilities for use, the Woods tube type is too cumbersome to build and operate whilst the thermal dissociator produces a relatively hot beam which is difficult to focus.

The discharge tube is made of Pyrex 1.5cm. diameter and 15cm. in length. The molecular hydrogen enters via an extension tube 30mm. in length with 3mm. inside diameter and an atomic beam leaves via an exit aperature 0.75mm. inside diameter and 5mm. long. Alternatively a multi-tube glass collimator can be used as the exit aperture if it is desired to reduce the beam flux into the source chamber pump. A variable coupling link connects the r.f. power, derived from an oscillator giving up to 50 watts of power at 27MHz., to the discharge tube.

The tube is cleaned carefully with dilute nitric acid and distilled water before being placed in the system. Apart from this no special internal surface

treatment is given to the tube (Phosphoric acid is sometimes used as a surface treatment agent). Thehydrogen discharge does not aquire its characteristic red glow until it has been used for several hours. After long periods of use the tube becomes blackened in the vicinity of the coupling electrode. This is possibly due to the production of black borosilicate products from internal surface decomposition. The tubes are normally replaced when this happens, but it has not been confirmed that this decomposition affects the performance of the discharge tube.

Molecular hydrogen is introduced into the tube using a conventional gas handling system. The source pressure is monitored using a Pirani gauge head positioned behind the discharge as shown in the diagram (fig. 4.2.) For initial hydrogen maser ringing signals, pressures varied between 0.2 and 1-torr, whilst for initial oscillation between 0.3 and 1.5 torr.

State Selecting Magnet

The purpose of the state separator is to remove atoms in the states $F=1, m_F=-1$ and $F=0, m_F=0$ from the atomic beam and to focus atoms in the states $F=1, m_F=1, 0$ on to the entrance aperture of the storage bulb.

Consider the behaviour of an atom having a magnetic dipole moment and falling into an inhomogeneous magnetic field. The additional energy required by a hydrogen atom in the states $F=1, m_F=\pm 1$ in a magnetic field $\underline{H}$ is described by $\underline{W}=-\mu\underline{H}$ where μ is the magnetic dipole moment of the atom. The force on an atom in an inhomogeneous field is

$$\underline{F} = -\nabla \underline{W} = -\frac{\partial W}{\partial H}\nabla \underline{H} = \mu_{eff}\nabla H$$

where μ_{eff} is the projection of μ on the direction of the field $\underline{H}$. Fig.(4.3). shows the variation of effective magnetic moment with the applied field.

When placed in a high field the hydrogen atoms have the magnetic properties of their valence electron. The effective magnetic moment is then $\pm\mu_0$ depending on whether the electron spin magnetic moment is paralell or

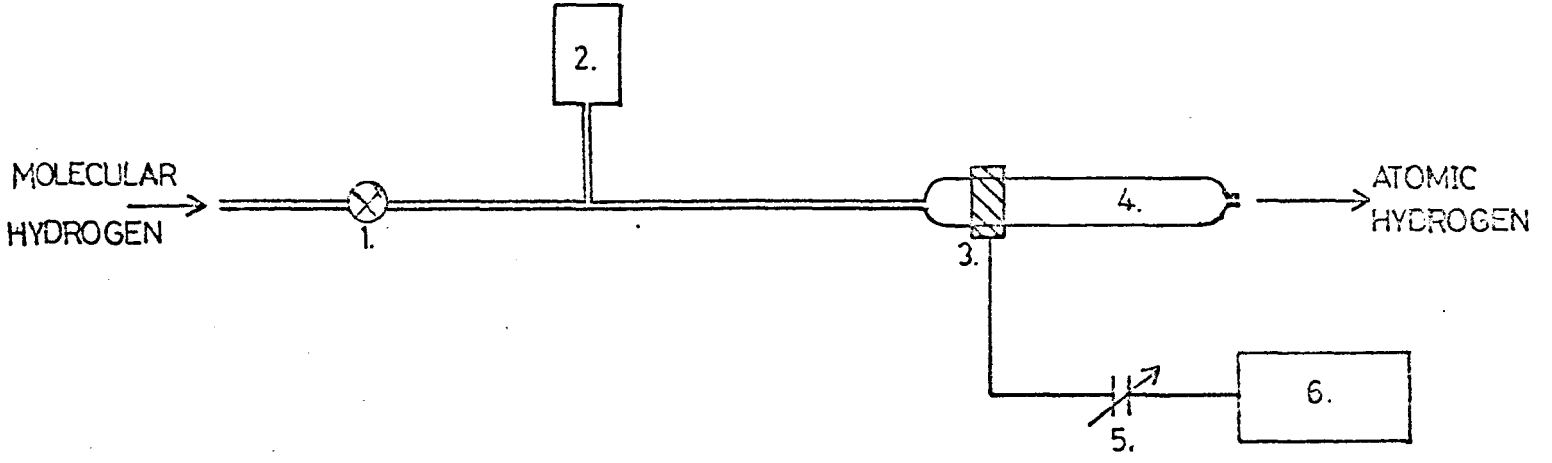

1. NEEDLE VALVE
2. PIRRANI GAUGE
3. R.F. COUPLING ELECTRODE
4. DISCHARGE TUBE
5. R.F. MATCHING UNIT
6. POWER OSCILLATOR (27MHZ.)

ATOMIC HYDROGEN SOURCE

FIG.(4.2)

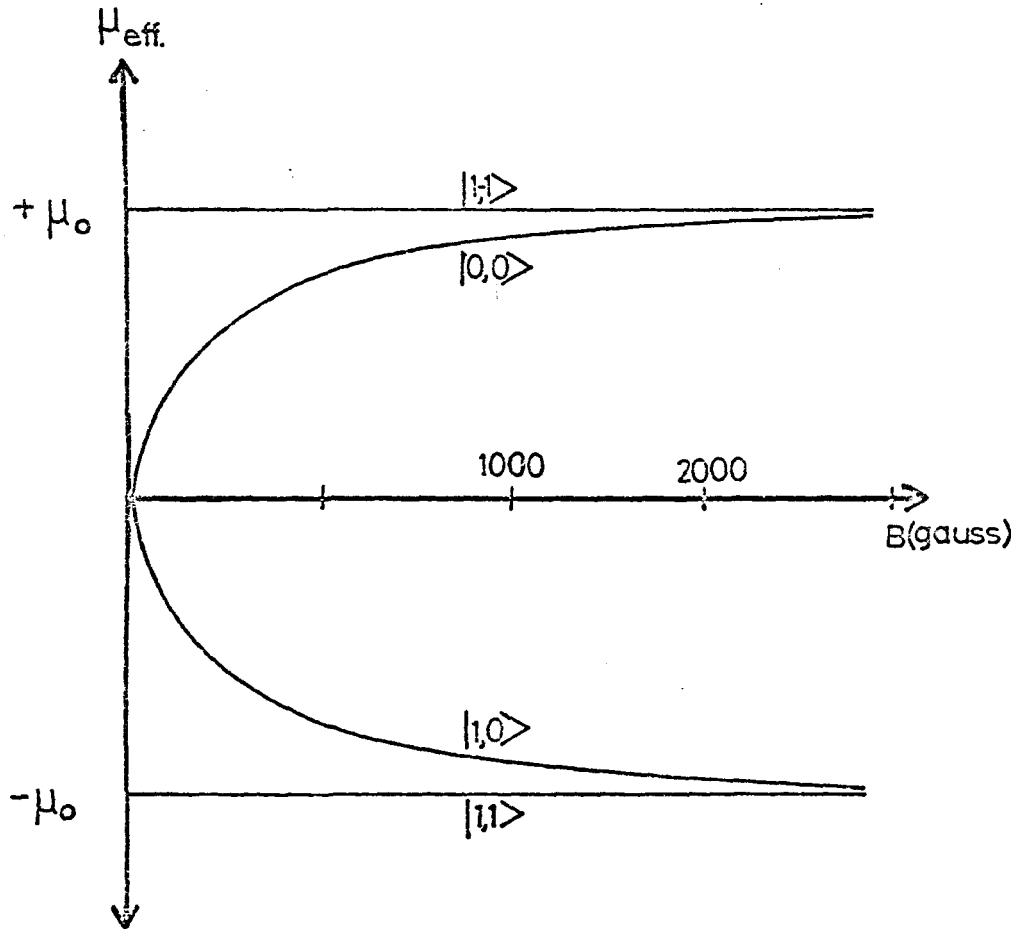

Variation of the effective magnetic moment of the four hyperfine levels of the ground state hydrogen atom, as a function of applied magnetic flux density.

FIG.(4.3)

anti-parallel to the direction of the magnetic field. μ_o is the Bohr magneton.

For the states $F=1, m_F=\pm1$, μ_{eff} is field independent and its modulus is μ_o. For the states $F=1, m_F=0$ and $F=0, m_F=0$ then μ_{eff} is field dependent. At $H=0, \mu_{eff}=0$ and as H increases $\mu_{eff} \neq 0$. In strong fields the magnetic moment of the atom is determined mainly by that of the electron and is nearly μ_o The increase in μ_{eff} with field occurs rather quickly and is practically μ_o for $H \simeq 1$kG. Since the field within the Mk.1 state separator is of the order 4kG, it may be assumed that $\mu_{eff} \simeq \mu_o$ for both $m_F=0$ and $m_F=\pm1$ states.

To consider μ_{eff} as constant it is necessary that when the atom moves in a variable magnetic field it must have the same value for the projection of the magnetic moment on the direction of the external field H. Thus it is necessary that the Larmor precession frequency ν_L of the atomic magnetic moment under the influence of H is much larger than the frequency ν of the variable external field. An atom whose motion takes it into a region of different strength sees the value of H as one alternating at a frequency

$$\nu = \bar{v}/\ell_2$$

$\bar{v}$= mean atomic velocity and ℓ_2= magnetic length. In the present case this results in $\nu \simeq 10$kHz. The Larmor frequency is

$$\nu_L = \frac{[\mu_J H]}{2\pi\hbar I} = \frac{g_J \mu_o H}{h} = 1.4 g_J H \text{(MHz)}$$

Thus with H for the Mk.1 magnet $\sim$4kG, $\nu_L \sim 5.6$GHz and hence $\nu_L \gg \nu$ so that μ_{eff} may be assumed constant.

For focusing the atoms with negative μ_{eff} i.e. $F=1, m_F=0,+1$ it is necessary to pick a magnetic field configuration such that (18)

$$\underline{F} = -D\underline{r}$$

where r is the distance from the beam axis and D is a constant. For a magnetic field configuration with 2n order symmetry (n=2,3,...) the magnetic flux density at a distance r from the symmetry axis is given by (19)

$$B/B_o = (r/r_o)^{n-1}$$

B_o is the magnetic flux density on a cylinder radius r_o. The radial force acting upon the atom is then

$$\underline{F} = \mu_{eff}(n-1)\left(B_o/r_o^{n-1}\right) r^{n-2}\frac{\underline{r}}{r}$$

for $n=3$

$$\underline{F} = 2\mu_{eff}\frac{B_o}{r_o^2} r\left(\underline{r}/r\right)$$

So if $$D = 2\mu_{eff}B_o/r_o^2$$

then for a hexapole magnet $$\underline{F} = -D\underline{r}$$

and the required state separation is possible. Thus the magnet acting in an analogous manner to a cylindrical lens in geometrical optics will be convergent for atoms with negative μ_{eff} and divergent for those with positive μ_{eff}. Atoms in the states $F=1, m_F=0,+1$ will then be focused along the magnetic axis. Focusing on to the entrance aperture of the storage vessel is also dependant on the magnetic fields, H', between the state separator and the bulb. As long as the change in H' is adiabatic the atomic spin projection on the instantaneous magnetic field is a constant of the motion. Hence the spins can follow the direction of H' into the cavity where the magnetic field is common to all atoms entering the storage bulb, and is in such a direction (i.e. along the cavity axis) to satisfy the selection rules for magnetic dipole transitions.

The state separator was designed following the principles suggested by Christensen and Hamilton (20), the cylindrical hexapole magnet giving the suitable r^2 dependence of field about its axis. The pole tips may be of arbitrary section as their shape is not of crucial importance as far as the radial field dependence is concerned. However, too large a pole tip angle (α) causes interpole flux leakage and hence reduces the field at the pole tips. For focusing, the critical dimensions are gap radius r_o and magnetic field length ℓ_2. The state separator is mounted in the bellows between the lower vacuum chamber and the discharge tube housing. The bellows is used to vary

the position of the magnet in situ and was used for initial optical alignment of the magnet with the atomic discharge source and entrance to the storage vessel. The Mk.1 state separator was magnetised at the National Physical Laboratory. Eight turns of 16 s.w.g. copper wire were wound onto each pole piece and a current passed through them by discharging two 2500μF capacitors in parallel by means of a thyristor discharge system, after raising them to a potential of 70 volts. The resulting field at the pole tips, of 4kG, was measured using a calibrated Hall probe. The magnet was then Araldited for extra rigidity.

As a result of the initial hydrogen maser ringing signals it was decided to fabricate another separator along similar lines but with the following modifications, in order to improve the rather low field of 4kG.

The pole tips on the second (Mk.II) magnet were made more rounded in section to avoid saturation effects at the tips which was probably happening with the rather pointed Mk.1 pole tips. The two magnets are shown for comparison in fig.(4.4). The magnet focusing gap was reduced to $\frac{1}{8}$" from the latter dimension giving too large a gap between poles in which to obtain high field values. The remaining dimensions were made to suit the overall space available in the system and the poles were made to have a large volume for storing magnetic energy whilst still keeping interpole flux leakage low. The higher the field, the better the focusing properties of the magnet. A sectional diagram of the basic magnet design is shown in fig.(4.5).

The yoke and pole tips of the magnet were made from Edgar Allen high permeability iron, the yoke being in two halves for ease of fabrication. The pole pieces were of Alcomax III, grain orientated along the magnetic radius (these were supplied ground and magnetised). Three magnets (1"x1"x$\frac{1}{2}$") were used equally spaced along each pole piece, which was held in position by two 4BA screws through the yoke. Two end plates were used to hold the two yoke

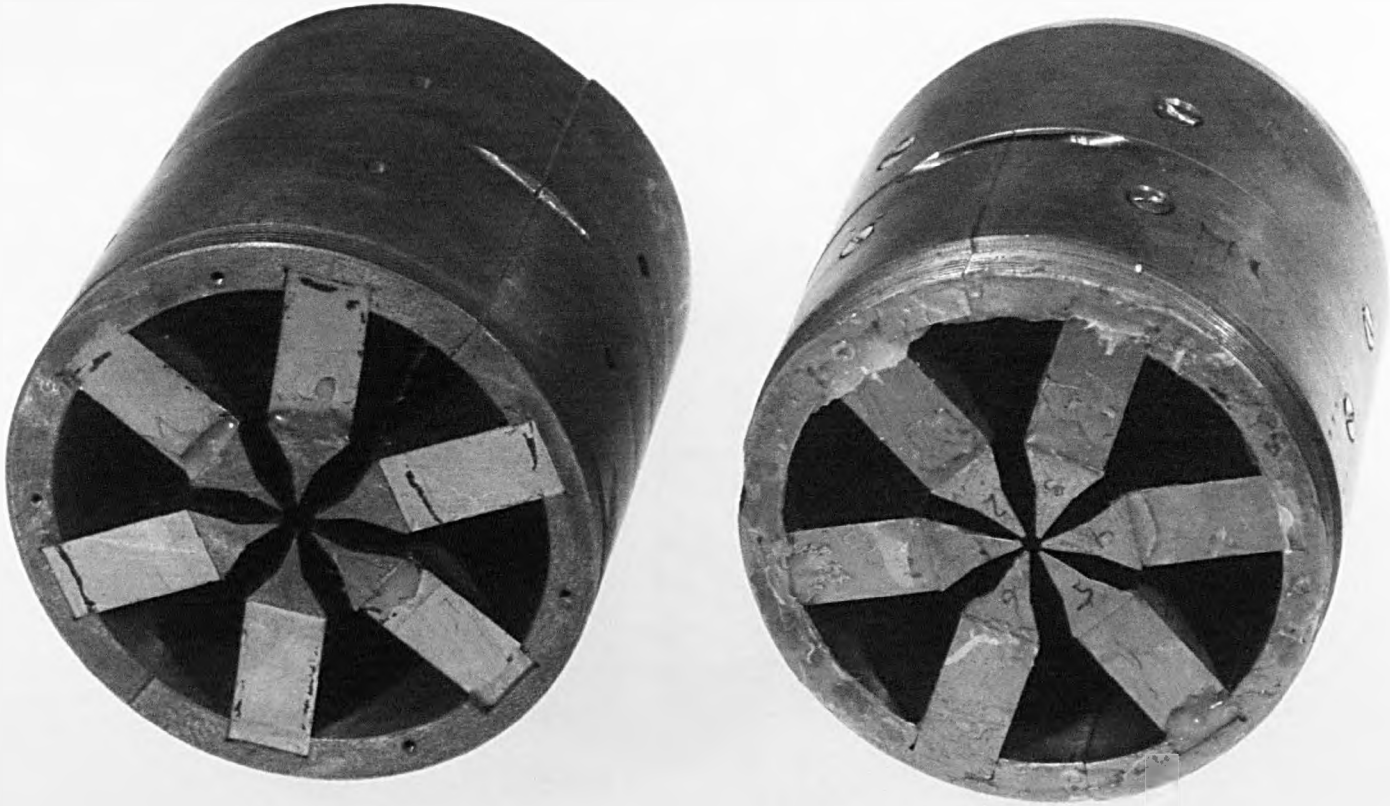

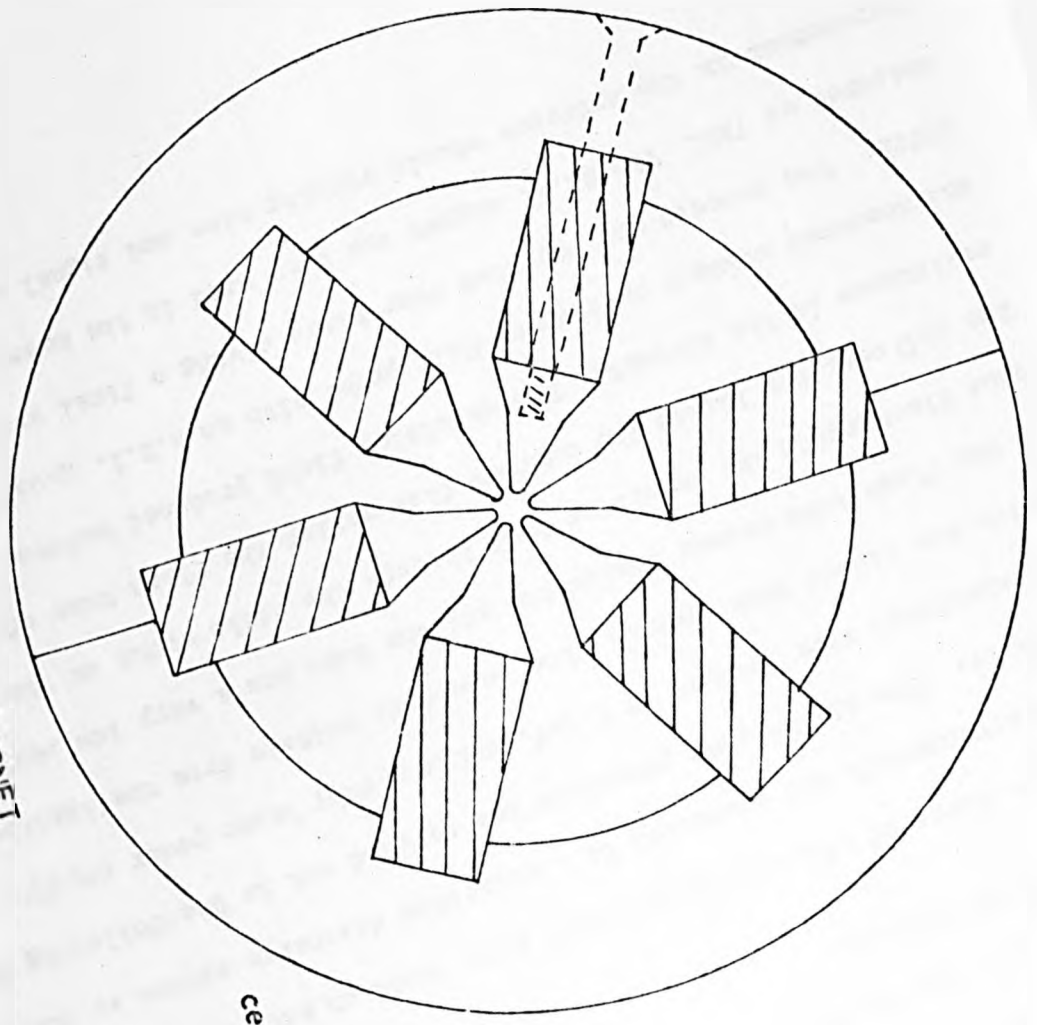

END VIEW OF 6 POLE MAGNET

FIG.(4.5)

halves together, one of the plates having a collar to locate the magnet in position in the bellows of the vacuum system. The end plates have holes drilled into them in order to facilitate pumping to remove hydrogen which is not focused. This avoids the unnecessary scattering of suitably state selected atomic hydrogen atoms. The magnet focusing region is $\frac{1}{8}$" in diameter ($2r_o$) and $3\frac{1}{2}$" long (ℓ_o); the diameter of the yoke is 3". The Mk.II was assembled and magnetised as follows.

Five turns of 16s.w.g. copper wire were wound on each pole and the whole wiring arrangement was connected to a capacitor discharge system as shown in fig.(4.6). The discharging procedure was carried out in the following manner. The capacitors were charged to 2.5kV. using a ruby laser power supply. The switch was closed then opened. The secondary voltage from the ignition coil to the flash tube causes ionization and the tube has a very low resistance, thus discharging the capacitor bank through the coils wound on the pole pieces. The 2kΩ resistor limits the current flow whilst the flash tube offers a low resistance in the circuit. The resulting field produced between the pole tips was measured using a calibrated Hall probe with an A.E.I. gauss meter type FB22B. The process was repeated four times giving a final average field measured as 7kG. The Mk.II magnet was then used in the maser with immediate improvement in the hydrogen atomic ringing time and signal amplitude.

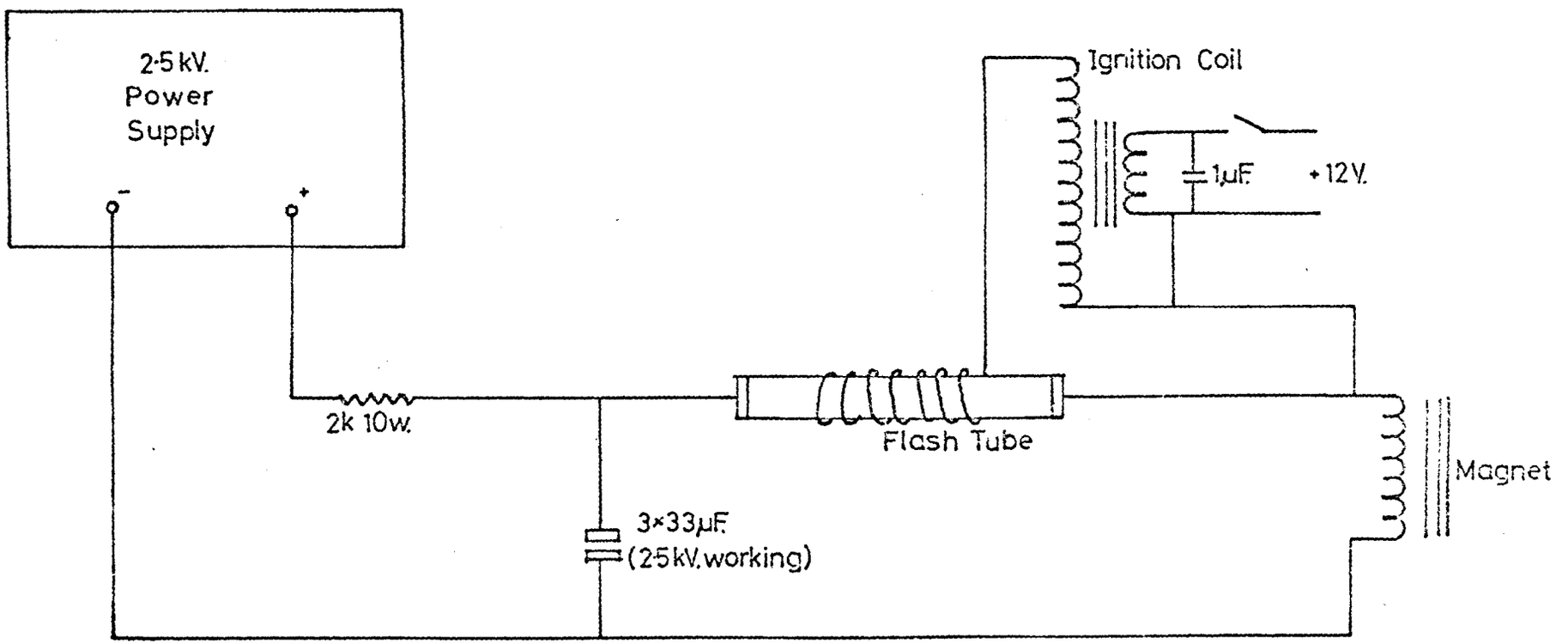

Capacitor Discharge Arrangement for Magnetization of Mk.II State Separator

FIG.(4·6)

Storage Vessel for Atomic Hydrogen

The quartz storage bulb has two functions; it forms a base for the Teflon film and is also a part of the vacuum system (hence the wall thickness must be such that it can withstand atmospheric pressure). This is the storage vessel for the atomic hydrogen, which has been state selected. The bulb material is chosen as quartz, the dielectric properties of this material ensuring that the Q of the microwave cavity is not appreciably deteriorated when the vessel is placed in position in the centre of the cavity resonator. Teflon is chosen as being one of the best coating materials; the probability of recombination of hydrogen atoms on a Teflon surface is nearly 10^{-5} (21). The bulb is of 150mm diameter and has a 150mm long, 30mm diameter neck by means of which it protrudes through the cavity base plate (see fig. (4.7)) and into the upper vacuum chamber where it is sealed in position using a dry-viton 'O'-ring assembly. The wall thickness of the vessel is 1mm.

Several attempts were made at putting a good continuous Teflon coating on to the inner surface of the bulb. The technique employed successfully was as follows.

Any previous unsuccessful coating was removed using a 48% HF solution. The mechanism here being that the HF diffuses through the Teflon and etches away the surface immediately below it, hence lifting the coating which can then be washed out with water. The bulb is rinsed with distilled water and dried by blowing dry nitrogen into it. A few c.c. of equal parts du Pont F.E.P. Teflon, product code 120 (this is a mixed polymer of fluropropylene) and distilled water is poured carefully into the bulb (frothing occurs if the solution is poured too quickly). The bulb is rotated until all the inner surface is wetted by the solution. The vessel is inverted and the excess liquid allowed to drain for about one hour. The coating is dried by gently blowing water vapour free nitrogen into the bulb. When dry the Teflon aquires

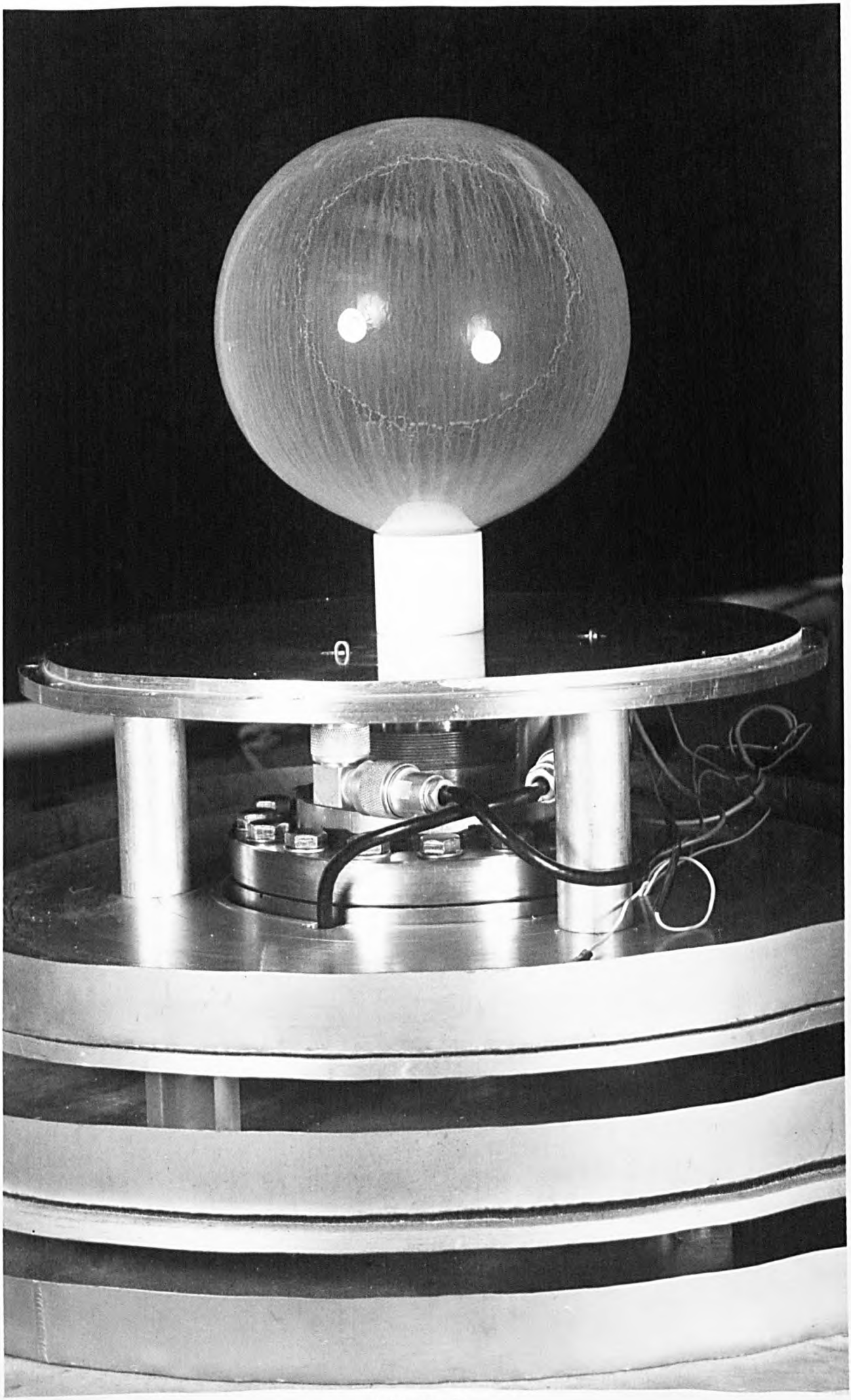

a chacteristic translucent or milky colour. At this stage the surface is carefully inspected for uncoated regions, pits, cracks and other defects. If there is any doubt about the quality of the coating it is much easier to remove at this point in time than after baking.

If the coating is satisfactory, the vessel is placed into an oven and the temperature raised slowly to 380°C over a period of about three quarters of an hour. The temperature is held at 380±10°C for one hour and the oven is switched off. The vessel is allowed to cool down slowly inside the oven. The resulting Teflon film is strong and clear and may only be removed using 48% HF as mentioned previously or by a solution which is 20% HF and 20% HNO_3. As a check on the quality and continuity of the baked-on Teflon, the 'water drop' test is employed. For this a small drop of water is placed in the bottom of the bulb and the vessel is rotated so that the water drop moves freely over the coated surface without wetting it in any place. If this can be done, the coat is assumed to be perfect and free from uncoated areas and cracks. If the coat is faulty the actual coating process can be repeated without removing the previous layer, until an acceptable Teflon surface is produced.

The neck of the vessel is tapered inwards at the point where it joins the bulb and it is in this position that a Teflon plug (see fig. (4.8)) is placed. The plug (with hole) is used to give an acceptable storage time, $\bar{\tau}$ for atoms entering the quartz bulb. The length and inside diameter of the hole in the plug determine the flow rate of atoms from the bulb. The storage time may be varied by simply inserting plugs with holes of differing length and cross-sectional area. The average storage time $\bar{\tau}$ of atoms in a spherical vessel of radius R admitting a beam through an aperture in a thin wall is equal to (18)

$$\bar{\tau} = \gamma^{-1} = \frac{16\pi R^3}{3A_e\bar{v}} = \frac{4V_b}{A_e\bar{v}}$$

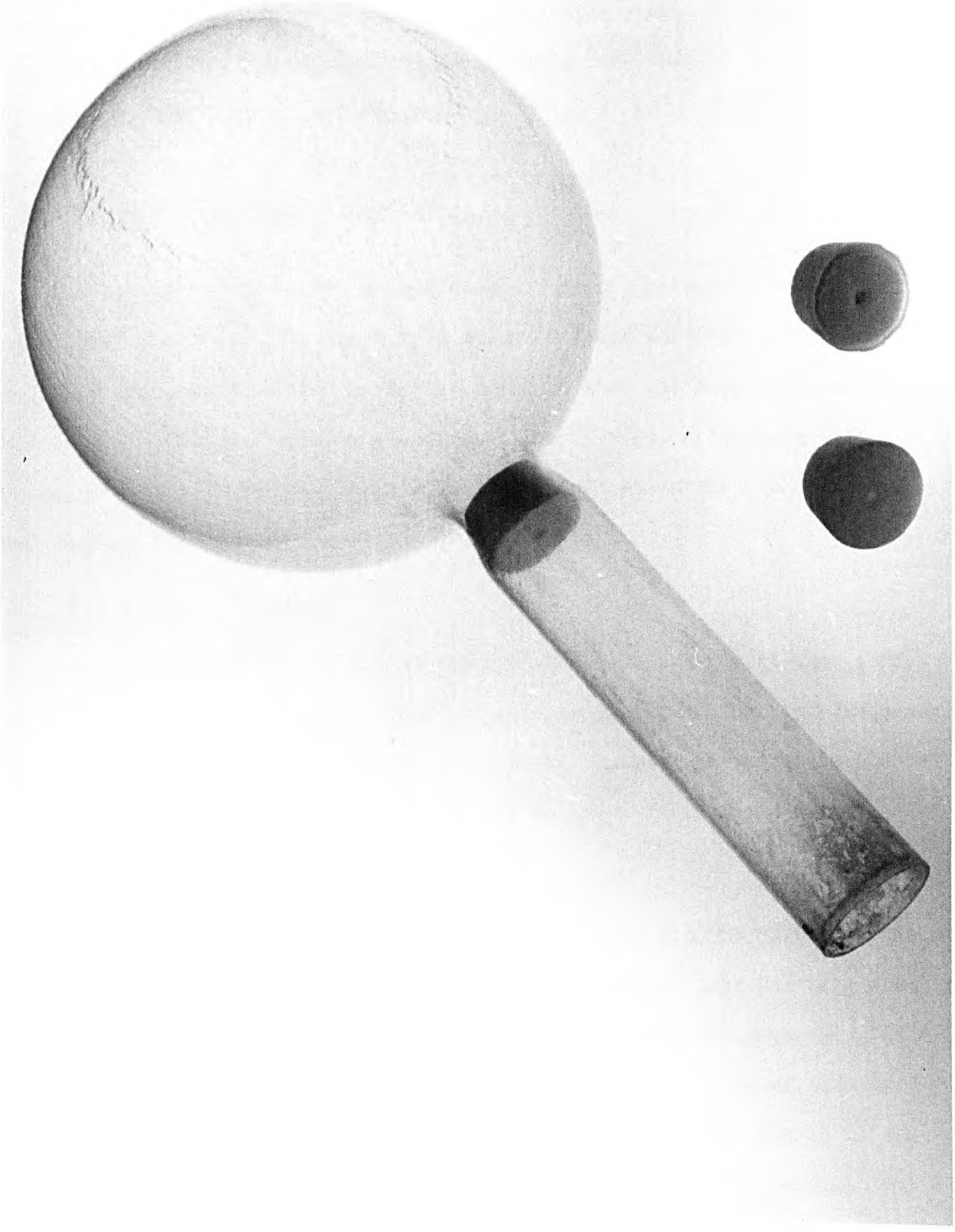

V_b is the volume of the storage bulb, A_e is the area of the exit aperture and $\bar{v}$ the mean velocity of atoms in the bulb.

Owing to the fact that the cross-section of the beam at the place where it enters the vessel is circular, it is possible to enhance the atomic flux admitted to the bulb by increasing its entrance area. However, in order not to diminish the lifetime of stored atoms, it is necessary to insert a duct of increased length in the entrance to the vessel. The average storage time of the atoms with a duct in place is then

$$\bar{\tau} = \frac{2R^3 l_d}{\bar{v} r^3}$$

l_d is the duct length and r its radius.

The coating of the storage bulb does cause an uncertainty in the unperturbed frequency of the hydrogen maser (23) and different samples of nominally the same materials have been found to give different frequency shifts (24). From a frequency standard point of view, this means that any frequency measurements must include an independent measurement of the wall shift due to the storage vessel coating material.

Cavity Resonator.

The cavity resonator of the atomic hydrogen beam maser must have a high Q and stable natural frequency; the magnetic component of the high-frequency field must have an anti-node at the place where the storage vessel is located in the cavity. These requirements are best met by a cylindrical cavity resonator tuned to the TE_{011} wave mode.

The TE_{011} mode is used because of its high Q value and the fact that the magnitude of the longitudinal component of the magnetic field for this mode is a maximum along the cavity axis; on moving away from the axis this field decreases according to a $J_c'(\delta r)$ law. Another important property of this mode is the absence of axial components of current on the lateral surface of the cavity and of radial components on its end surfaces. For this reason, the

surface discontinuities run along rather than across the microwave current flow lines (eg. between the surface of the cylinder and the base) and do not result in a deterioration of the cavity Q due to moveable plates and tuning plungers.

The cylindrical microwave cavity is made from aluminium. One advantage of using aluminium is the possibility of thermally tuning the cavity due to the large temperature coefficient of the metal, this being approximately fifty times that of fused silica which is a more frequently used material. Other desirable attributes of the aluminium cavity are: it is electrically opaque, has a reproducible high Q, is mechanically stable and the good thermal conductivity assures uniformity of temperature over the cavity. The cavity body is machined from extruded tubing and the end plates from sheet aluminium. The inside diameter of the resonator is 274mm. and the maximum physical length 256mm. The lower end plate is fixed and has two coupling loops each halfway along a radius line from the centre of the cavity through the loops. The axial position of the upper end plate is adjustable; coarse tuning is by turning three threaded pillars (see figs. (4.9) and (4.10)) with 24 threads per inch, which move the plate in or out and fine tuning by moving an 8mm. diameter aluminium tuning rod in or out by means of a micrometer screwthread.

The material from which the cavity body was made has a possibility of 0.5% of Fe present. This could produce extraneous magnetic fields in the region of the storage bulb. The effect of these fields can manifest itself in various ways. For example, the presence in the cavity resonator of a magnetic field whose vector is not directed along the axis of the resonator makes it necessary for the solenoid to produce a high H field since the vector of the resultant field must be orientated along the cavity axis to satisfy selection rules for the atomic resonance. The presence in the magnetic field

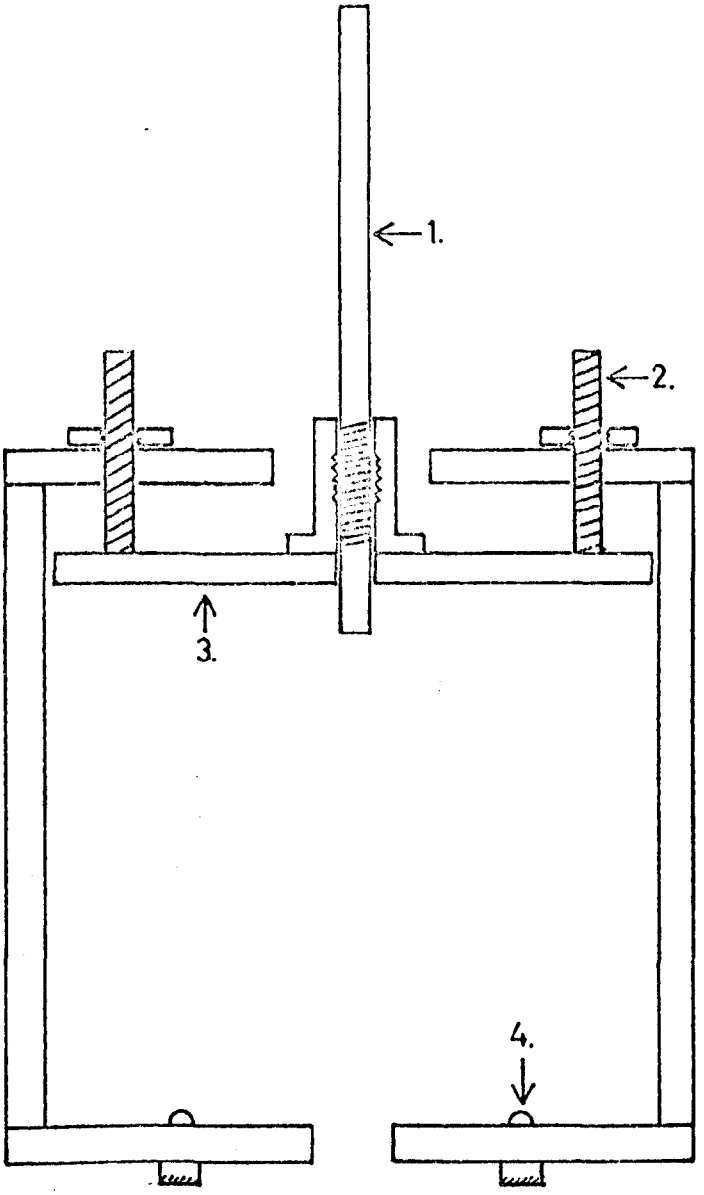

1. Fine Tuning Rod
2. Coarse Tuning Pillars
3. Top Plate
4. R.F. Coupling Loops

MICROWAVE CAVITY

FIG. (4.9)

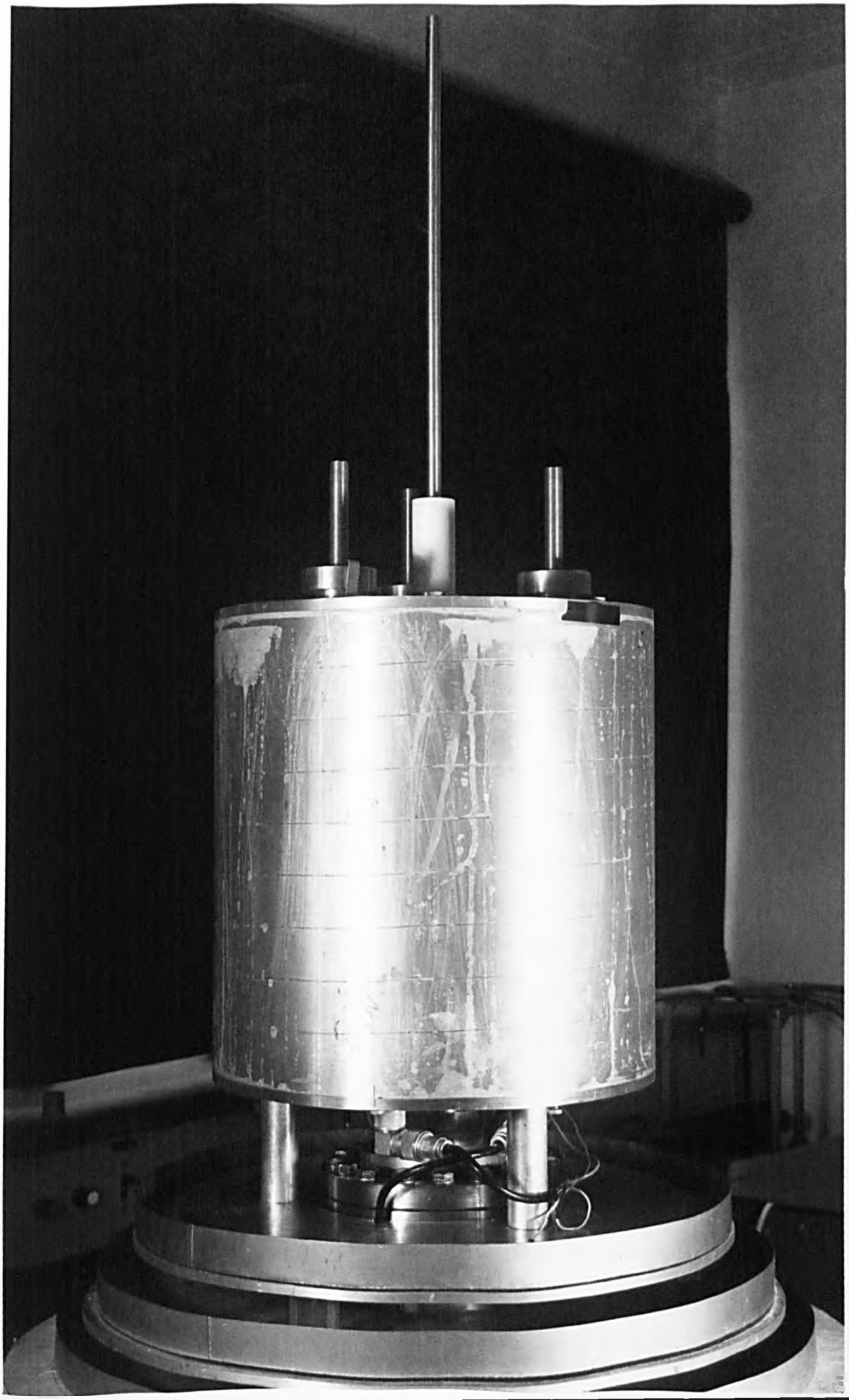

of an inhomogeneous transverse component in space causes a depletion of atoms in the working level of the maser due to the stimulation of Zeeman transitions $\Delta F=0$, $m_F=\pm 1$. This is due to the fact that atoms moving in the bulb experience a time varying magnetic field at such a frequency, and in the required direction, as to induce the transitions between the upper quantum states.

The determination of the operational mode for the cavity was done by observation of the cavity response to a transmitted signal, frequency modulated over the range 1.3 to 2.0 GHz. Without the storage bulb in place the TE_{011} resonance was identified, with the cavity at its maximum physical length, at a frequency of 1433.2 MHz. The resonant frequency of a right circular cylinder is given by

$$\nu = \frac{c}{2\cdot 54}\left[\frac{1}{4}\frac{n^2}{L^2} + \left(\frac{u_{\ell mn}}{\pi}\right)^2 \frac{1}{D^2}\right]^{1/2}$$

where c is the velocity of light in free space, $u_{\ell mn}$ is the m^{th} root of the Bessel function $J_\ell'(u)$, n is dependent on cavity mode designation, $TE_{\ell mn}$, as are ℓ, m and L, D are the length and the diameter of the cavity in centimeters respectively. Application of this equation to the cavity indicates that the cavity should be 306mm. long electrically to give the TE_{011} resonance at 1420.4 MHz (the maser frequency). With the storage bulb in place the TE_{011} mode was found to be at 1420.4 MHz with the cavity length measured to be 260mm. This would indicate that the presence of the 150mm. diameter quartz storage bulb increased the electrical length of the cavity by 46mm. This increase is of the same order of magnitude as that observed by other experimenters with similar size bulbs (18), (24). The absence of modes other than the TE_{011} in the cavity at the maser frequency indicates that the cavity design is successful in the suppression of unwanted modes and that the frequency degeneracy of the TE_{011} and TM_{111} modes has been lifted by the presence of the storage bulb in the cavity. Measurement of the cavity Q factor indicates a loaded Q factor of 3×10^4, which is an acceptable value if maser oscillation is to be achieved. Details of techniques used to measure Q are

given in the appendix. The input cavity coupling loop has an area of $1cm^2$ and the output loop $1.5cm^2$. Since the oscillation level of the maser is not substantially affected by heavy loading on either of the loops, the cavity can be assumed to be somewhat under-coupled.

If the hydrogen maser is to be used as a frequency standard, one of the important factors affecting the frequency stability and reproducibility is the stability of the natural frequency of the cavity resonator. The change in oscillation frequency $\Delta\nu_o$ when the cavity is detuned by $\Delta\nu_c$ is given by

$$\Delta\nu_o = \Delta\nu_c Q_c / Q_\ell$$

Q_ℓ is the line Q, Q_c is the cavity Q. For a cavity of coefficient of thermal expansion α ($=24\times10^{-6}/^\circ C$ for Al) the cavity frequency shift is

$$\Delta\nu_c = -\alpha T_c \nu_c$$

T_c is the temperature change in the cavity, $\Delta\nu_c/\nu_c = 24\times10^{-6}/^\circ C$ so

$$\Delta\nu_c \simeq 35kHz/^\circ C$$

But for a maser frequency stability of 1 part in 10^{13} it is necessary for $\Delta\nu_c \simeq 7Hz$ and hence a temperature stability of

$$\Delta T_c \simeq 2\times10^{-4}{}^\circ C$$

In the initial experiments to obtain maser oscillation the cavity was uncompensated for thermal drifts and the assumed temperature stability was $0.1^\circ C$ short term, hence the estimated frequency stability due to this factor is of the order one part in 10^{10}. To obtain a frequency stability of use in standards work, the aluminium cavity must be carefully thermally controlled.

Frequency shifts due to air pressure and humidity changes in the cavity may be reduced by evacuating the cavity and facility for this at a later stage has been designed into the apparatus.

The possibility of thermally tuning the cavity which is one of the advantages of using such a metal cavity, was foregone in the first instance since the time delay between adjustments due to the large thermal capacity of

the cavity would be unacceptable for initial setting up of the maser system as a whole.

Magnetic Shields and Field Coils

For hydrogen maser frequency standard application it is desirable to reduce the ambient magnetic field at the storage bulb to as low a value as possible owing to the quadratic field dependence

$$\nu = \nu_0 + 2750 H_0^2 \ (Hz) \qquad H_0 \text{ in oersted}$$

of the maser oscillation frequency between the levels $(F=1, m_F=0)$, $(F=0, m_F=0)$. This is most satisfactorily achieved by the use of magnetic shields (see fig. (4.11)). In the ideal case these completely eliminate the external magnetic field and then a small uniform static field is applied by passing a current through a solenoid placed around the cavity and inside the innermost shield (see fig. (4.12)).

The low field limit at which the maser oscillates is determined by either (i) the magnitude of the residual field which may lie in an undesirable direction or (ii) the gradients in the residual field which can cause undesirable atomic transitions as the Zeeman frequency between the F=1 sub-levels is reduced. In (i) the applied H_0 field must be large enough so that the oscillating magnet is substantially parallel to the oscillating field. Even then owing to (ii) gradients of the residual transverse field can cause relaxation due to random motions of the atoms. This relaxation rate is uniform at low fields and drops rapidly when the Zeeman frequency exceeds the mean 'rattle frequency' of atoms in the bulb. Consequently, large gradients neccessitate a relatively large uniform applied field.

In the maser system the external fields are shielded by the use of concentric magnetic shields. The configuration used is as follows: the shielding comprises three coaxial cylinders fabricated from 0.081cm. Mu-metal. The innermost of 38cm. diameter, 66cm. long; the middle 43cm. diameter,

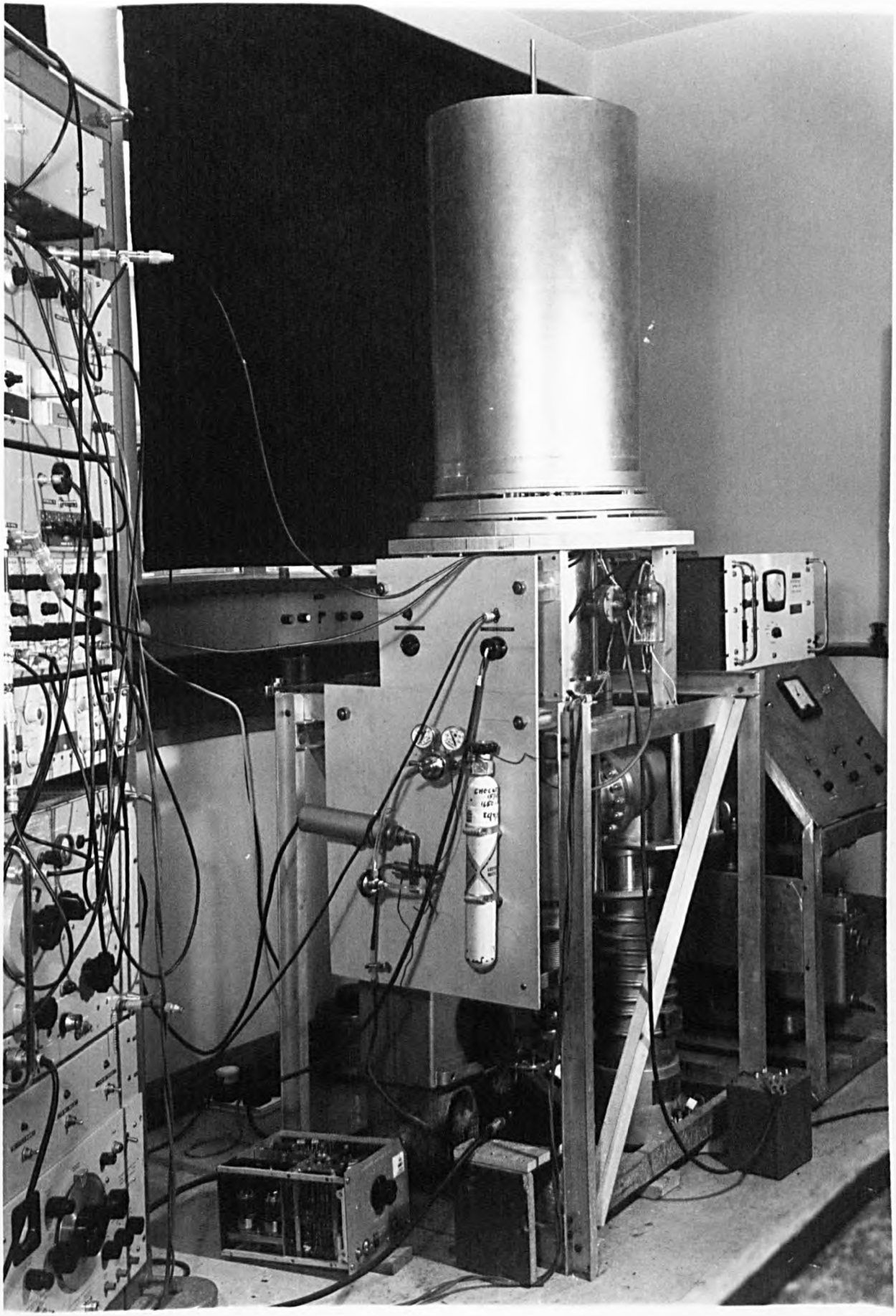

FIG.(4.11)

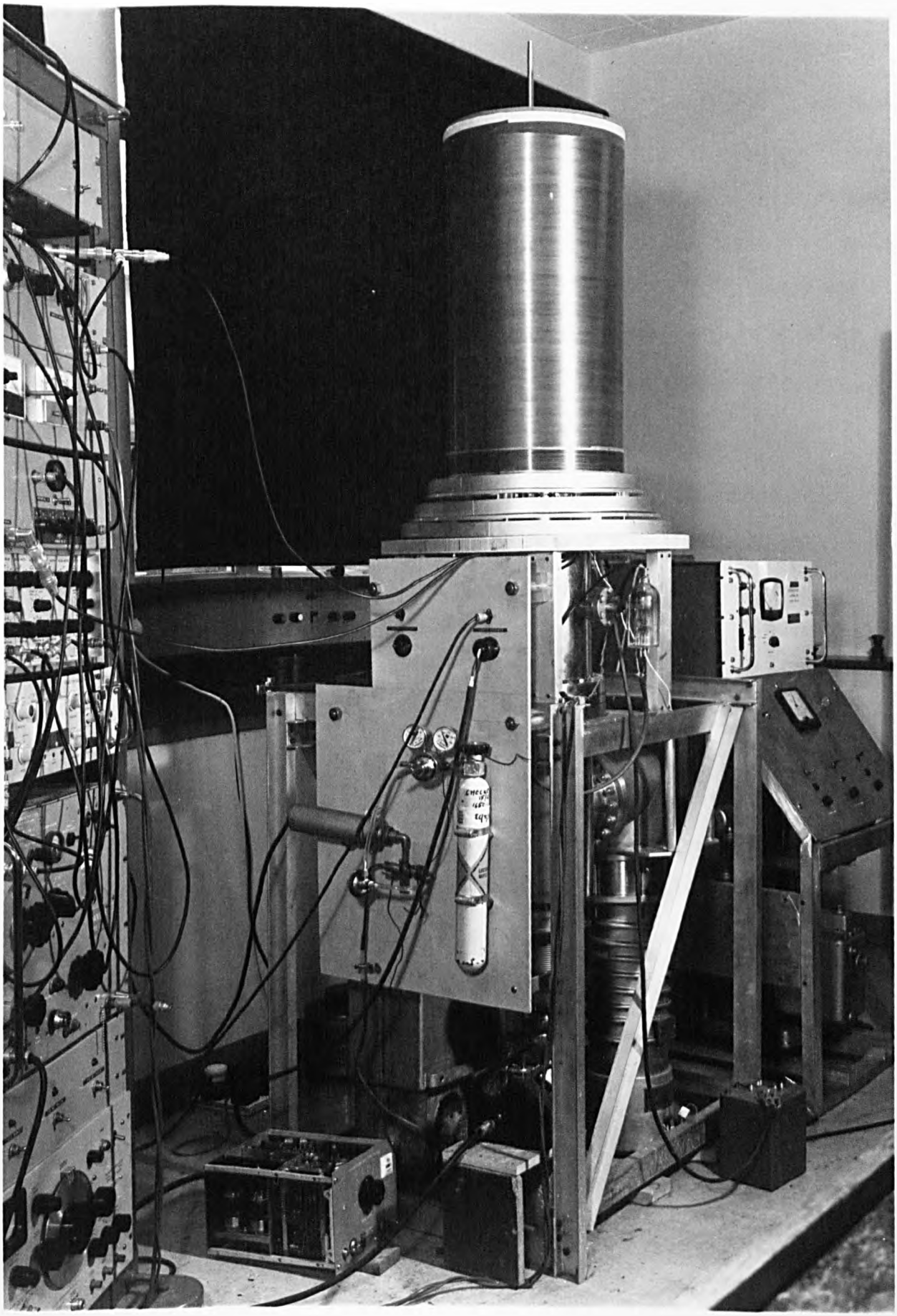

FIG.(4.12)

74cm. long and the outer 48cm. diameter, and 81cm. long. All the shields have end caps spun from Mu-metal and drilled to take coaxial cables. The shields and lids were annealed by the manufacturer (Magnetic Shields Ltd. Kent). The static H_0 field is applied by means of a solenoid of 1000 turns of 22 s.w.g. wire wound on a 30cm. inside diameter plastic former of 1 meter in length and placed coaxially around the cavity. A correction coil of 50 turns of 26 s.w.g. wire is wound over the main coil near to the bulb entrance at the lower end of the shields. This correction coil is used to reduce the effect of stray magnetic fields in the vicinity of the apertures in the shield lids, for the bulb neck and cables.

Proper demagnetization is essential to the shield's performance. To achieve this a 50 Hz demagnetizing current is passed through the main H_0 coil The current is brought up rapidly to 6A. by means of a 'Variac' and then reduced slowly to zero over a period of about one minute.

The chief function of demagnetization is to raise the flux level in the shields to a point at which the shield magnetization can favourably reorientate itself. Although large permanent fields are effectively reduced by the shields, they are much less effective in reducing small variations of magnetic field since the incremental permeability drops off rapidly at low field strength. Addition of extra shields does not help matters since the shielding contribution is counterbalanced by the decrease in permeability of the inner shields which now operate at lower magnetic flux.

ELECTRONIC DETECTION SYSTEM

Introduction

The elctronics associated with the maser may be divided into two sub-systems. The first delivers a pulse to the microwave cavity input at the maser frequency, which is approximately 1420.4 MHz. The second sub-system is a double super-hetrodyne receiver for the detection of the extremely low

HYDROGEN MASER DETECTION SYSTEM –

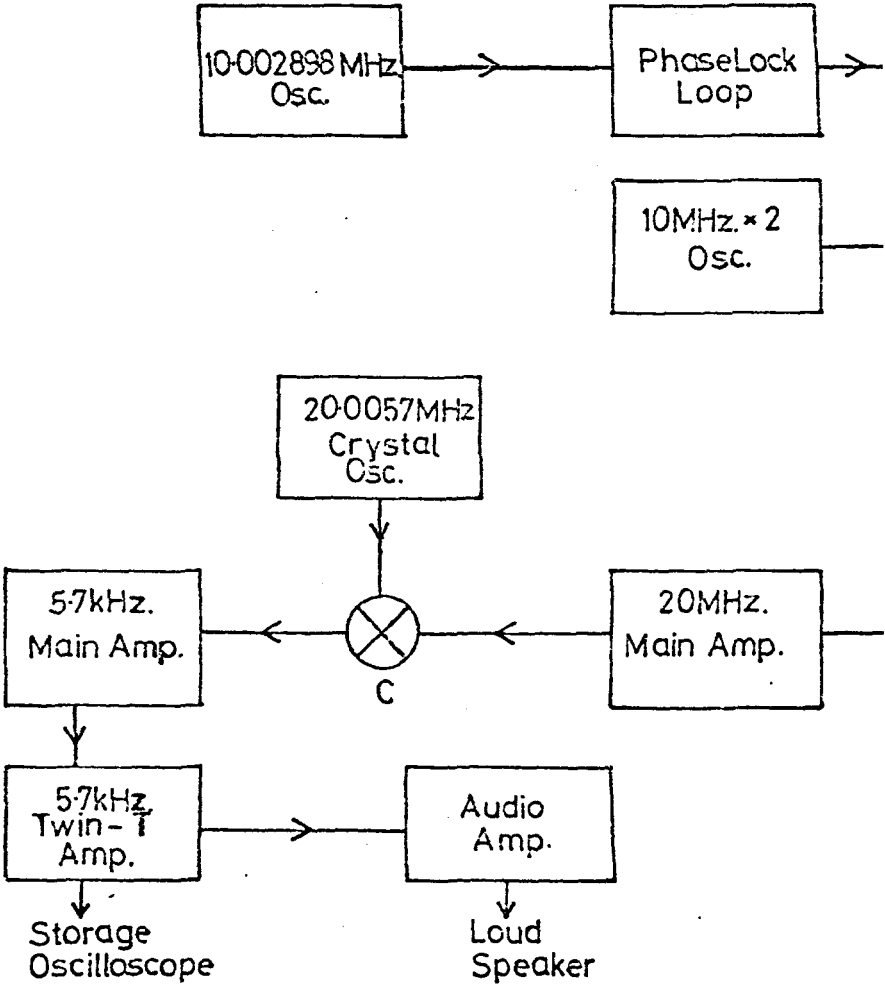

FIG(4·13)

- BLOCK DIAGRAM

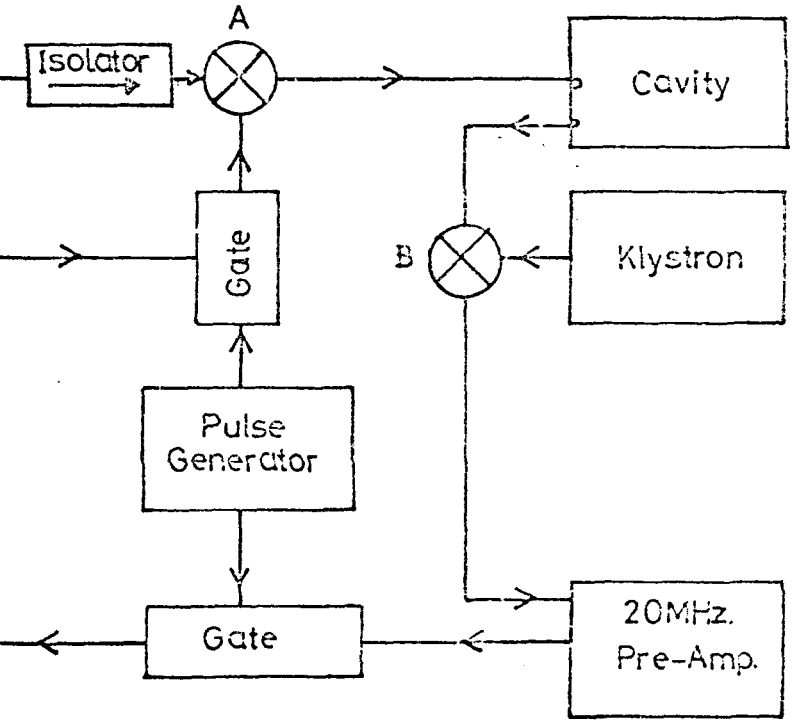

level maser signals ($\sim 10^{-15}$ W.) fromthe cavity output.

The system is shown in block form in fig. (4.13). Fixed attenuators and microwave tuning elements are not shown. The signal applied to the cavity input is produced by mixing two signals at A. One at 1400 MHz is derived from a Bradely 510X transistor oscillator, phase-locked to a stable 10 MHz crystal oscillator. The other is a pulsed 20 MHz signal obtained by doubling the output from another 10 MHz crystal and switching using a Hatfield MD4 modulator. The pulsed 1420 MHz upper side-band from the coaxial mixer (Radiall type R6390), is accepted by the cavity which acts as its own filter and rejects the lower 1380 MHz side-band. The isolator is used in the position shown to protect the 510X unit, which appears very sensitive to output load change.

The maser output signal is mixed, in the microwave mixer at B, with a 1400 MHz signal from the klyston oscillator (Saunders Type CT478), the 20 MHz side-band from B passing to the input of the I.F. stage pre-amplifier. This latter unit and the main I.F. amplifier are separated by an MD4 modulator switching device, which serves to 'silence' the I.F. amplifiers for the duration of the high level pulse applied to the cavity and thus avoids saturation of the receiver. The amplified I.F. signal is mixed at C with a signal from an STC crystal oscillator (type 4013) to give a resultant output from the mixer at 5.7 kHz. This passes into the first low frequency amplifier and then into a narrow band twin-tee amplifier tuned to 5.7 kHz. The narrow band output is displayed on a storage oscilloscope and simultaneously, after audio amplification, is fed into a loudspeaker.

As there are several signals in the region of the I.F. frequency and since the overall gain of the system is of the order of 150 dB, efficient screening of the individual units is essential.

20 MHz Pre-Amplifier

This is a low noise stage to amplify the very small signal from the microwave mixer B. The pre-amp. is tuned with a series tuned circuit to 20.0 MHz but does not need a very narrow bandwidth because the main 20.0MHz amplifier is more sharply tuned and this governs the overall bandwidth of the I.F..

The circuit (fig. (4.14)) has the following main characteristics. The BF115 is a low noise r.f. transistor giving optimum noise figure from a source impedance of a few hundred ohms. The two balanced mixer crystals have effective resistance of a few hundred ohms at the I.F frequency and so they can be a.c. coupled directly to the transistor base without an impedance matching transformer, and the overall noise figure will still be low. The TI407 stage is a standard x10 current amplifier giving nearly zero output impedance at the emitter of the second transistor. It is thus easy to match the output of the pre-amp. to 50Ω by using the series 47Ω resistor. (Units in the electronic receiver have been standardized to have 50Ω inputs and output. All interconnecting coaxial cables have characteristic impedances of 50Ω.).

The amplifier has a centre frequency of 20 MHz, a bandwidth of 1 MHz and an overall gain of 30dB.

Bradley 510X Phase-Lock System

This uses as its reference source, an HCD 35 crystal oscillator with a frequency of 10.002898 MHz and short term frequency stability of 1 part in 10^9 The amplified 10 MHz from the crystal is fed into the 50Ω input on the 510X unit, where it is internally multiplied to 100 MHz and this signal is then used as the referance to phase lock a transistor oscillator to 1400.40575 MHz. The power output at 1.4 GHz is 200mW into 50Ω

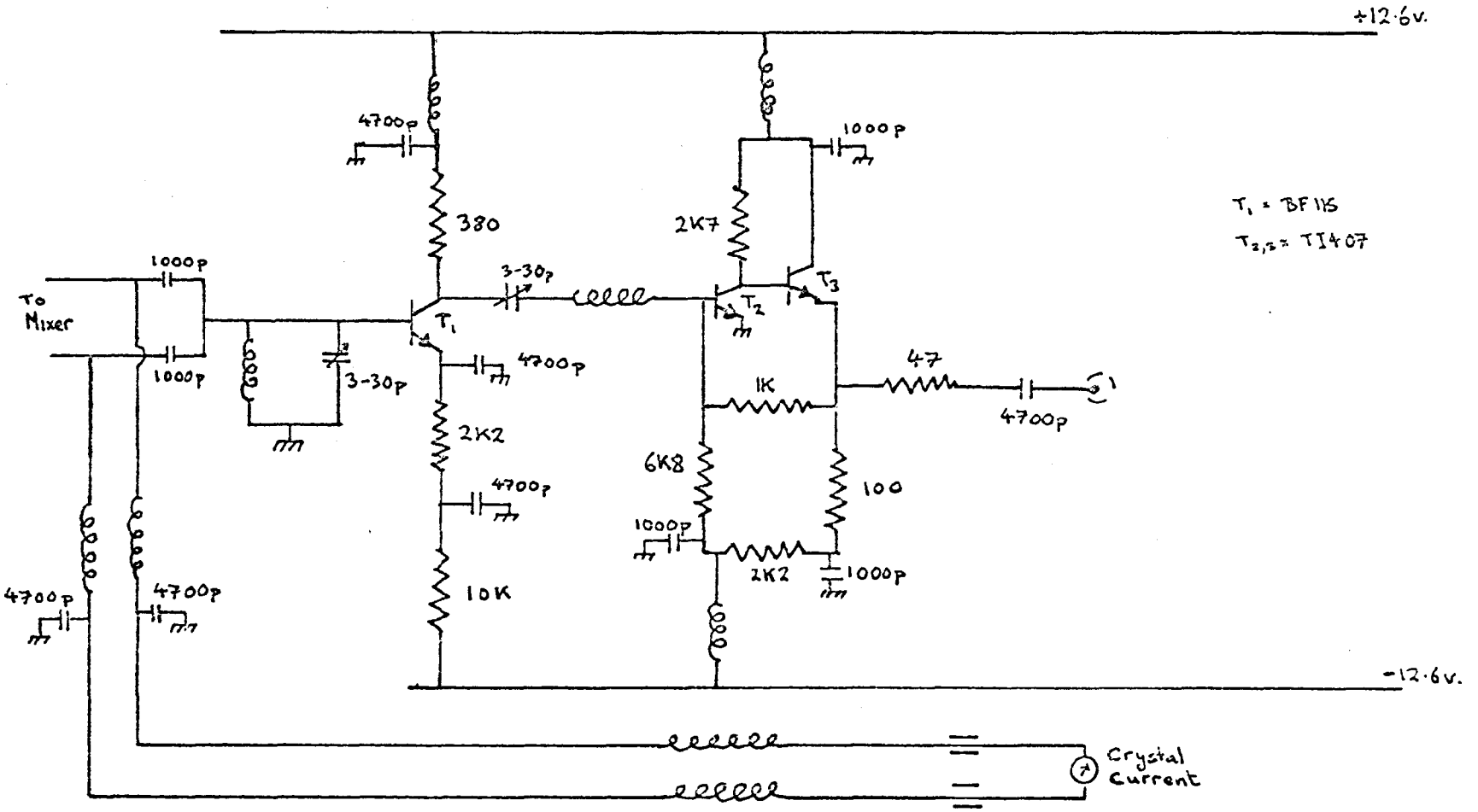

20MHz. Pre-Amplifier

FIG.(4·4)

20 MHz Main Amplifier

A circuit, originally designed at Jodrell Bank, (fig. (4.15)) is used for this application. The amplifier has low noise characteristics and input and output impedances matched to 50Ω. The bandwidth of the unit governs the overall I.F. bandwidth, the value being 600 kHz centred at 20 MHz. The gain of the stage is 45dB.

Balanced Mixer

The high frequency mixer, B, used is an MEL type L493/2, L-band mixer for use in the frequency range 1.0 to 1.7 GHz. A typical noise figure at the crystal current used (i.e. 1mA) is 6dB. This gives an overall receiver noise figure of 6dB plus the pre-amplifier noise figure. By using well matched crystals, noise figures below 6dB can be obtained from the mixer. For receiver applications the use of the port marked No.2 on the mixer as the input achieves the best matching of the device to the amplifier chain.

Amplifier Silencing Unit

The switching modulator between the pre and main 20 MHz amplifiers is normally kept in an 'on' condition with a +ve d.c. bias applied by means of a resistive potential divider network from the amplifier d.c. rail. By applying a suitable -ve d.c. level to null this 'on bias', the modulator may be switched to the 'off' condition and hence no r.f. signal passes into the main amplifier. By applying a negative pulse at the same time and of equal duration to that applied to the cavity, the I.F. can be switched off or 'silenced' whilst the cavity pulse is on. Hence saturation of the receiver, due to direct transmission and detection of the cavity pulse, is avoided. A semi-schematic diagram of the arrangement is shown in fig. (4.16).

20.0057 MHz Oscillator

This produces the signal which is mixed with the amplified 20 MHz I.F. in the MD4 modulator at C in the block diagram. The output from the modulator

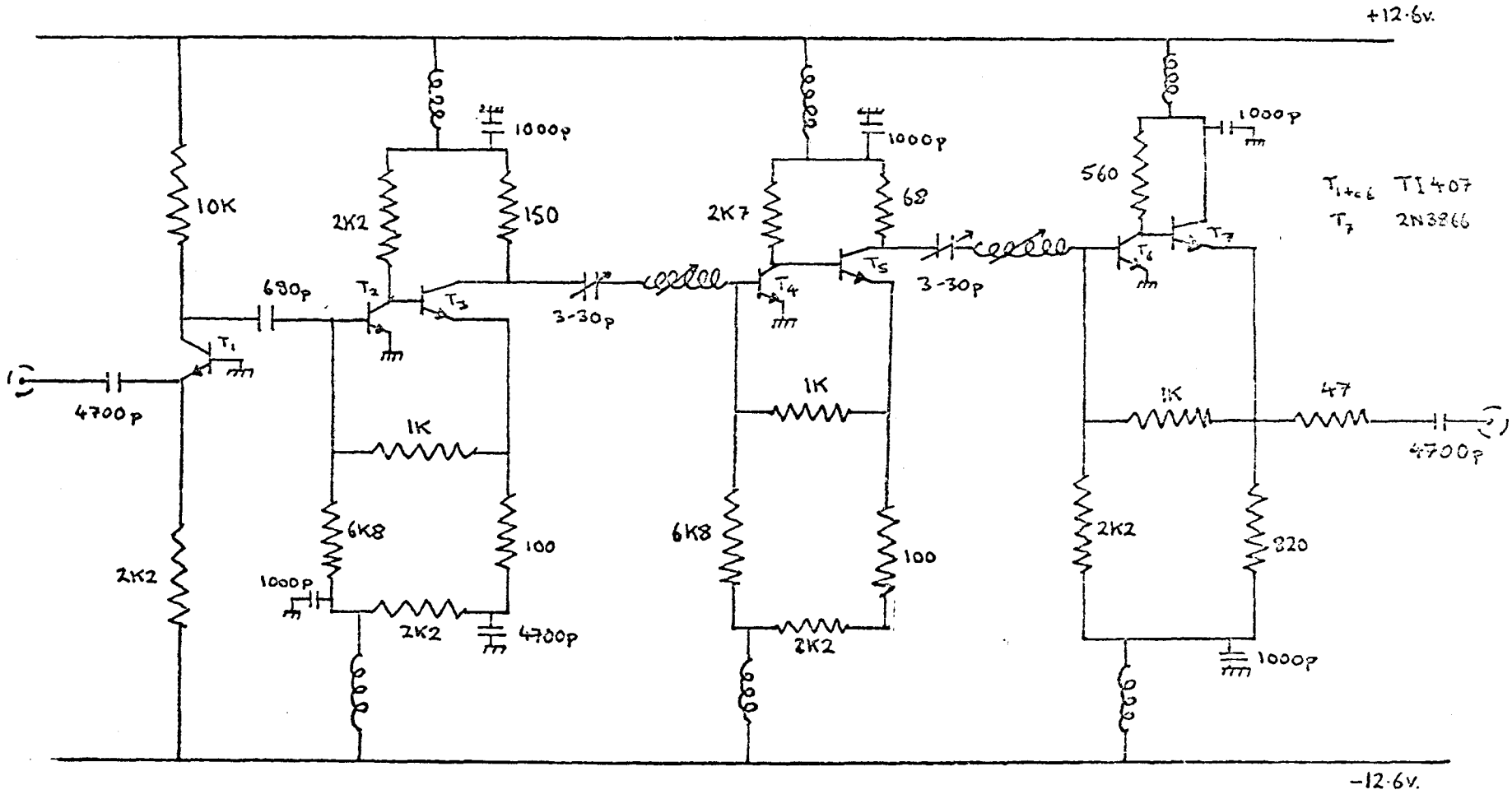

20MHz. Main Amplifier

FIG(415)

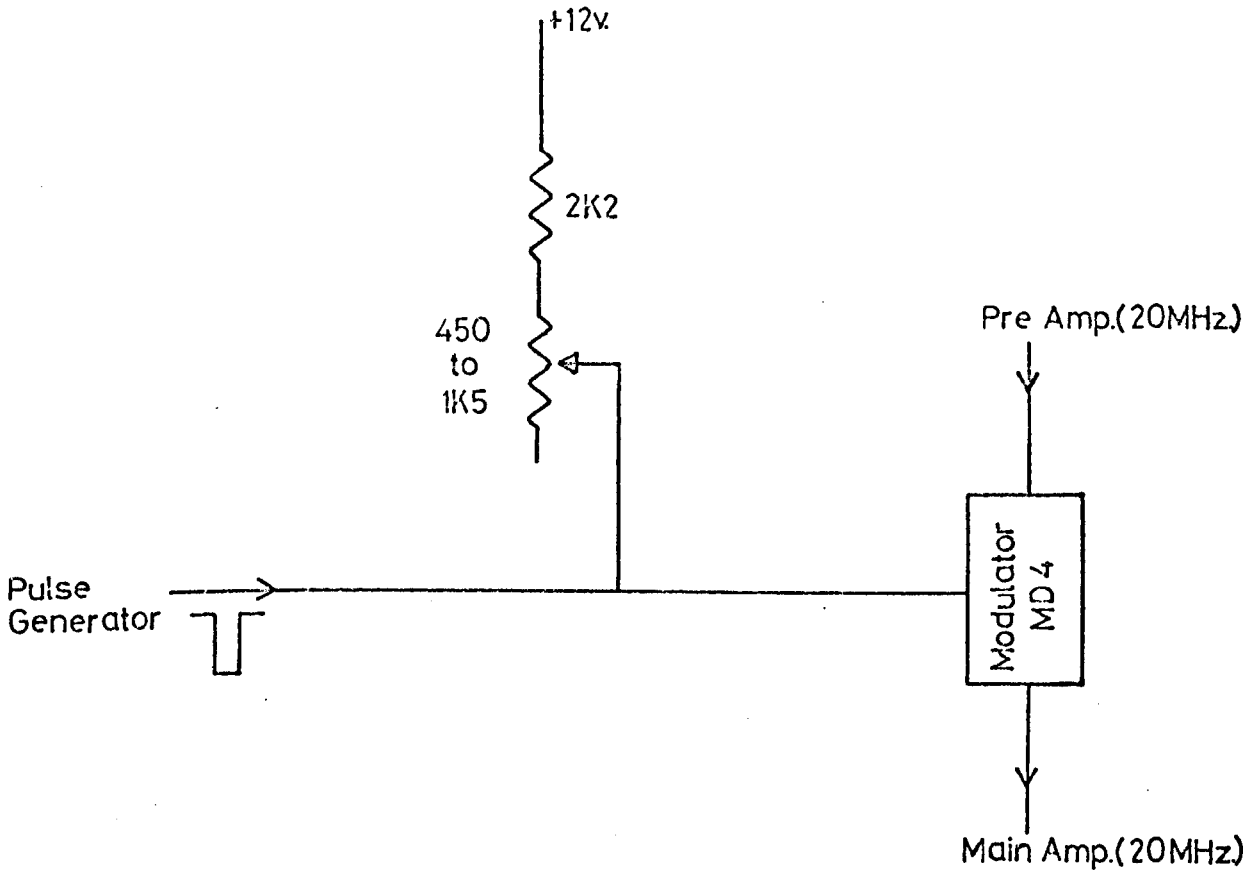

I.F. Amplifier Silencing Unit

FIG.(4.16)

then passes into the first stage of low frequency amplification. The oscillator circuit is shown in fig. (4.17).

10 MHz x2 Amplifier/Doubler

The requirement here is to produce a 20 MHz signal to mix with the 1400 MHz from the phase locked loop. The 1400 MHz signal has a short term variation of 10 Hz and hence to have comparable stability from the 20 MHz requires a stability of 5 parts in 10^7. The basic oscillator used is a 10 MHz HCD 70 with short term frequency stability of the order 1 part in 10^7

The 20 MHz is produced by doubling the amplified output from the HCD 70. Amplification of the oscillator output is necessary in order to obtain a useful level of 20 MHz signal from the doubler circuit. The output from this device is fed into the gate as shown on the block diagram. A circuit is given in fig. (4.18).

Low Frequency Amplification Unit

The complete amplifier unit at 5.7 kHz comprises a filter, low noise broadband amplifier, narrow band amplification stage and audio output stage.

The sideband frequencies fromthe MD4 modulator are 5.7 kHz and 20.0057 MHz. The latter sideband is removed by means of the initial filter which short circuits the r.f. to earth whilst passing the 5.7 kHz signal into a low noise amplifier with broad band-pass characteristics. The very narrow band feature of the complete low frequency unit is produced using a twin-tee feedback amplifier with the tuned filter at 5.7 kHz in the feedback loop. The filter has maximum impedance (theoretically ∞) at the resonant frequency and hence gives the unit maximum gain at this point. The output from the twin-tee amplifier is fed directly to an oscilloscope and simultaneously into the audio amplifier from which it passes to a loud speaker. This allows both visual and audible observation of the maser signal.

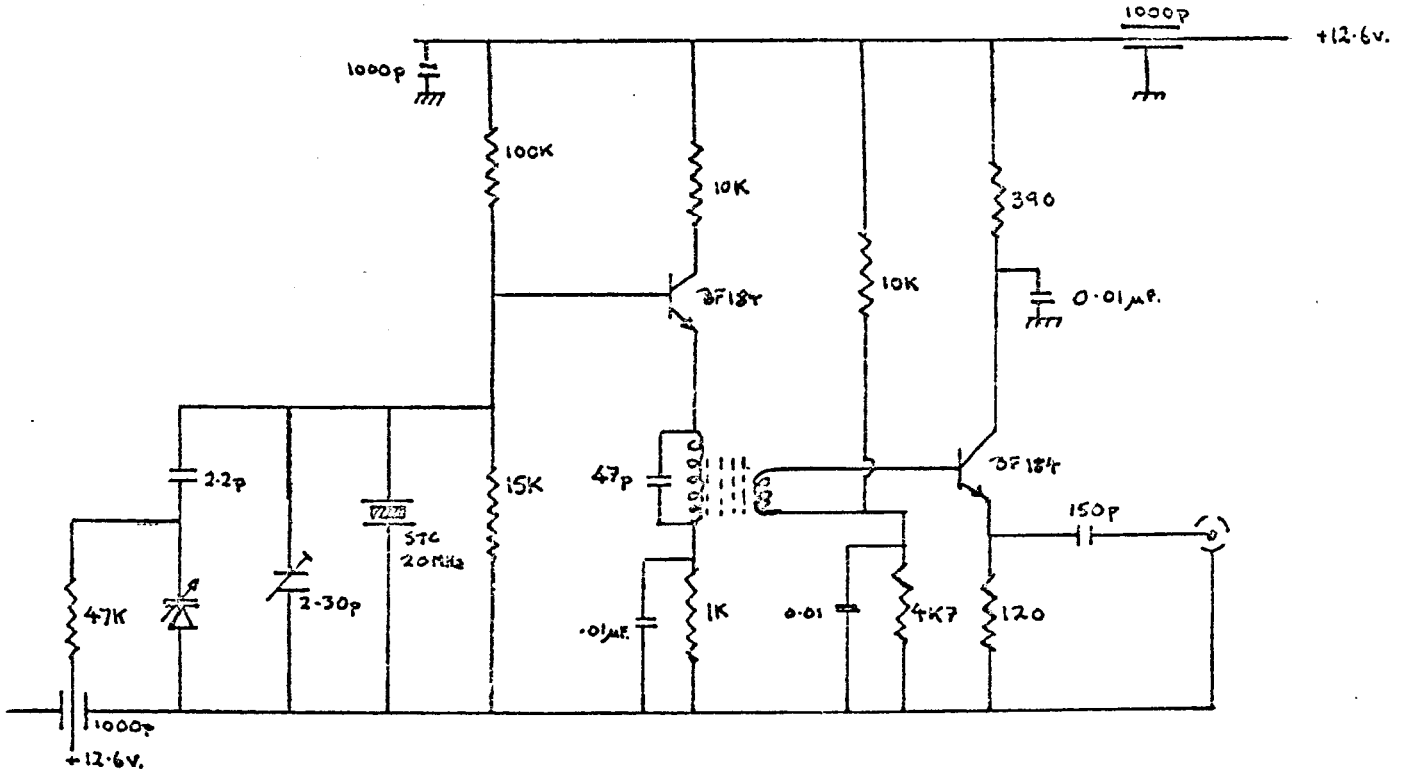

20MHz.- Offset Oscillator

FIG. (4·17)

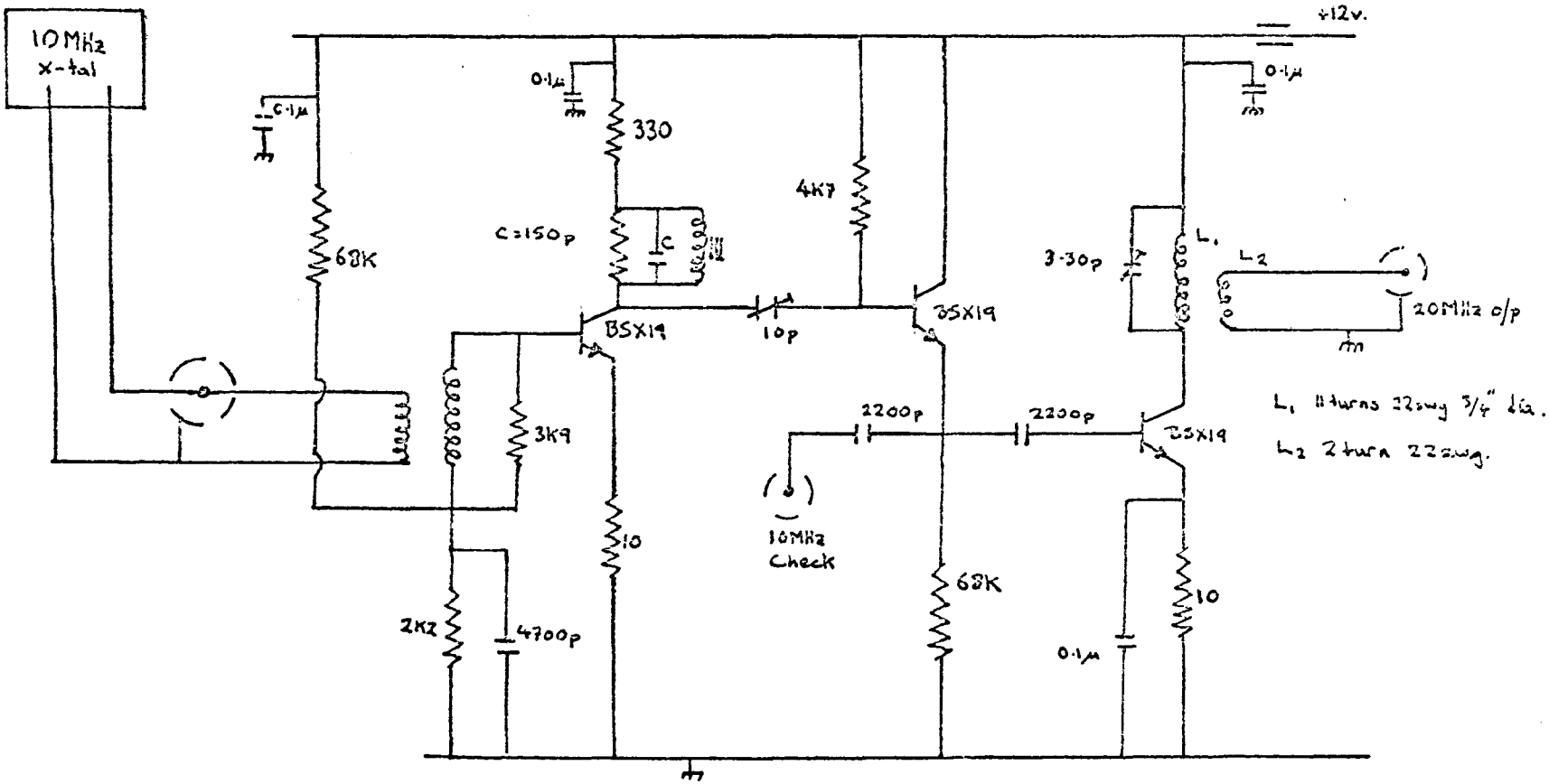

10MHz.×2 (Doubling Unit)

FIG.(4·18)

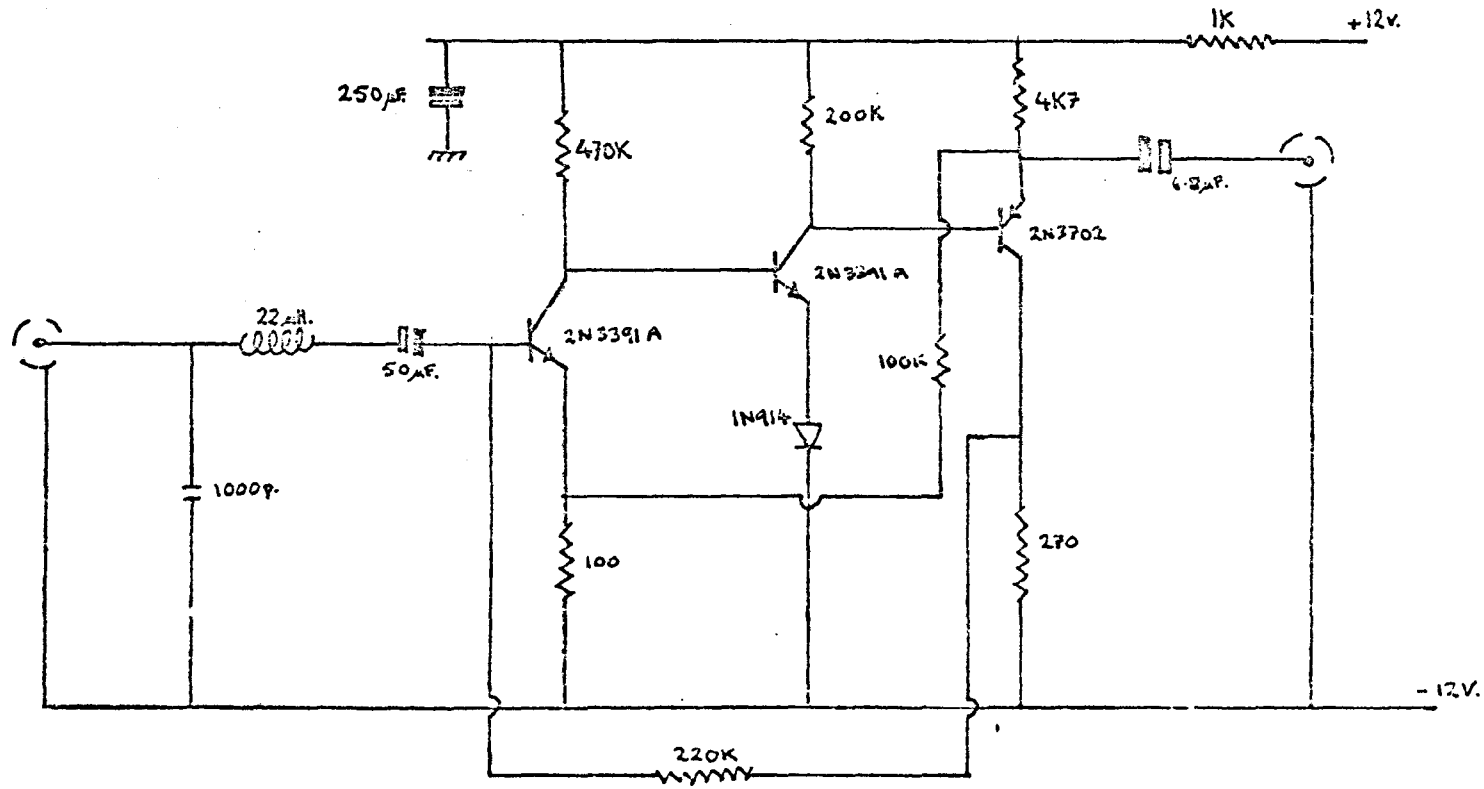

Low Noise A.F. Amplifier

FIG. (4·19)

5·7 kHz. Tuned Amplifier

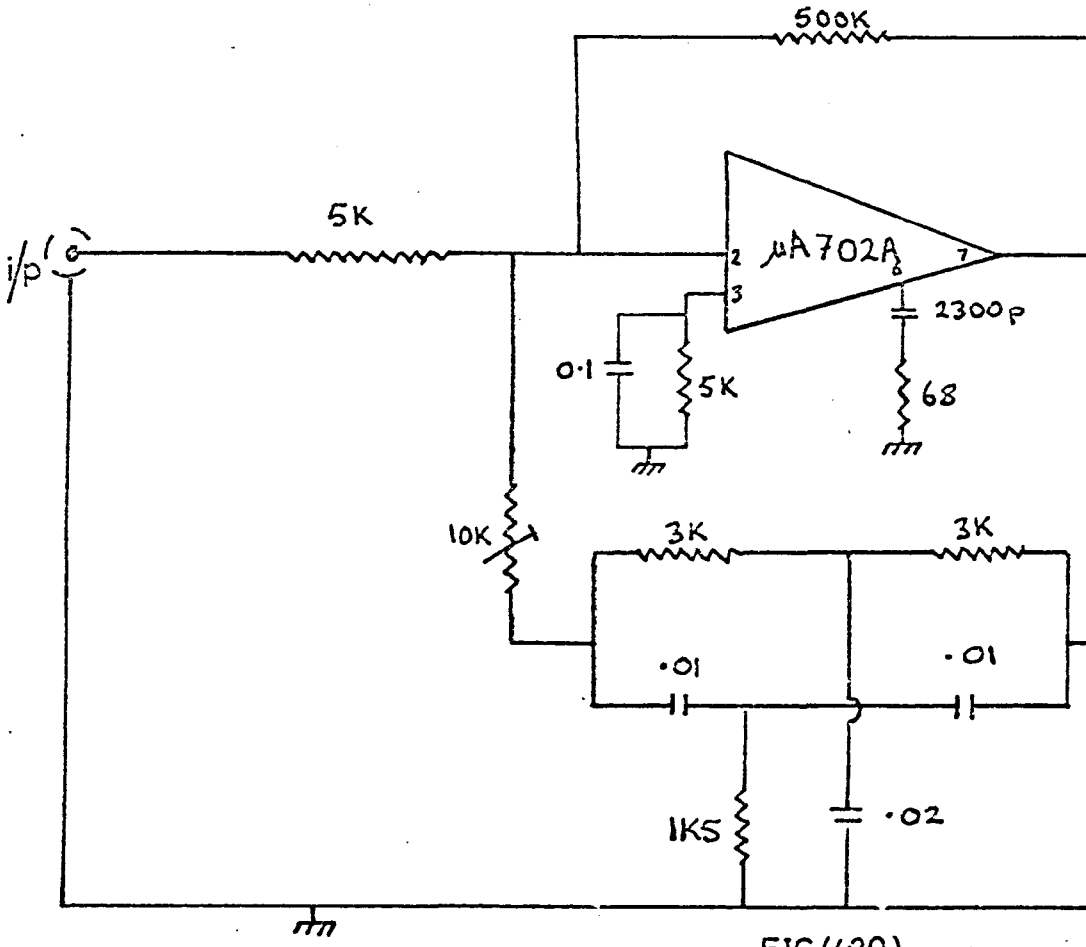

FIG.(420)

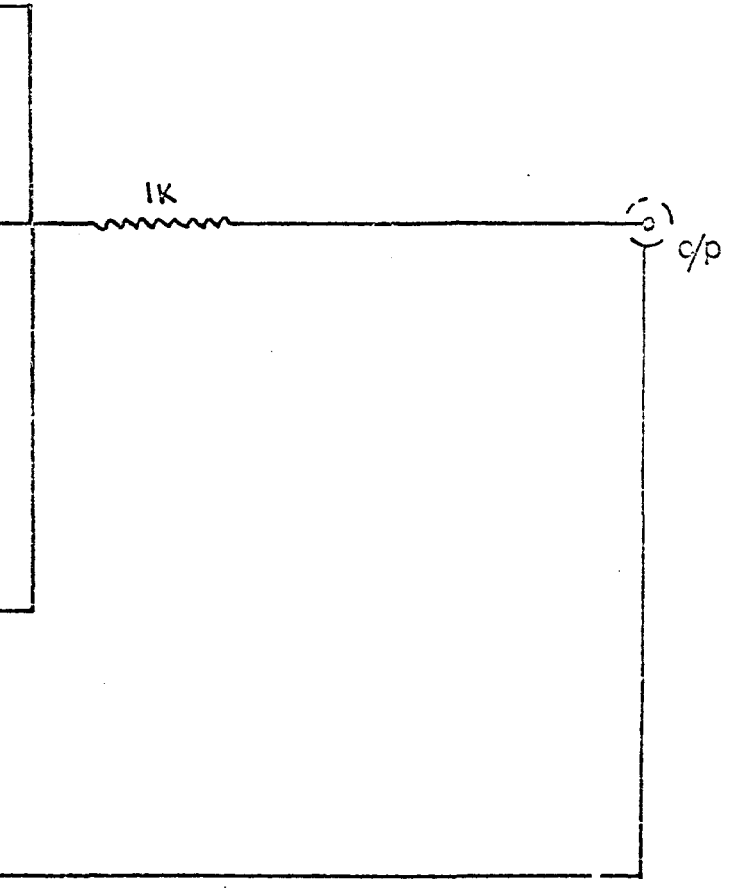
1K
o/p

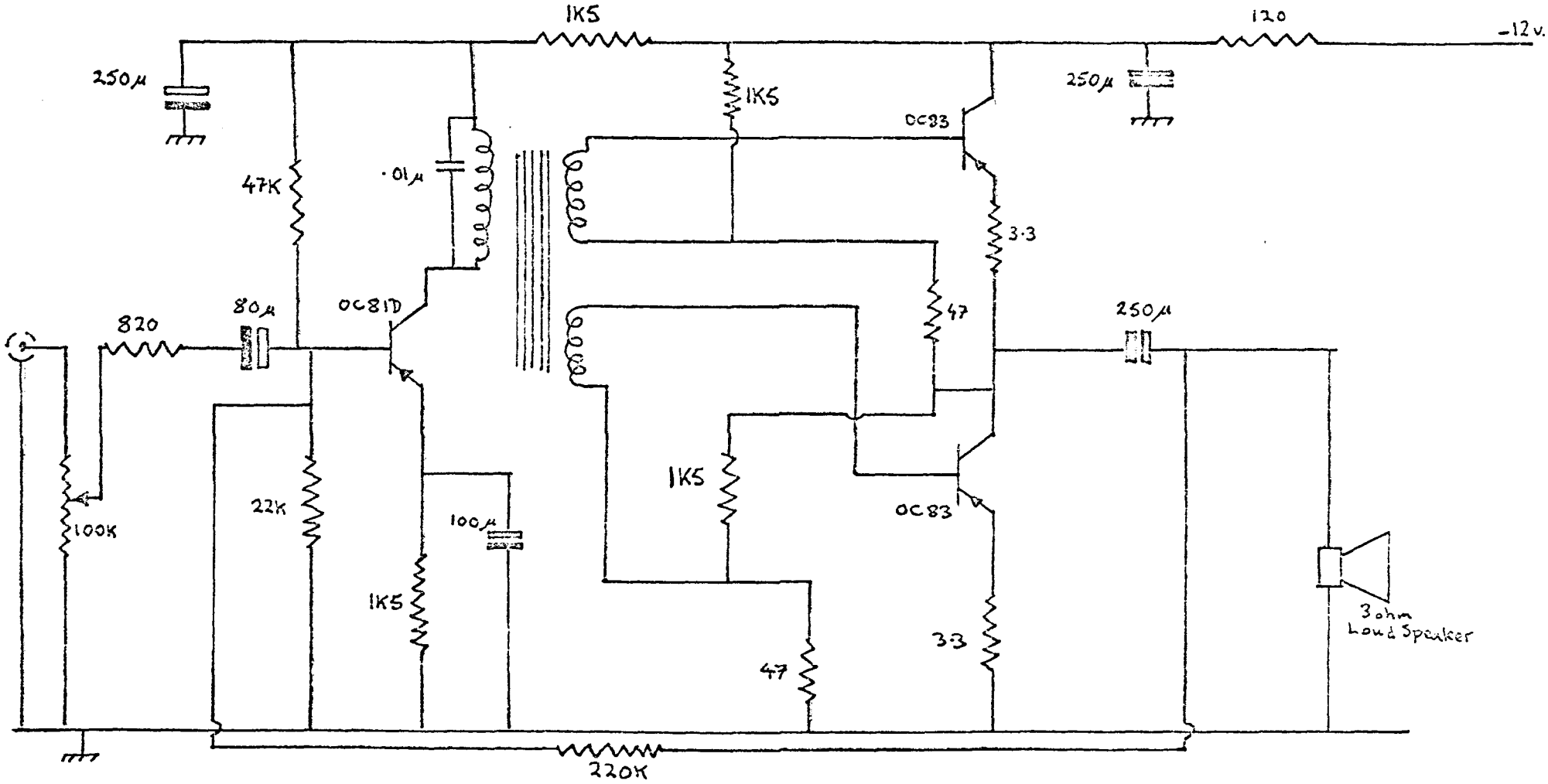

Audio Output Stage

FIG(421)

The overall gain of the complete low frequency unit is 80dB and the bandwidth, which is governed by the twin-tee filter is 143 Hz centred on 5.72 kHz. Circuit diagrams are shown in figs. (4.19,20,21).

CHAPTER FIVE

MASER PERFORMANCE BELOW AND ABOVE OSCILLATION THRESHOLD

Form of the Observed Maser Ringing Signals

Following the application of a pulse of radiation to the resonant cavity at the atomic transition frequency, the resultant coherent spontaneous emission signal, due to the hyperfine transition of atoms in the ground state of atomic hydrogen, varies in power according to

$$P_s = \frac{\omega \mu_o^2 \eta I^2 Q_L^2}{2\pi V \gamma^2 Q_c} e^{-2\gamma t}$$

where ω is the cyclic emission frequency of the hydrogen atoms, μ_o the Bohr magneton, I the intensity of the atomic beam admitted to the storage vessel Q_L the loaded cavity Q, η the cavity filling factor ($\eta \simeq 3$), Q_c the cavity coupling Q, v the volume of the cavity and γ the total atomic relaxation rate.

By measuring the charateristic damping time of the radiation signal from the hydrogen maser, it is possible to determine the relaxation rate of the hydrogen atoms and their lifetime in the excited state. As mentioned in Chapter 1, there are several processes contributing to the relaxation of atoms in the storage vessel. The total relaxation rate γ is comprised of the sum of the independant relaxation rates γ_i.

$$\gamma = \sum_i \gamma_i$$

A block diagram of the experimental arrangement for the observation of the coherent spontaneous emission signals is shown in fig. (4.13). The trigger pulse applied to the I.F. amplifier blanks this unit and avoids its saturation whilst the excitation r.f. pulse is applied to the cavity.

If atoms in the state $F=1, m_f=0$ are present in the cavity a signal of power P_s is detected at the receiver after termination of the r.f. pulse to the cavity. The signal voltage at the receiver input is of the form

$$u(t) = u_o e^{-\gamma t}$$

Assuming there are no non-linear distortions of the signal (this is true at low power levels) the shape of the signal envelope displayed on the oscilloscope screen is described by the function

$$A(t) = A_0 e^{-\gamma t}$$

Measuring the time in which the amplitude of this signal decays by a factor $1/e$, it is possible to determine the radiative lifetime, γ^{-1}, of the atoms in the storage vessel. The error in this measurement is of the order 10%.

Relation Between the Observed Signals and the Magnetic Dipole Moment per Unit Volume:

In the pulse experiment, the atoms are stored in the microwave cavity for the order of 1 sec. and are put into a radiating state by a pulse of a few milliseconds (6ms. is typical) duration. Whilst this pulse is on, an atom makes over 100 transits of the storage bulb. Each atom sees the same time-averaged driving field and attains the same level of excitation. A uniform oscillatory magnetic moment per unit volume, M(t), is established.

Following the pulse, the atoms give up energy to the cavity at the rate

$$-\frac{dU}{dt} = \int \underline{M}' \cdot \frac{d\underline{H}}{dt}\, dV \qquad (5.1)$$

where U is the internal energy of the atoms (U does not include the energy of the electromagnetic field. It is identical, apart from an additative constant, to the expectation value of the hydrogen spin Hamiltonian), H' is the magnetic field, and integration is over the volume of the storage bulb.

In the maser, with a constant magnetic field along the axis (the Z-axis) of a cylindrical cavity operated in a TE_{on} mode.

$$\underline{M}' = M(t) \sin \omega t\, \underline{k}$$

$$\underline{H}' = H(r,t) \cos \omega t\, \underline{k}$$

where $\underline{k}$ is a unit vector along the Z-axis. $\underline{M}(t)$ and $\underline{H}(r,t)$ are slowly varying functions of time: the fractional changes in these quantities in the time it takes an atom to cross the bulb and in an oscillation period are roughly 10^{-4} and 10^{-9} respectively. If dU/dt is averaged over several oscillation periods, then

$$-\left(\frac{dU}{dt}\right)_{av.} = -\frac{\omega M(t)}{2}\int H_z(r,t)\, dV = -\frac{\omega M(t)}{2}\langle H_z \rangle_b(t) V_b$$

where $\langle H_z \rangle_b(t)$ is the magnitude of the Z-component of the oscillating magnetic field at the time t averaged over the volume of the bulb V_b.

Let the energy stored in the cavity field be W and the loaded cavity Q be Q_L. The rate of dissipation of energy in the cavity walls and the detection system is $\frac{\omega W}{Q_L}$. As atoms leak out of the bulb or undergo relaxation collisions and as field energy is dissipated, the energy stored in the field changes in time thus;

$$\frac{dW}{dt} = -\frac{\omega W}{Q_L} - \left(\frac{dU}{dt}\right)_{av.} \qquad (5.2)$$

W is a function of $\langle H_z \rangle_b$ since H_z and the magnitude of the total oscillatory field, H, are related by the cavity mode and equations, and

$$W = \frac{1}{8\pi}\int H^2 dV = \frac{1}{8\pi}\langle H^2 \rangle_c V_c \qquad (5.3)$$

where $\langle H^2 \rangle_c$ is the square of the magnitude of the total oscillatory magnetic field averaged over the volume of the cavity, V_c. The average quantities $\langle H_z \rangle_b^2$ and $\langle H^2 \rangle_c$ are related by a number which depends on the cavity mode. For convenience the ratio is defined as

$$\eta = \langle H_z \rangle_b^2 / \langle H^2 \rangle_c \qquad (5.4)$$

Substituting equations 5.3 and 5.4 into 5.2 and rearranging, one obtains

$$\frac{d\langle H_z \rangle_b}{dt} = -\frac{\omega}{2Q_L}\langle H_z \rangle_b - \frac{2\pi\eta V_b \omega}{V_c} M(t) \qquad (5.5)$$

If the beam flux, cavity Q and decay rate, γ, are such that the maser is not close to oscillation, and the applied r.f. pulse is not too intense then M(t) is independent of $\langle H_z \rangle_b$. Equation 5.5 applies only after the pulse, once uniform magnetization M(t) has been established. If M(t) is assumed to be of the form

$$M(t) = M_0 e^{-\gamma t} \qquad (5.6)$$

where M_0 is the magnetization per unit volume at the end of the pulse, taken to be time 0, then 5.5 has the solution

$$\langle H_z \rangle_b = -4\pi\eta Q_L \frac{V_b}{V_c} M_0 e^{-\gamma t} + C e^{-\frac{\omega}{2Q_L}t} \qquad (5.7)$$

where C is an integration constant and it is assumed that $\omega/2Q_L \gg \gamma$

$$C = 4\pi\eta Q_L \frac{V_b}{V_c} M_o + \langle H_z \rangle_b(0) \qquad (5.8)$$

The second term in 5.7 is a transient solution corresponding to the ringing decay of the empty cavity. It decays with a time constant $2Q_L/\omega \simeq 10^{-5}$ sec. The current induced in the coupling loop is proportional to the radial field near the wall at one end of the cavity, which in turn is proportional to $\langle H_z \rangle_b$. Since the detector is linear, the observed signal following the transient is a direct measure of $M(t) = M_o e^{-\gamma t}$.

Equation 5.5 was solved assuming $M(t)$ independent of H_z, and that the radiation field following the pulse does not itself induce a change in the magnetic moment of a hydrogen atom. This is equivalent to the requirement that

$$\frac{\mu_o}{\hbar} \int_o^\infty \langle H_z \rangle_b(t) dt \ll \pi/2 \qquad (5.9)$$

For a pulse of length τ which has just put the atoms in the optimum radiating state

$$\langle H_z \rangle_b(0) \simeq \frac{\pi \hbar}{3\mu_o \tau} \qquad (5.10)$$

For the transient signal corresponding to the ringing of the empty cavity, the left hand side of 5.9 is

$$\frac{\mu_o}{\hbar} \int_o^\infty \frac{\pi \hbar}{3\mu\tau} e^{-\frac{\omega}{2Q_L} t} dt = \frac{\pi Q_L}{\omega \tau} \qquad (5.11)$$

For $Q_L \simeq 3 \times 10^4$ and $\tau \simeq 6 \times 10^{-3}$ sec. the inequality in 5.9 is satisfied. The requirement on the hydrogen signal is

$$4\pi\eta Q_L \frac{V_b}{V_c} M_o \frac{\mu_o}{\hbar} \int_o^\infty e^{-\gamma t} dt \ll \pi/2 \qquad (5.12)$$

or

$$4\pi\eta Q_L V_b M_o \mu_o / V_c \hbar \gamma \ll \pi/2 \qquad (5.13)$$

If the atoms have been put into the optimum radiating state,

$$M_o \simeq \eta \mu_o = I \mu_o / \gamma \qquad (5.14)$$

where n is the population density difference for the hyperfine states $F=1, m_F=0$ and $F=0, m_F=0$, I is the state selected flux density diffence of these two states and γ is the total depolarization rate. The requirement on I is then

$$I \ll \hbar \gamma^2 V_c / 8 \mu_o^2 Q_L \eta V_b \qquad (5.15)$$

which, to within a factor of 2, is just the condition that $I \ll I_{th}$ is the flux density at which the maser begins to oscillate.

Experiments Leading to Maser Oscillation

The first coherent spontaneous emission or ringing signal from the Keele maser is shown in fig.(5.1). This was a noisy low level signal of extremely short ring time. (The term 'ring time' $\tau(=\delta^{-1})$ is being used for the time taken for the signal to decay to $1/e^{th}$ of its initial amplitude). The modulation present was due to leakage, through the cavity, of the stimulating 1420MHz pulse, causing amplitude modulation of the detected maser signal. The frequency of the modulation envelope was variable and depended on the magnetic field applied to the maser region by the solenoid around the cavity. This behaviour was consistent with a fixed frequency leakage signal modulating the magnetic field dependent maser signal.

To improve the maser signal, the MkII state separator was fitted into the system. This device had a 7kG average field, measured between the pole tips of the magnet, in contrast to the rather weak average value of the MkI which was only 4kG. Maser signal amplitude and ring time improved as a result of this change. The decay times measured from oscilloscope traces were of the order 500ms. Following this result, other areas for system modifications were considered.

The Teflon plug in the neck of the storage vessel contained a duct of 5mm. diameter and 2mm. length. This allowed a relatively large flux of atomic hydrogen into the bulb and hence the hydrogen-hydrogen (H-H) spin exchange contribution to relaxation in the bulb was high. Also with such an entrance aperture, the escape rate of useful atoms fromthe storage vessel was high. It was therefore, decided to alter the dimensions of the duct in the neck. Because pumping the system down from atmospheric pressure was a problem with the R.E.F. (Radial Electric Field) pump, the change in the duct dimensions was drastic in order to effect a noticeable variation in maser performance due to this change. The entrance aperture was reduced to 2mm. diameter and the length of the duct increased to 15mm. This would limit hydrogen flux into

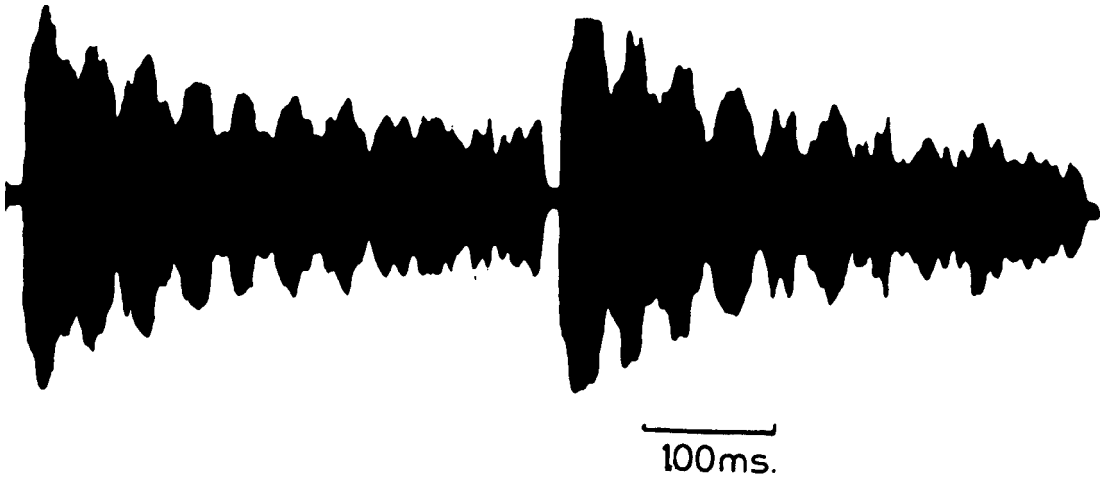

(a)

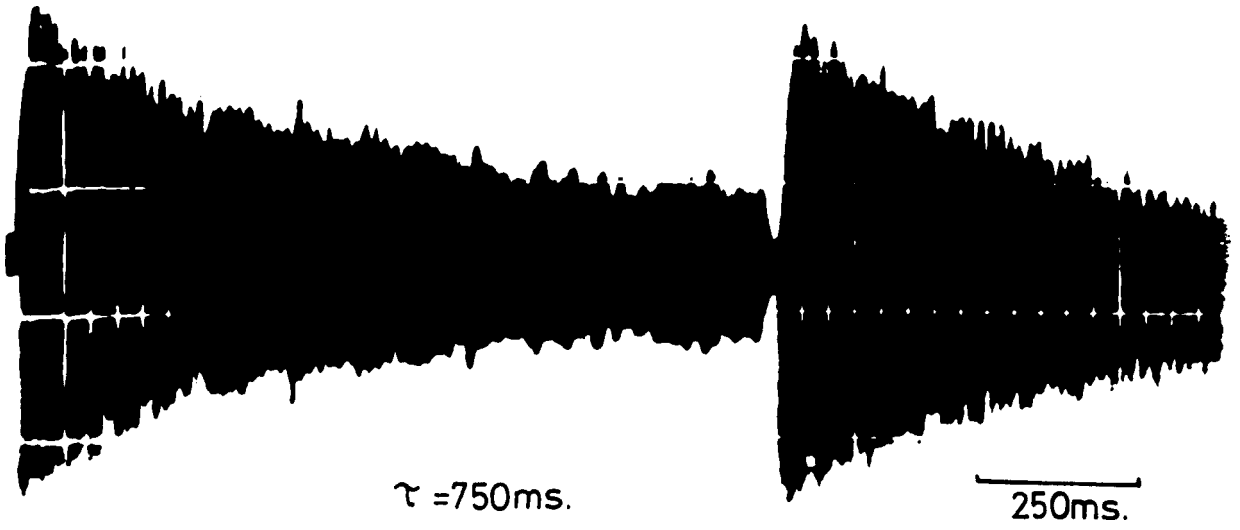

(b)

Oscilloscope Traces of Coherent Spontaneous Emission

FIG.(5.1)

the bulb and so reduce H-H spin exchange relaxation, whilst improving the storage time of atoms in the vessel. The results can be seen from the photograph of fig.(5.1(b)), which shows the ring time improved to 750ms. The dimensions of the aperture were clearly near an optimum.

After a vacuum failure which necessitated replacing the R.E.F. pump with a vacion type, an experiment to optimize the duct diameter in the Teflon plug was carried out. The results are shown in the graph of fig.(5.2). The poor values for the ring times were due to the fact that the hydrogen discharge was showing the wrong colour (bluish) due to an air leak, which would cause spin exchange effects with the atomic hydrogen in the bulb, thus reducing ring time.

Without gas contamination and with a fresh Teflon coating put on to the storage bulb, the Teflon plug containing the duct giving maximum ring times in the previous experiment was used in the system. With this arrangement, atomic ringing signals of the order over 800ms. in length were observed. Optimisation of the signal amplitude and ring time by variation of the other externally adjustable parameters of the maser, resulted in no further improvement. It was decided to try the MkI and MkII state separators in tandem in order to improve state selection and the focusing efficiency for the atomic hydrogen beam. The MkI magnet was placed downstream from the MkII magnet in the vacuum system to achieve better atomic beam collimation by using a stronger magnet, with a narrower gap, first. This modification was successful and ring times of 1 sec. duration were observed (Fig.(5.3(a))). A bulb with a fresh Teflon coating was then used in the system and ring times were improved to around 3 sec.. Here, regenerative narrowing of the atomic resonance line was taking place and the conditions for self sustained oscillation were nearly satisfied. The photograph in fig.(5.3(b)) shows a signal with this long ring time.

With the maser signals now close to the oscillation threshold, an effect

Optimization of Storage Bulb Exit Apperture (Duct Length 15mm.)

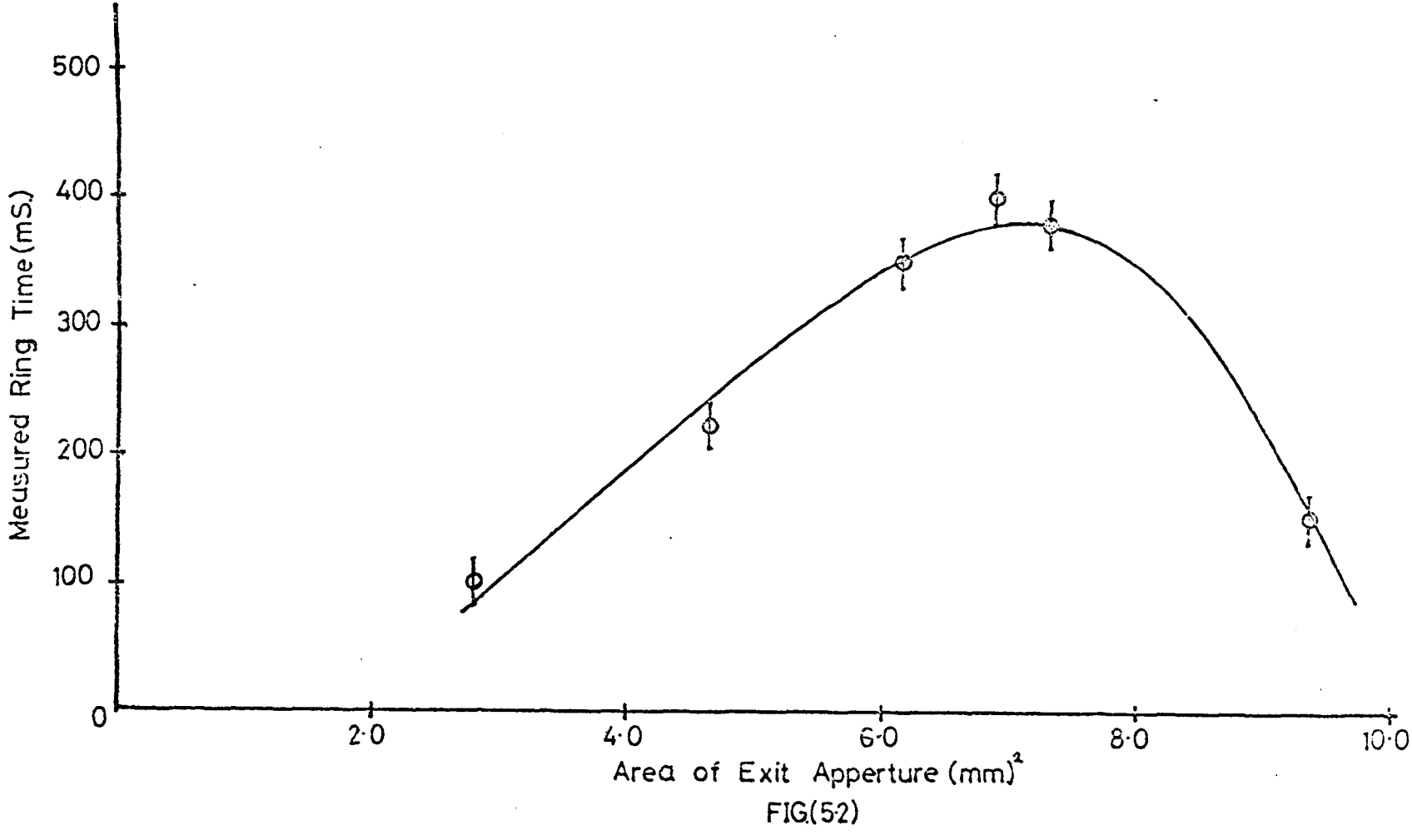

FIG(5·2)

(a)

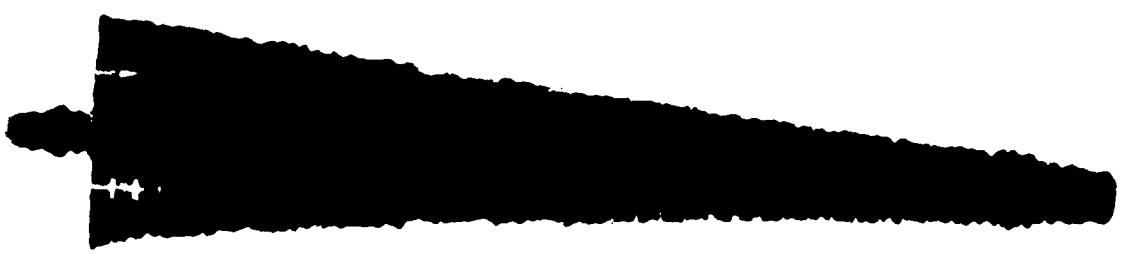

(b)

Coherent Spontaneous Emission on Nearing Oscillation

FIG.(5.3)

was observed which was termed a 'phasing' effect. This manifested itself in that the initial height of the detected signals varied in a random fashion when using pulse repetition frequencies of 0.5Hz or faster. The variation was either an increase or decrease in the level of the signals obtained, in comparison with those using a series of well spaced manually applied pulses. Hence, for consistency of results at long ring times, pulsing is carried out manually leaving a sufficient interval of time between successive pulses to avoid any interference with any previous pulse and hence avoid this so termed 'phasing effect'. The term 'phasing effect' is used since the resultant magnetization vector following a microwave pulse at the resonant frequency depends on the phase (and amplitude) of the decaying magnetization vector due to any previous pulse. Thus the amplitude of the resultant signal varies randomly in amplitude because the phases of the stimulating and decaying magnetization vectors are random.

Once these 3sec. ring time signals were observed, the externally variable parameters of the maser system were optimised. This involved cavity fine tuning, gas pressure adjustment, bellows alignment to peak the atomic beam optics and the adjustment of the values of applied H_0 and correction fields.

Self sustained maser oscillation was eventually achieved. The initial signals are shown in fig.(5.4). The signal to noise ratio is better than 10 to 1. Only one magnetic shield was in position at this time. Addition of a second shield resulted in a small improvement in signal level, but the third shield made no observable difference to the oscillation amplitude.

OSCILLATION CHARACTERISTICS OF THE MASER

Once self sustained maser oscillation was obtained, the behaviour of the maser with respect to externally variable parameters was studied.

The characteristic variation of oscillation level with respect to the relative pressure of hydrogen behind the discharge tube is shown in fig. (5.5). The onset of oscillation is fairly rapid as the oscillation threshold flux into

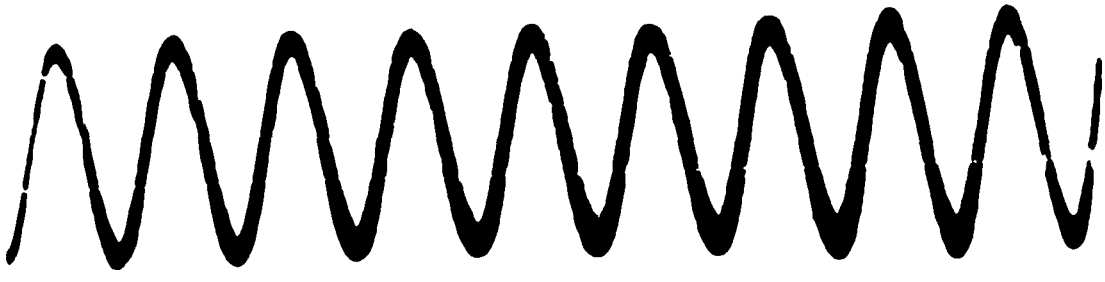

100μs.

Initial self sustained maser oscillation signal obtained using the present system. The phase-locked loop is used as the local oscillator to achieve the necessary stability for the detection of oscillation signals.

FIG.(5.4)

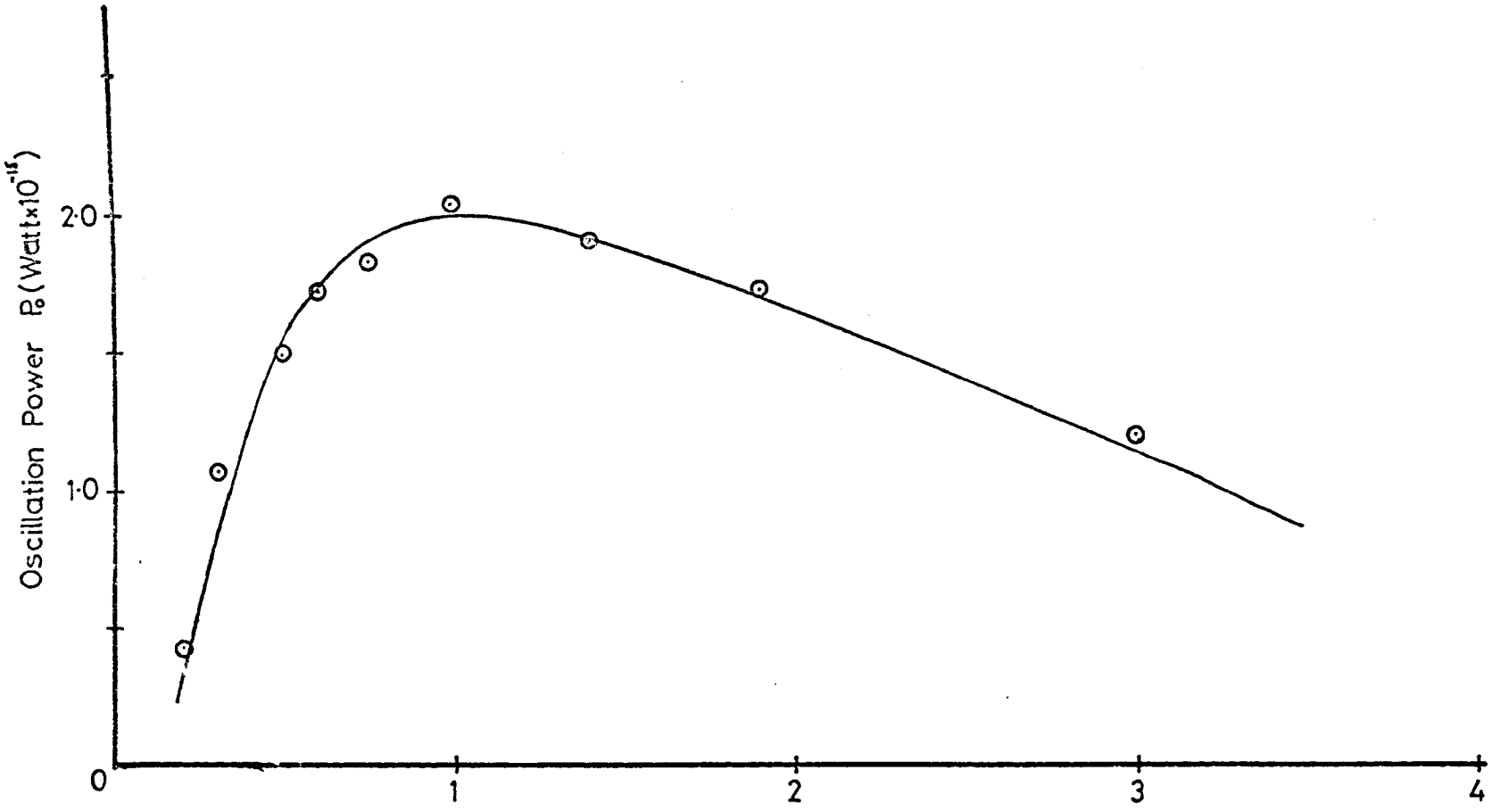
Oscillation Power P_0 (Watt×10^{-15})
2·0
1·0
0
1
2
3
4
Relative Gas Pressure

FIG(55)

the storage bulb is reached. The level increases with gas pressure to a maximum and then starts to decline until oscillation stops. This is due to the fact that at relatively high atomic hydrogen densities in the storage bulb, the relaxation effect of hydrogen-hydrogen spin exchange (which is directly proportional to the density of hydrogen) becomes dominant and so the level of oscillation is gradually reduced, finally ceasing. Ringing signals only, are then obtainable. Reducing the flux level back to the optimum value allows oscillation to build up from the thermal noise in the cavity. The power of the oscillation signal at the receiver input, was measured to be 2×10^{-15} W at the maximum amplitude.

The signal power from the maser was determined by comparison with a calibrated noise source. This source gave 22.5dB noise power above kT per unit bandwidth and was applied to the input of the detection system. The output signal level at 5.7kHz with 14Hz bandwidth was measured. The noise source was replaced by the maser signal and the I.F. attenuator adjusted until the output was at the same level. The maser power was then determined by adding (if attenuation increased) or subtracting (if attenuation decreased) the attenuation change in dB to the value 22.5dB of the noise source. This calibration procedure must be repeated on all experimental runs in order to have an absolute value for the output power from the maser during experiments.

With the magnetic shields in place, the cavity is tuned by the fine tuning rod which protrudes through the holes in the top of the shields. The effect of fine tuning on oscillation level is shown in fig.(5.6). This was plotted with 3cm. of the tuning rod protruding below the cavity top plate at the optimum output level. The tuning is sharp and smooth at this setting but as the amount of rod in the cavity is reduced the tuning becomes asymmetrical and with a small degree of insertion is very flat. Since an aluminium cavity is used, thermal drifts cause the cavity to detune and so it preferable to have the tuning rod inserted to a depth where the tuning will be sharp and

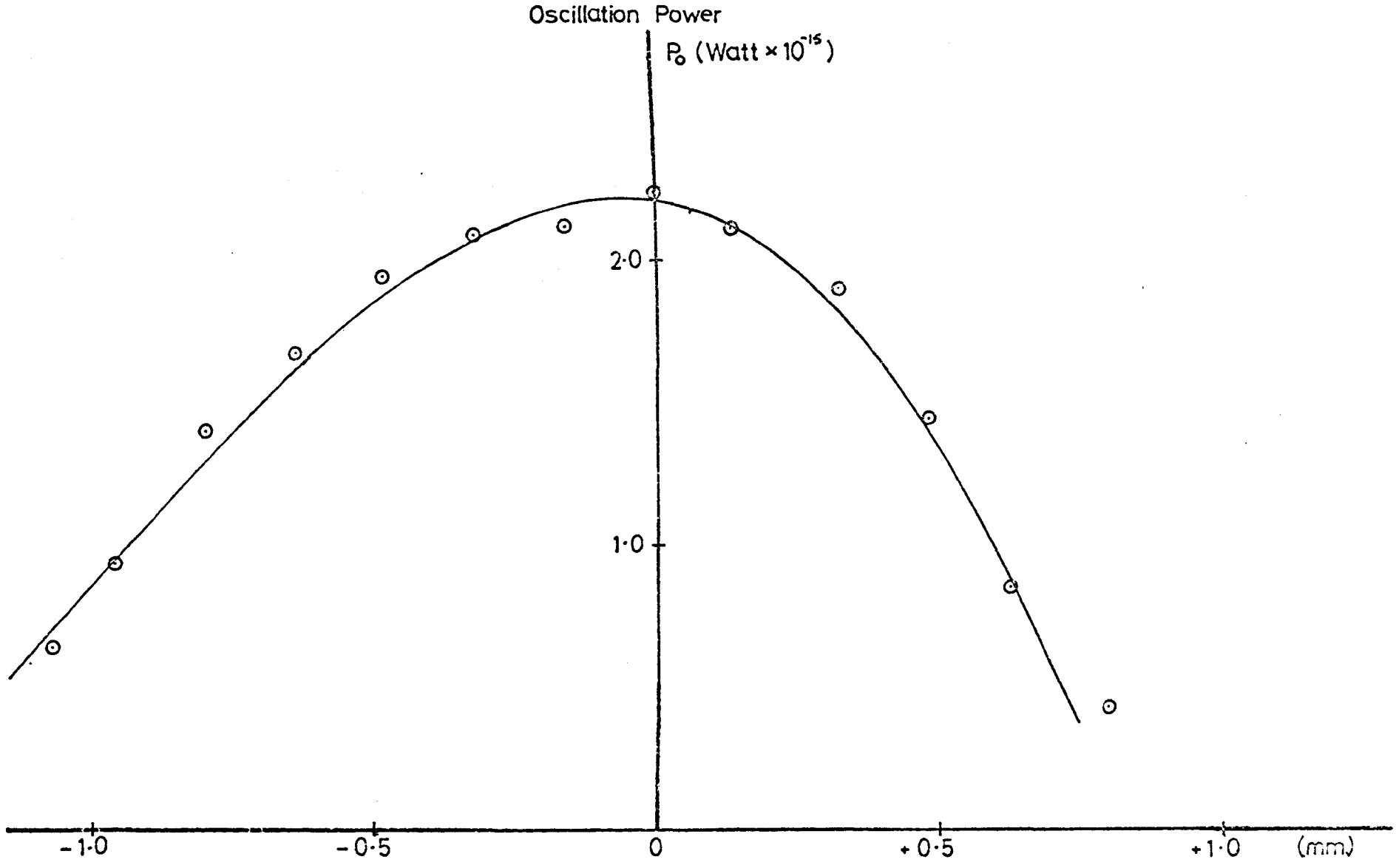

Fine-Tuner Insertion Around Optimum Position

FIG.(56)

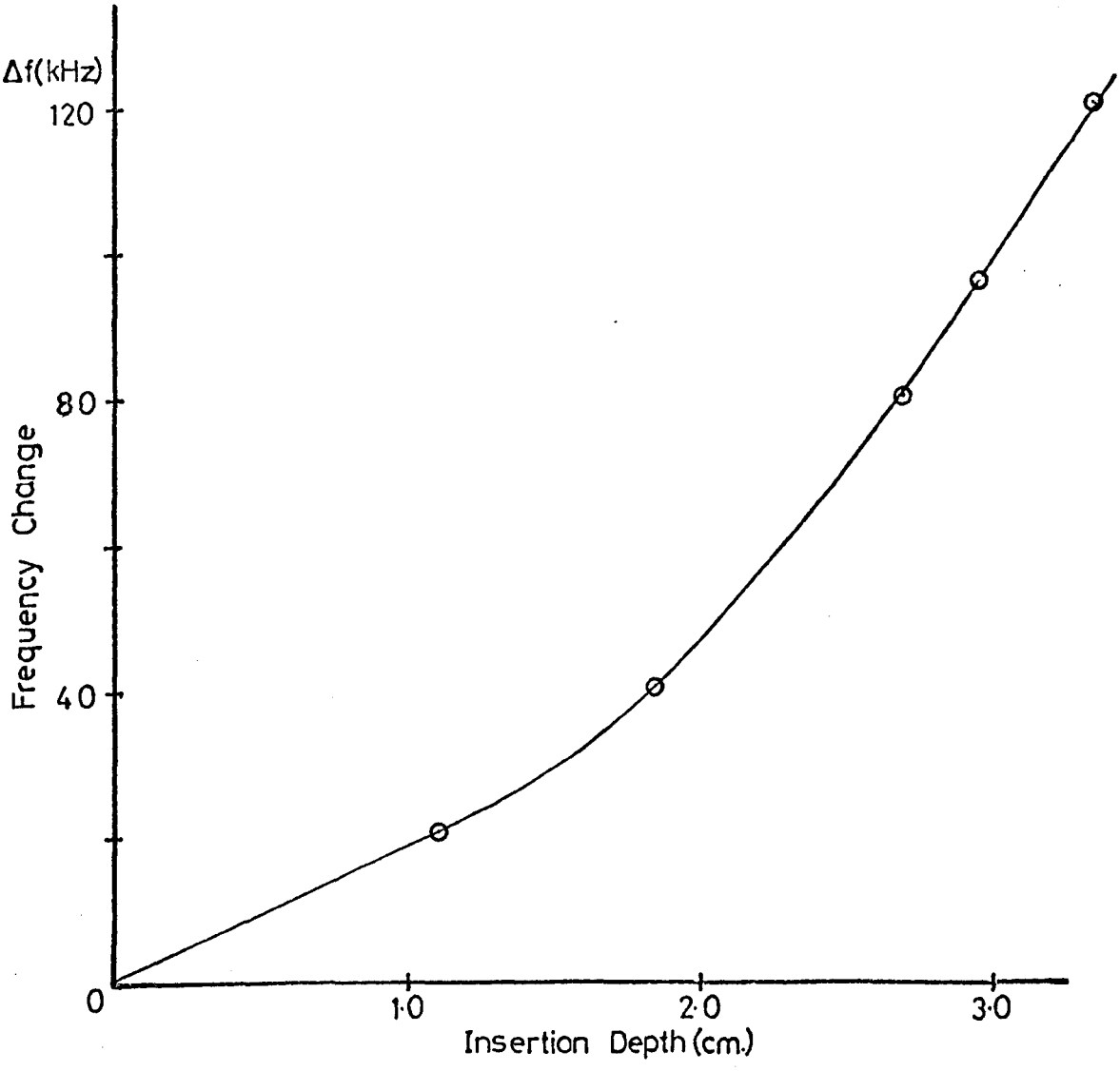

Theoretical dependence of the frequency of the cavity on the depth of insertion of the fine tuning rod.

FIG(5·7)

symmetrical. Also larger drifts can be compensated for by fine tuning and there is no necessity to remove the magnetic shields to reach coarse tuning adjusters. The theoretical tuning effect of an 8mm. diameter rod inserted into a cavity of the dimensions used is shown in fig. (5.7).

Maser oscillation is possible over a wide range of static magnetic fields H_o. The variation of amplitude with magnetic field around a particular value of H_o is shown in fig. (5.8) for a low and a high applied field. It can be seen that the variation with H_o at higher fields is much sharper than at lower field values. This behaviour is to be expected since the maser transition frequency with applied magnetic field varies as the square of the field.

$$\nu = \nu_o + 2750 H_o^2 \qquad \text{Hz/gauss}^2$$

Hence the effect of varying the field about any peak position will be much sharper at higher fields.

A typical H_o value for oscillation is with the current in the field coil set at 50mA (these readings are converted to gauss as described later). The correction field applied then shows a peak value for oscillation amplitude with H_o fixed. This is due to the small correcting field being applied at the lower end of the main coil to compensate for the lack of shielding caused by the apertures in the shield lids, for taking coaxial cables and the top vacuum flange. By applying a suitable field via the correction coil it is possible to optimise the homogeneity of fields in the cavity region and so obtain maximum oscillation level. A typical curve showing this effect is given in fig. (5.9). Compensation of this type at the upper end of the main coil has not been found necessary. The applied correction at the lower end of the coil becomes less effective as the value of H_o is increased. This is to be expected since the local field due to the applied correction coil is small in comparison to H_o, which would dominate. In later experiments with higher levels of oscillation, the correction field may be removed for all values of main field, without any adverse effect, but oscillation is quenched by application of

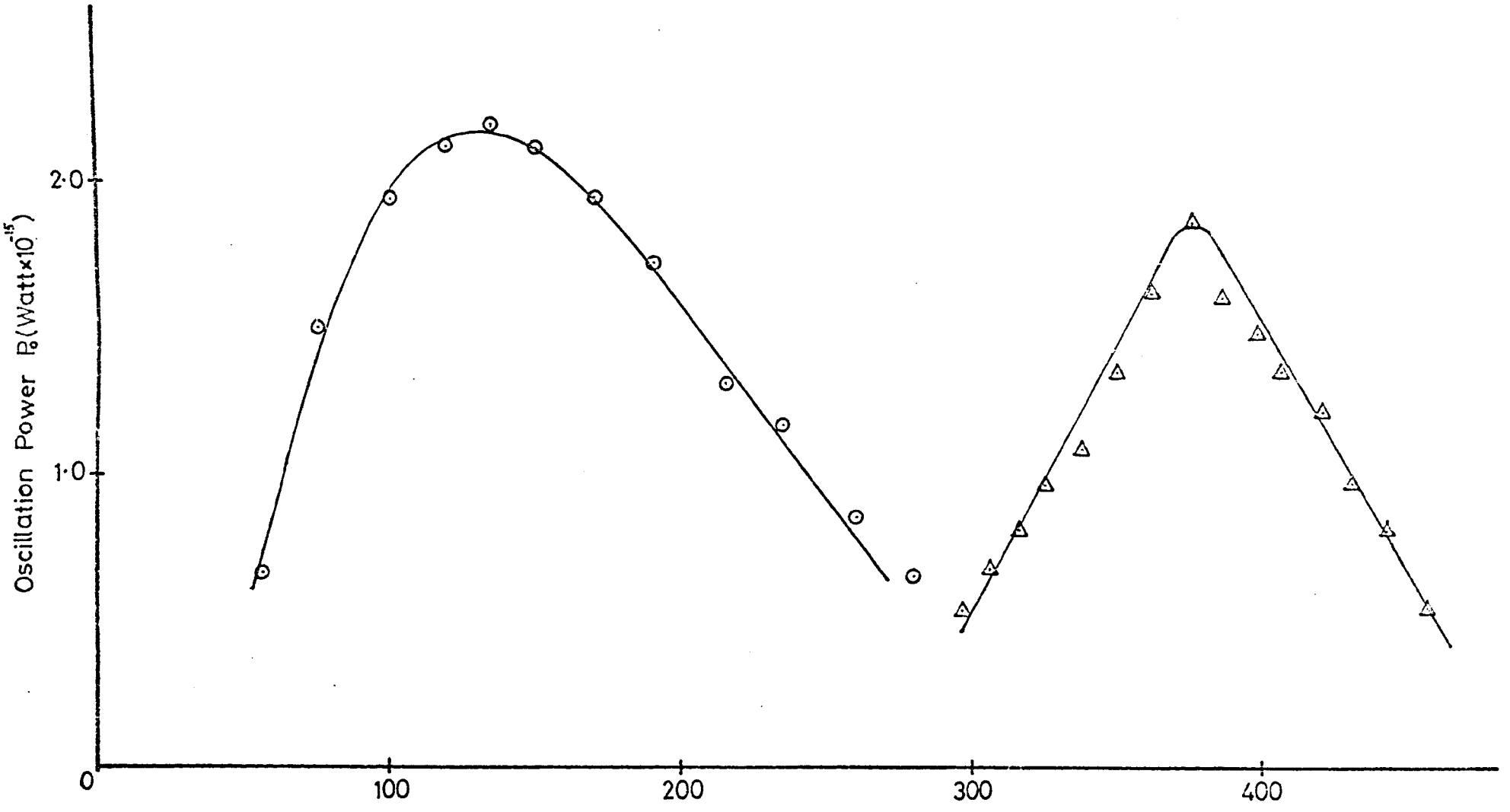
Oscillation Power P_0(Watt×10^{-15})
2·0
1·0
0
100
200
300
400
Applied H_0 Field (mG.)

FIG.(5·8)

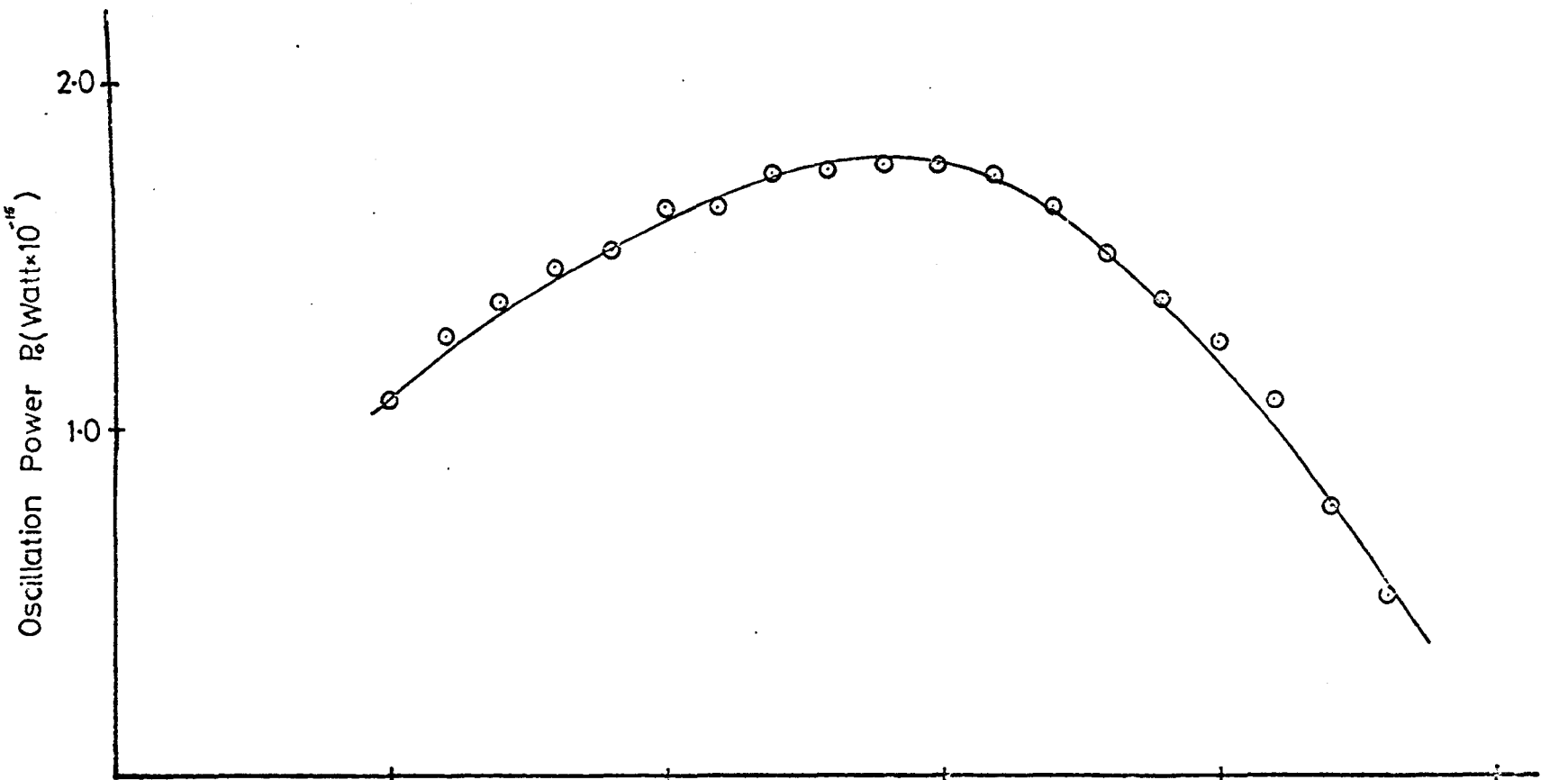
2·0
1·0
0
Oscillation Power P_0(Watt×10^{-15})
1·0
2·0
3·0
4·0
5·0×10
Correction Coil Current (mA.)

FIG(5·9)

excessive correcting fields in all cases.

The measurement of the resultant static magnetic field in the region of the storage bulb is determined by an oscillation quenching technique using double resonance. This is standard procedure in hydrogen maser work, for the in situ measurement of H_o.

The principle of the technique is that transitions between F=1 Zeeman sub-levels can be induced by the application of a magnetic field, of suitable frequency, in the x-y plane inside the cavity (fig. (5.10)). This causes depopulation of the F=1 m_F=0 upper maser energy level and hence quenches the oscillation. Removal of the applied field allows the maser signal to build up to its previous level from the thermal noise power in the cavity. The upper levels in the ground state of atomic hydrogen are field dependent. The application of the oscillating field in the x-y plane causes transitions resulting in oscillation quenching only when the frequency of the applied field corresponds to the transition frequency between the upper levels at the particular value of H_o. The variation in frequency of the Zeeman transitions depends on the value of H_o in the following manner

$$|\Delta\nu_z| = 1.4 \times 10^6 H_o \qquad \text{Hz/gauss}$$

where $\Delta\nu_z$ is the frequency separation of the F=1, m_F= 1 and F=0, m_F=0 levels. Hence, if at the point of oscillation quenching, the frequency of the applied quenching field is measured, the value of H_o in gauss may be determined from the formula quoted.

In the case of any electrically transparent cavity such as one made from quartz, the application of the double resonance field has been performed (Essen et.al.) using a loop of wire wound on the outside of the cavity body, and by a loop of cavity dimensions inside the cavity in the case of metallic resonators such as those of invar and aluminium. However, in the present work the coupling loop in the cavity base plate, which is not used under oscillation

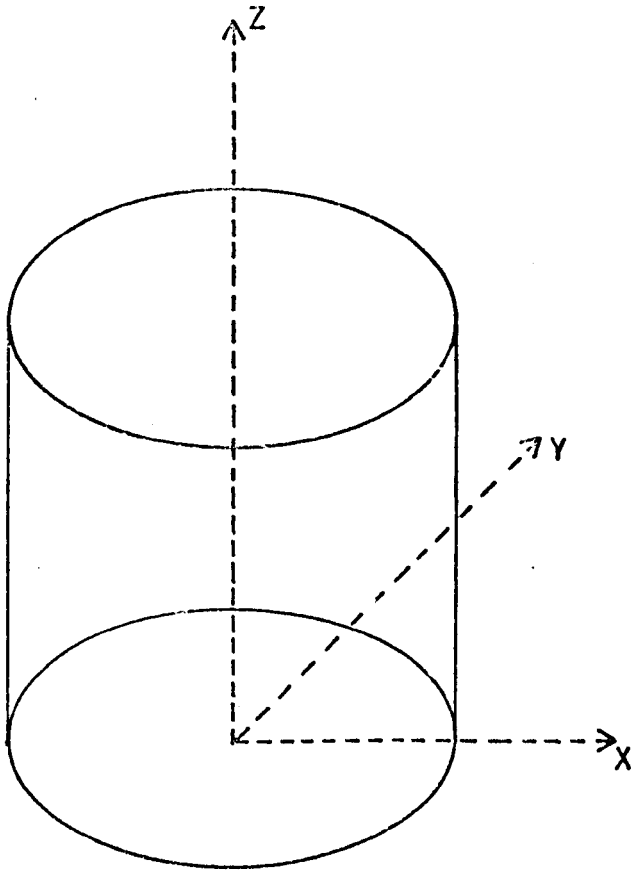

AXES FOR MAGNETIC FIELDS IN THE CAVITY

FIG. (5.10)

conditions, was found useful for signal injection.

A high power variable frequency oscillator was used. An output power of over 1 watt was needed because the loop area is extremely small in comparison with techniques using a loop of cavity dimensions. The oscillator was swept through the frequency range slowly by hand. At low levels of oscillation the quench position was fairly broad and although easy to find, the exact position of quenching was inaccurate. With higher levels of oscillation, the sweep must be much slower and the quench position is more accurately determined. The disimilarity is due to the different levels of maser oscillation. A low level requires only approximate quench position to be found in order that this mechanism can reduce the population inversion to a value below the oscillation threshold. However, with higher levels, the quench frequency must be more accurate if it is to stimulate sufficient atomic transitions to depopulate the upper maser level and hence stop oscillation.

The double resonance effect is illustrated at low oscillation level, in fig. (5.11). The frequency sweep is manual. At (a) quenching occurs as the frequency of the applied field reaches the appropriate value determined by H_o. On passing through this position, oscillation builds up from thermal noise. Reversing the direction of the sweep causes quenching at (b), near the frequency of that at (a). The average of the two readings at (a) and (b) gives $\pm$ 10kHz, a value for the double resonance quenching frequency from which H_o is calculated. In this case $\Delta\nu_L$=830kHz giving a value for H_o of the order 580mG.

Theoretically, the maser will oscillate, with perfect shielding, at virtually zero applied magnetic field and this is the most favourable condition, as indicated earlier, for its operation as a frequency standard. The lower limit for H_o at which the present system will still oscillate was determined by reducing the current in the H_o coil and retuning to keep the cavity following the oscillation frequency until self sustained oscillation was just

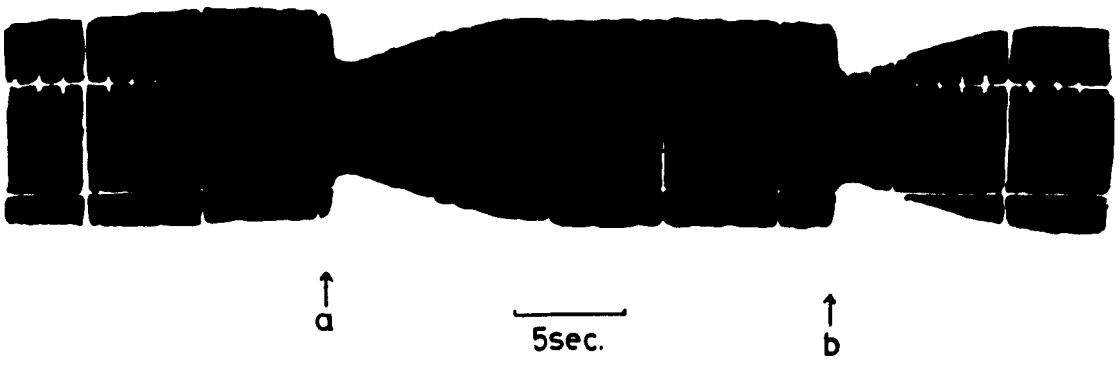

Photograph showing the effect of the injection of the double resonance signal into the cavity. At (a) quenching occurs as the resonant frequency (830kHz in this case) is reached. At (b) the resonant frequency is reached during the reversal of the manual frequency sweep. Time increases left to right. After quenching, oscillation builds up from thermal noise in both cases.

FIG.(5.11)

obtainable. The limit was lower for higher levels of oscillation under similar conditions. The lower limit was determined when the applied field was no longer strong enough to produce a uniform field along the cavity axis and hence the relaxation effects due to field inhomogeneity cause oscillation to cease. For frequency standards work of the quality of other laboratories, the lower limit must be reduced to around 1mG. At present it is 28mG. and this should be greatly improved by using a quartz cavity and by re-annealing and more thorough degaussing of the magnetic shields.

If under conditions of self sustained maser oscillation, the atomic hydrogen flux is removed by switching off the r.f. drive to the discharge tube, the maser oscillation decays in the manner illustrated by the photograph of fig. (5.12). A graph of signal amplitude versus time, after switch-off, is plotted (fig. (5.12(b))) from measurements made on a series of these photographs. The resulting curve is exponential in shape and the time taken for the amplitude to fall to $1/e^{th}$ of the maximum can be measured from it. The value ontained is 0.8sec. and this gives a measure of the parameter γ^{-1} for the system, where γ is the total relaxation rate of the atoms in the bulb.

Since the graph of fig. (5.5) of oscillation amplitude versus gas pressure behind the discharge tube was uncalibrated with respect to pressure, the pressure gauge head was replaced with one which gave reliable readings in Torr. Thus with a new calibrated curve, useful comparisons could be made with any later characteristics of this type, which may be plotted. The resulting graph is shown in fig. (5.13).

After a period of just over two weeks of semi-continuous operation, effects resulting in the eventual loss of self sustained oscillation were observed.

Firstly, a reduction in the level of oscillation, in comparison with the initial signals obtained, was observed. Optimisation of the variable

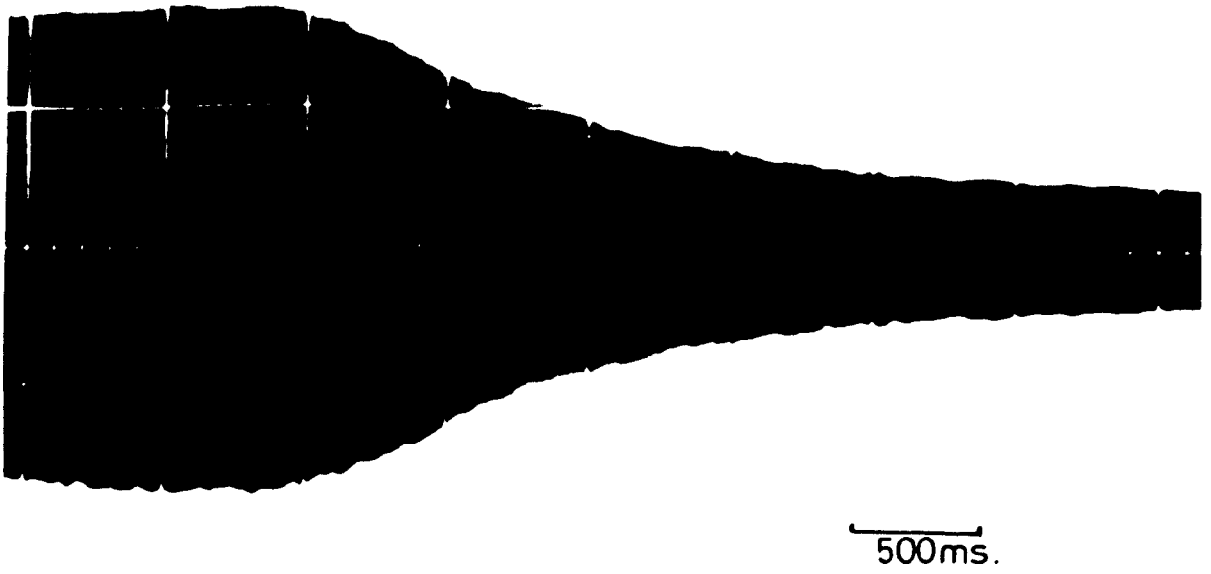

Oscilloscope trace showing the decay of the oscillation signal after the atomic hydrogen discharge is switched off.

(a)

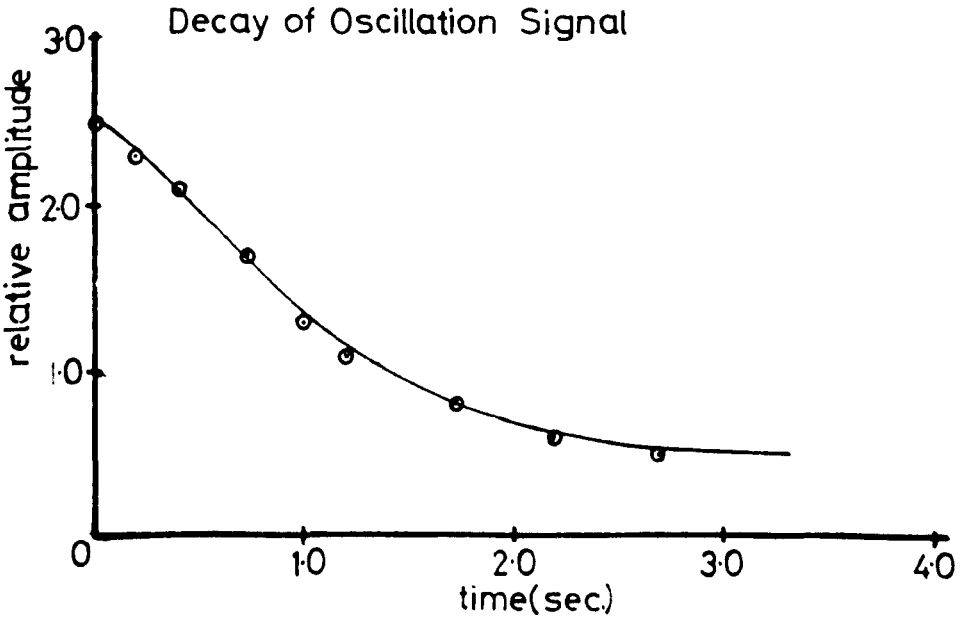

Graph of the oscillation decay plotted from values obtained from a series of photographs of the above type.

(b)

FIG. (5.12)

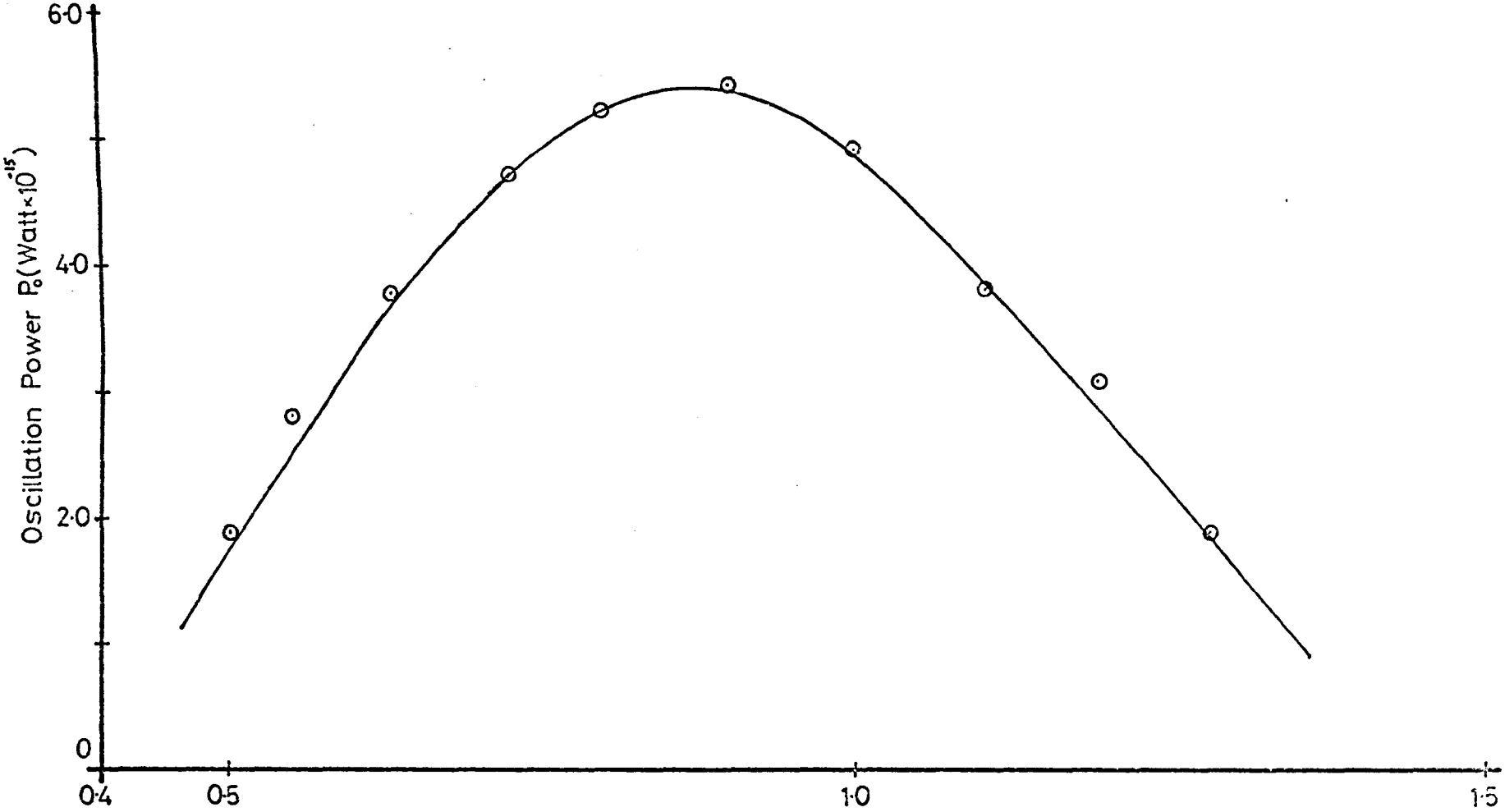
6·0
4·0
2·0
0
Oscillation Power P_0(Watt×10^{-15})
0·4
0·5
1·0
1·5
Discharge Gas Pressure (torr)

FIG(5·13)

parameters of the system was not successful in regaining previous signal amplitudes. The second stage in the process was the decrease in output level over the period of the working day. At this point in time it was noticed that the inside walls of the Pyrex discharge tube were becoming blackened. This was probably due to the formation of black boro silicate deposits as observed by Kleppner et. al. (24) who, however, reported that this had no adverse effect on the level of oscillation. Because the discharge drive power was 20W in our case (10W Ramsey, 5W N.P.L.), it was decided to forced-air cool the tube to avoid any effect coupled with the discolouration, which may be due to overheating in the atomic hydrogen source. The rate at which the oscillation signal decayed from its 'switch on' amplitude continued to increase until oscillation was lost after a period of only about 30 sec. from the time of first switching on the maser. If the discharge was switched off for a minute or so after the signal was lost, oscillation was again possible but the time of degrading was still as short as previously mentioned. Removing the air cooling from the discharge tube under conditions of oscillation, caused an even more rapid decline in signal level.

With the air cooling replaced, oscillation became impossible to sustain for even a few seconds. The discharge tube was replaced with a clean one of the same dimensions. This did in fact re-establish oscillation but a decline in level was again apparent after a few hours of use. Such an effect could not be due purely to the discharge tube degrading since the previous tube had been in use for several months. The time taken for oscillation to stop again became shorter until it was not possible to get the maser to oscillate at all. The maser atomic ringing signals were then observed and these degraded to give ring times as poor as 400ms. A further change in discharge tube did not improve matters. However, removal and recoating the storage bulb produced immediate oscillation on its replacement. The signal level was higher than had been achieved previously. This indicated that total failure was probably

due to the bulb coating. The difficulty was now to resolve the mechanism of the failure.

A search through the hydrogen maser literature revealed other references to a similar type of oscillation degrading. Mungal et.al. (25) refer to the discolouring of discharge tubes and in 'extreme cases' of blackening, the failure of these tubes to produce atomic hydrogen. Actual loss of oscillation is referred to as being associated with the destruction of the Teflon bulb coating by the atomic beam.

The most detailed account of a similar type of problem is given by Nitikin and Strahkovskii (26). Here the vacuum system employed oil diffusion pumps and nitrogen cold traps. Results almost identical with those at Keele were observed. Replacement of the oil pump on the upper vacuum chamber with a vacion type pump, extended the time scale of the effects observed by the Russian experimenters from several weeks to eighteen months. The overall results explained by Nitikin and Strahkovskii as the appearance of the hydrocarbon formations, due to oil contamination in the bulb, facilitating the recombination of hydrogen atoms on the inside surface of the storage bulb. No mention is given to any discharge tube discolourations.

From the results of the Russian paper, the loss of oscillation appears to be caused by oil contaminants reacting with atomic hydrogen in the bulb, but the time scale of events is only similar to that at Keele when Nitikin et. al. use only oil pumps for evacuation of their system. The extension of this time to eighteen months is achieved when an ion pump is used to give a system almost identical to that at Keele. In our system however, only a water cooled baffle was used on the diffusion pump and this may allow more rapid contaminiation due to oil vapour.

The results of Mungal et. al. (25) indicate a possible destruction of the bulb coating by the hydrogen flux into the bulb and no oil contamination

is possible because of the exclusive use of ion pumps. Although discolouration of the discharge tube was observed, it was considered only for the reason that it fails to produce atomic hydrogen and hence oscillation cannot be possible under any circumstances.

The effect of inner surface contamination in the effuser is that atomic hydrogen recombination at the tube surface is increased causing a reduction in the useful beam flux. In extreme cases, contamination results in the failure of the tube to produce any atomic hydrogen. This would obviously result in oscillation failure, but under normal circumstances the contribution to failure from the discharge tube is negligible.

The problem with the storage vessel cannot be so clearly defined, since failure takes place both with and without the presence of oil vapour from diffusion pumps. Two distinct effects seem probable. In the case of oil contamination, this would appear to produce relaxation centres under the influence of the atomic hydrogen on any oil contaminants present in the bulb and so cause sufficient relaxation at the walls of the bulb to prevent oscillation. Where there are no oil pumps in use, it would appear that the actual surface of the Teflon is destroyed by the action of the atomic beam i.e. energetic atoms from the hot discharge impinge on the Teflon surface causing it to disintegrate on a microscopic scale and eventually oscillation failure results due to excessive relaxation at the walls of the storage vessel.

A combination of these effects may explain why, even when using an ion pump on the upper chamber, the time scale for the degrading of oscillation performance is of the order of only weeks in the present case. It is likely that all the above effects are simultaneously involved: discharge tube contamination leading to the hydrogen recombinations, oil contamination of the storage bulb and the production of a very hot beam due to the high r.f.

drive level supplied to the discharge. The temperature in the discharge was measured to be in excess of 230°C. The only rapid solution to the problem has been the replacement of the bulb coating and discharge tube as soon as signs of failure appear. A more long term solution to the problem would be the replacement of the oil pump with a vacion type, an improvement in discharge efficiency to reduce power inputs and hence have a cooler beam.

Also the inside of the discharge tubes may becoated to avoid the the formation of compounds on the walls which might facilitate hydrogen recombinations.

With the maser oscillating once more, it was decided to replace the discharge tube with one different only in its length being increased from 15cm. to 20cm. The aim was to have a larger area of tube and hence produce better cooling due to more conduction of heat away from the effuser. With the new dischrge tube in place the characteristic output power versus pressure behind the atomic hydrogen source was plotted (fig. (5.14)). The peak power is $\sim 2.5 \times 10^{-15}$ W (22.5dB above $KT\Delta f$). The main features are again the sharp rise of signal amplitude from the onset of oscillation and the now extremely flat top at relatively high gas pressures. The improvement in signal amplitude is due to the fresh bulb coating and the flat top response of the curve shown is probably caused by the presence of the extended discharge tube.

At this improved level of oscillation, amplitude transients were investigated by switching the discharge supply on and off manually . After some optimisation of signal level and adjustment of discharge tube gas pressure, displays of the type shown in fig. (5.15) were observed on the storage oscilloscope. The sweep is left to right, the discharge being switched off at (1) and on at (2). As can be seen on the build up of the oscillation from noise, there is an overfulfillment of the steady state oscillation conditions and an amplitude transient is apparent. Transient behaviour using switching techniques of 'spoiling' the magnetic field in the cavity was not

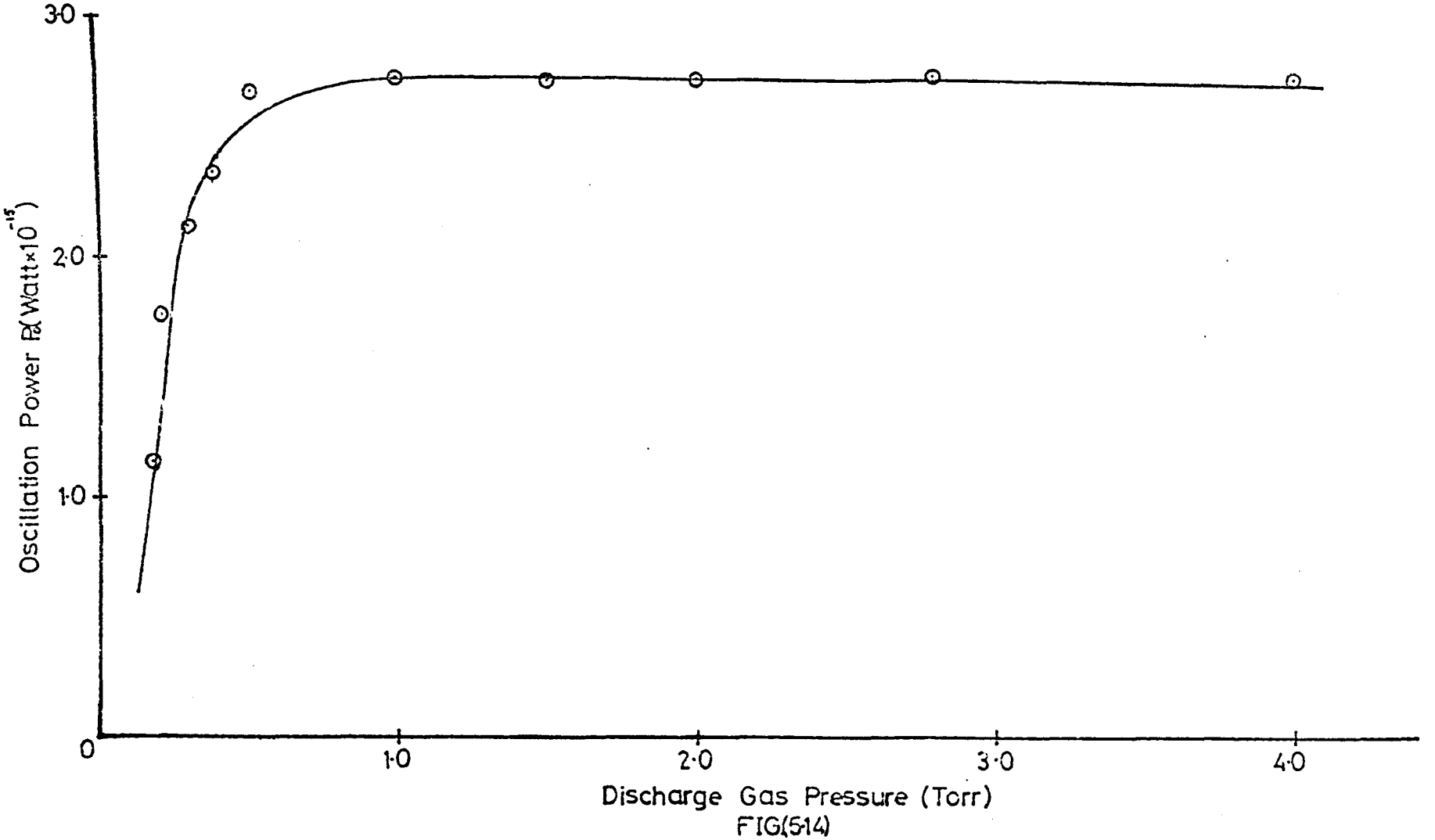
3·0
2·0
1·0
0
Oscillation Power P(Watt×10⁻¹⁵)
1·0
2·0
3·0
4·0
Discharge Gas Pressure (Torr)
FIG(5·14)

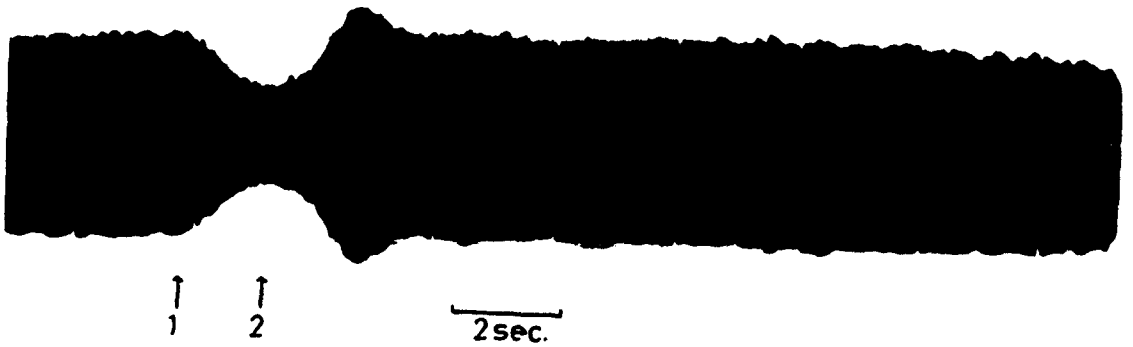

(a)

Oscillation amplitude transient produced by switching the atomic hydrogen source of (1) and then back on (2).

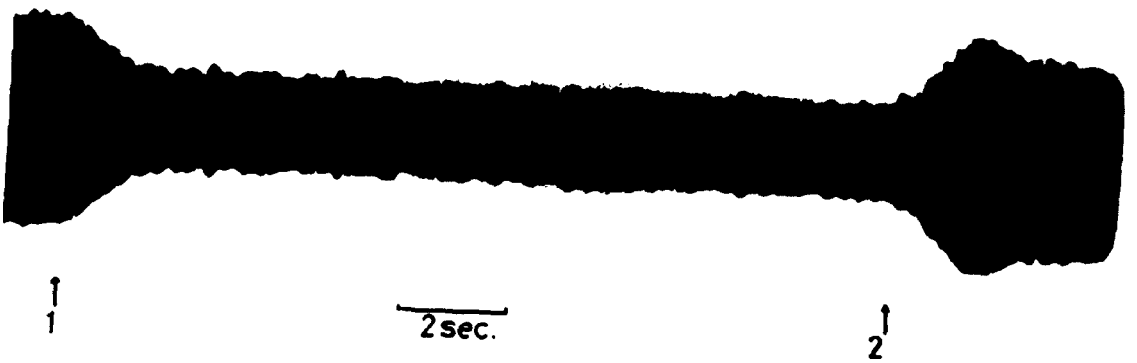

(b)

As (a) but with the time during which the beam is off now much longer. Time increases left to right.

FIG.(5.15)

obvious at this level of oscillation.

The results of the investigations carried out in this section, serve to characterize, under conditions of steady state oscillation, the basic static properties of the constructed maser oscillator. The amplitude transients reported in the last paragraph are properties of the dynamic behaviour of the maser and these are investigated more fully in the following chapter.

CHAPTER SIX

ON AMPLITUDE TRANSIENTS

Introduction

The strength of the observed oscillation amplitude transients is directly dependent on the level of steady state maser oscillation. Thus to observe stronger transients due to beam switching techniques and to see transient behaviour with less effective methods of production, the maser output power needed to be improved.

A fresh Teflon coating was placed on the inside of a storage vessel and this was used in the system. By this means, the output power of the maser oscillation was increased by a factor of three to 7.3×10^{-15} Watt. Various methods of amplitude transient production were then investigated. The results are reported and discussed in this chapter.

Theoretical Considerations of the Transient Behaviour of the Hydrogen Maser

The approach taken here is along the lines of that followed by Audoin (27)

Assuming the validity of the two level approximation applied to the ground state hyperfine levels of hydrogen it can be established Audoin (28) that the whole set of spins confined in the storage bulb fulfills a Bloch equation of the type;

$$\dot{\underline{M}} = -\underline{M}\times\underline{H} - \frac{M_1\underline{k}_1 + M_2\underline{k}_2}{T_2} - \left[\frac{M_3}{T_1} - I(t)\right]\underline{k}_3 \qquad (6.1)$$

where $\underline{M}$ is the magnetization vector and $\underline{H}$ the magnetic field vector T_1 and T_2 are the overall longitudinal and transverse relaxation times respectively, $\underline{k}_1$, $\underline{k}_2$ and $\underline{k}_3$ are unit vectors and $I(t)$ is the excess of flux of atoms inthe upper state over the flux in the lower state.

The validity of the Bloch equation (in suitable representation) for atoms in a hydrogen maser, arises both from the simple structure of the hydrogen atom ($I=\frac{1}{2}$) and the fact that the population inversion is performed

outside the microwave cavity and atoms are confined for a long time in the storage bulb. All the properties of the hydrogen maser can then be calculated and compared qualitatively to experimental observations to give information on atomic processes.

In the hydrogen maser, the effect of the induced magnetic dipole moment $\mu_0 M_1$ of all the atoms driving the electromagnetic field in the resonant cavity, is calculated from Maxwell's equations. For experimental purposes and for the sake of completeness, an excitation at a frequency ω, produced by an external generator, connected to the cavity through a coupling loop, is also considered. To avoid the use of a coupling coefficient this excitation is defined such that the amplitude of the cavity response H_1, is equal to the amplitude of the excitation field H_e when the cavity contains no atoms and when the excitation frequency is the same as the resonant frequency, ω_c of the cavity.

H_1 is then a solution of the equation

$$\ddot{H}_1 + 2\dot{H}_1/T_c + \omega_c^2 H_1 = K\ddot{M}_1 - 2\omega_c H_e/T_c \qquad (6.2)$$

where T_c is the cavity time constant $T_c = 2Q_c/\omega_c$. The parameter K depends on the cavity filling factor η and volume V_c such that

$$K = 4\pi\eta\mu_0^2/\hbar V_c$$

Equations (6.1) and (6.2) allow exact calculation of all the macroscopic properties of the maser either in the free running conditions ($H_e=0$) or when driven externally ($H_e \neq 0$). The directly measurable parameters are the frequency, the amplitude and the phase of the electromagnetic field in the cavity. Thus amplitude may be calculated as a function of time by looking for amplitude solutions of the above equations.

The following boundary conditions are set;

$$H_e = 0$$

$$H_1 = b\cos(\omega t + \phi)$$

$$M_1 = m\sin(\omega t + \psi)$$

T_1, T_2, T_c are much longer than the hyperfine transition period, b is the reduced electromagnetic field ($b=\mu_c\langle H_z\rangle_{bulb}/\hbar$) and m is the amplitude of the total magnetic moment divided by the Bohr magneton. The parameters b, m, ϕ, ψ are also slowly varying functions of time.

In the hydrogen maser cavity time constant is much smaller than the atomic relaxation times and hence the cavity electromagnetic field follows, with negligible delay, the variations of its excitation level. Thus for practical experimental situations the following simplified differential equation describes the amplitude variations;

$$\frac{d}{dt}\left(\frac{\dot{b}}{b_o}\right)+\frac{1}{T_1}\left(\frac{\dot{b}}{b_o}\right)+\left(b^2-b_o^2\right) = 0 \qquad (6.3)$$

These variations are thus defined by the values of the T_1 relaxation time and the steady state oscillation level b_o. This is related to the fact that the oscillation level is bounded by the saturation of the atomic resonance and that the population difference varies with the T_1 time constant.

For small variations around the steady state level, equation (6.3) can be linearized by putting $b=b_o+\varepsilon$, for $\varepsilon \ll b_o$. The return to the steady state after removal of any perturbation which causes the oscillation level to change from the steady state value, is described by;

$$T_1\ddot{\varepsilon} + \dot{\varepsilon} + 2T_1 b_o \varepsilon = 0 \qquad (6.4)$$

From this it is easily shown that when the amplitude of oscillation is low ($8T_1^2 \times b_o^2 < 1$), the buildup amplitude transient is just a damped exponential and that the amplitude variations are slower as the level is reduced. This conclusion may be verified by operation of the maser just above the oscillation threshold.

For high oscillation levels ($8T_1^2 \times b_o^2 > 1$) the amplitude transient takes the form of a damped oscillation of the form;

$$\varepsilon = C\exp(-t/2T_1)\cos(\omega_1 t+\phi) \qquad (6.5)$$
$$\omega_1^2 + 1/4T_1^2 = 2b_o^2$$

where C, ϕ are the constant parameters.

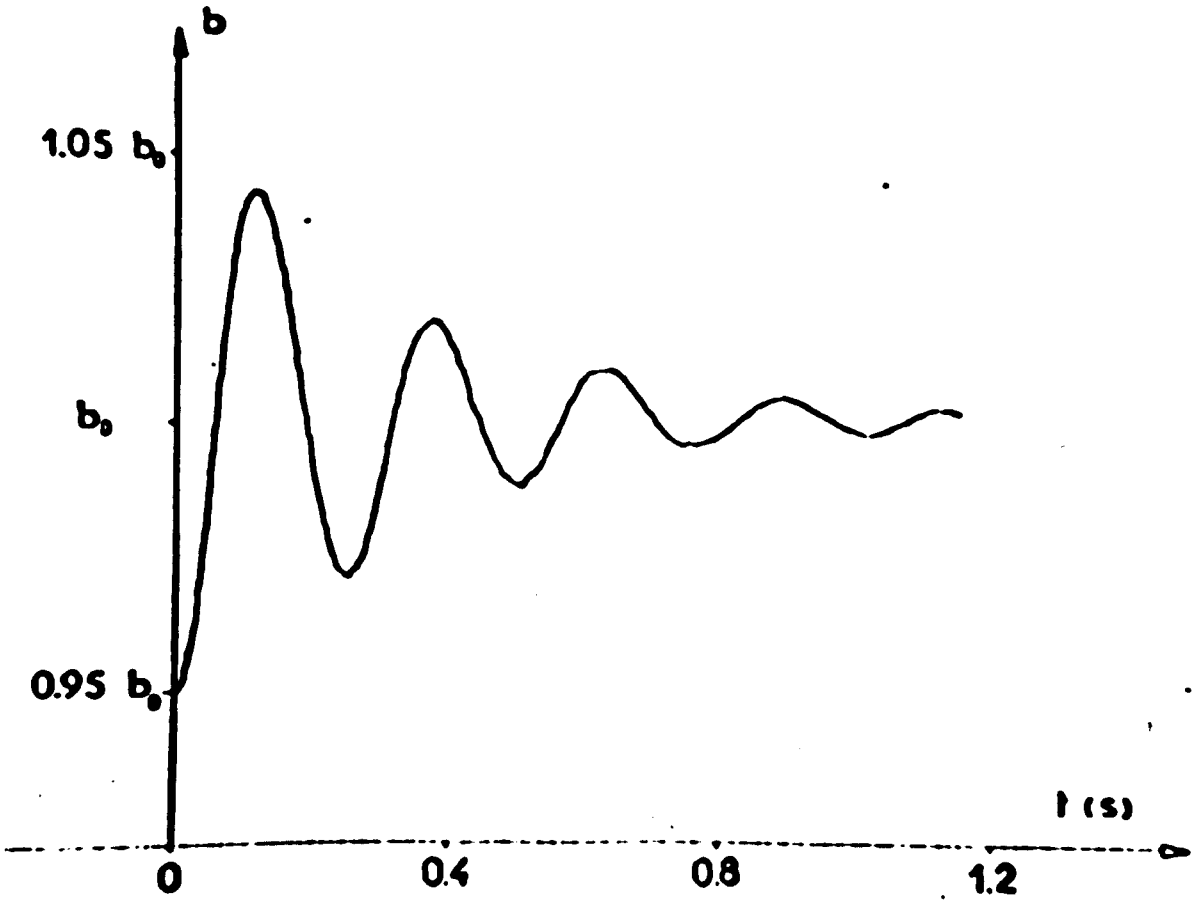

Example of recorded amplitude transient.

(After Audoin)

Fig. (6.1)

This type of behaviour has been reported for the Ammonia maser (29), the Proton maser (30) and the Hydrogen maser (31), (32).

An example of an amplitude transient recorded by Audion et. al. is shown in fig. (6.1). This was induced by the removal of an inhomogeneous static magnetic field previously applied to the atoms in the cavity. The apparent Q factor of the cavity was increased by connecting a feedback loop, comprising a variable gain amplifier together with a phase shifter, to the microwave cavity.

Investigation of Techniques for Producing Oscillation Transients

In all the following experiments, the power output from the maser under steady state conditions was measured to be 7.3×10^{-16} W.

The transient produced by switching the discharge supply off and then back on was first observed under the improved oscillation conditions. Fig. (6.2(a)) is a typical photograph of the transient which results. A comparison with fig. (5.15) reveals that the overshoot of the oscillation amplitude on buildup is initially larger and that a minimum amplitude occurs before the steady state level is reached. At the new improved level of oscillation, other methods of transient production were investigated.

Successful results followed the re-establishment of the oscillation signal after quenching by (i) double resonance, (ii) the proximity of a strong externally applied static magnetic field, (iii) the application of excessive correcting magnetic field. These techniques and the initial results from them are now briefly described.

(i) Double Resonance:

The procedure followed here is almost identical to that used when measuring the value of H_o. The main variation is in the 'quench' being removed more quickly, (in about 0.5sec., which is approximately the time taken to move the frequency dial of the oscillator quickly off resonance

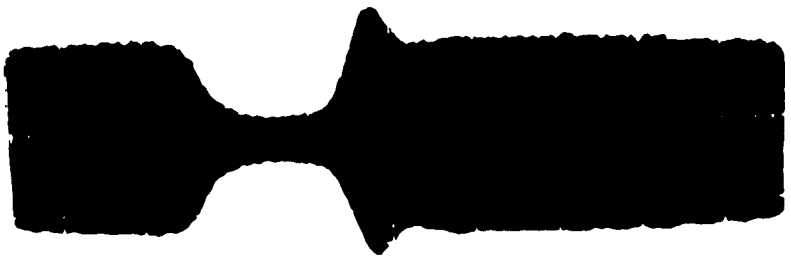

(a) Beam Switching

2 sec.

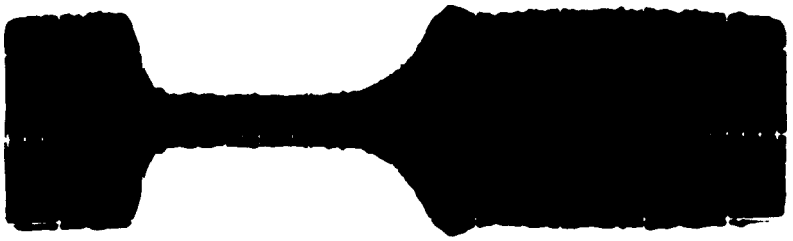

(b) Double Resonance

(c) Permanent Magnet

Oscillation Transient Type

Fig. (6.2)

(d) Permanent Magnet

2 sec.

(e) Repeat (d) then (c)

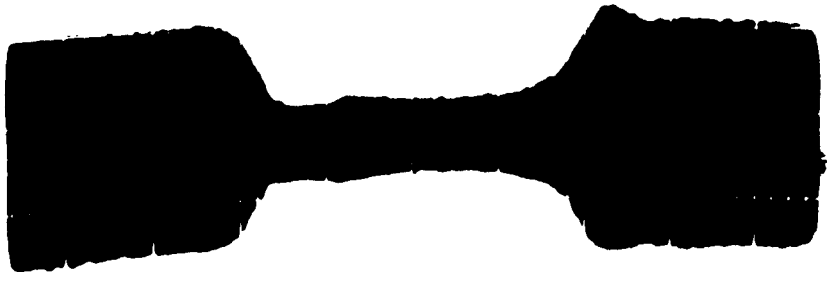

(f) Excess Correction Field

Fig. (6.2)

by hand. As is shown in fig. (6.2(b)) there is a transient overshoot in the initial amplitude of the oscillation signal. This overshoot was not observed under the same conditions with the lower levels of oscillation and for thoses cases fig. (5.11) is a typical response.

(ii) External Magnetic Field:

The initial technique used here was very primitive. A strong horseshoe magnet was introduced by hand to the region at the upper end of the vacuum system, below the lid of the magnetic shield. The stray static magnetic field produced by this magnet was sufficient to quench oscillation and by removing the magnet rapidly, oscillation was re-established and transient behaviour observed. Fig. (6.2(c)) shows the result for the magnet used with the N.&S. poles left and right respectively when viewed from behind the magnet. Fig. (6.2(d)) is the result with N.&S. poles rightto left respectively. The orientation of poles is only important in the sense that locally the value of B_o, since the sign of the magnetic field changes with the pole reversal. The general effect is a result of the production of a stray magnetic field at right angles to the B_c field along the cavity axis.

Both orientations of the magnet produce amplitude transients on its removal. However, in fig. (6.2(c)) a slight increase in steady state oscillation prior to quenching was observed. This was not a further transient, but appeared to be the result of a momentarily more favourable orientation of the nett local magnetic field seen by the atoms in the region of the bulb entrance as the magnet is moved into the quenching position. The characteristics shown by these oscilloscope traces (c), (d) are due to the effects of the magnetic fields produced by the horseshoe magnet, in itsdifferent orientations, as seen by the active atoms inside the storage vessel. This was demonstrated by adding another magnetic shield to the one already in use. The ensuing results are shown in fig. (6.2(e)). Going left to right along the trace, first (d) and then (c) was repeated. It can be seen that in the first case

the quenching is no longer complete and a transient is barely observable. In the second, the extra shield removes the effect producing the pre-quenching increase for oscillation and again quench is not complete, but more definite here. The resulting transient has a larger initial overshoot. Although this type of technique for producing amplitude transients has been successful, it is not sufficiently reproduceable since the process depends to a large extent on the position and orientation of the magnet and the quality of the magnetic shielding.

(iii) Excessive Correction Field:

As a result of the observations in (ii), oscillation transient production was attempted by applying an excessive correcting field current at the lower end of the solenoid. Reducing this excess applied field back to its steady state value (by manually varying the potentiometer controlling the current in the coil) transients were produced as shown in fig. (6.2(f)).

In summarising the above results, it may be said that there are basically two different responses observed. These are transients produced by beam switching and those due to all the other methods used. The beam switch technique produces a much more prominent response in camparison with the others. This is consistent with earlier results where at the lower levels of oscillation, only transients due to beam switching were observable.

Further improvement in the power of oscillation was necessary to investigate the above transients in more detail. Optimization of the external parameters of the system and the improvement in the atomic hydrogen discharge, as a result of its ageing, produced power levels under steady state operation of 31dB above kT per unit bandwidth or 2.64×10^{-14} Watt. With this much improved level of oscillation, the amplitude transient types were studied in more detail.

Transients Data Using Chart Recording Technique:

In addition to the observation of transients using the storage oscilloscope,

the 5kHz output from the receiver was rectified and the resulting signal recorded by means of a chart pen-recorder. The results produced using the various techniques are shown for comparison in figs. (6.3,4,6). Fig. (6.3(a)) shows the transient produced by switching the atomic beam, (6.3(b)) that due to the high level correction field and (6.3(c)) the result of the double resonance sweep.

In fig. (6.3(a)) a second maximum is visible during the transient response and also a very large initial overshoot of the transient in comparison with the other techniques. The decay envelope of oscillation varies depending on the quench method used as does the time taken for the oscillation to build up, back to the original steady state level.

Fig. (6.4) shows the results of applying the excess current pulse to the correction coil using a capacitator discharge arrangement. (A sketch is shown in fig. (6.5)). This technique was more precise than a manual application of an excess current which required varying the potentiometer controlling the current flow and winding back to the optimum position to remove the quench. With the electronic technique, the correction field current is normally at the optimum position until the excess current pulse is applied. Then the capacitor in the circuit discharges through the correction coil. It is apparent that there is a minimum applied voltage to the capacitor, below which the excess current produced in the coil is not sufficient to completely quench the maser oscillation and hence produce an observable transient. This value is 15V. in this case. Increasing the voltage above the value necessary to obtain a complete quenching does not affect the amplitude of the transient.

The transient recorded in fig. (6.6) is a result of quenching oscillation by pushing on the fine tuner protruding through the top of the magnetic shields. This tilted the top plate in the cavity and hence caused a detuning effect (Q-degrading also taked place) such that the conditions for oscillation are no

(a) Beam Switching

(b) Correction Field

(c) Double Resonance

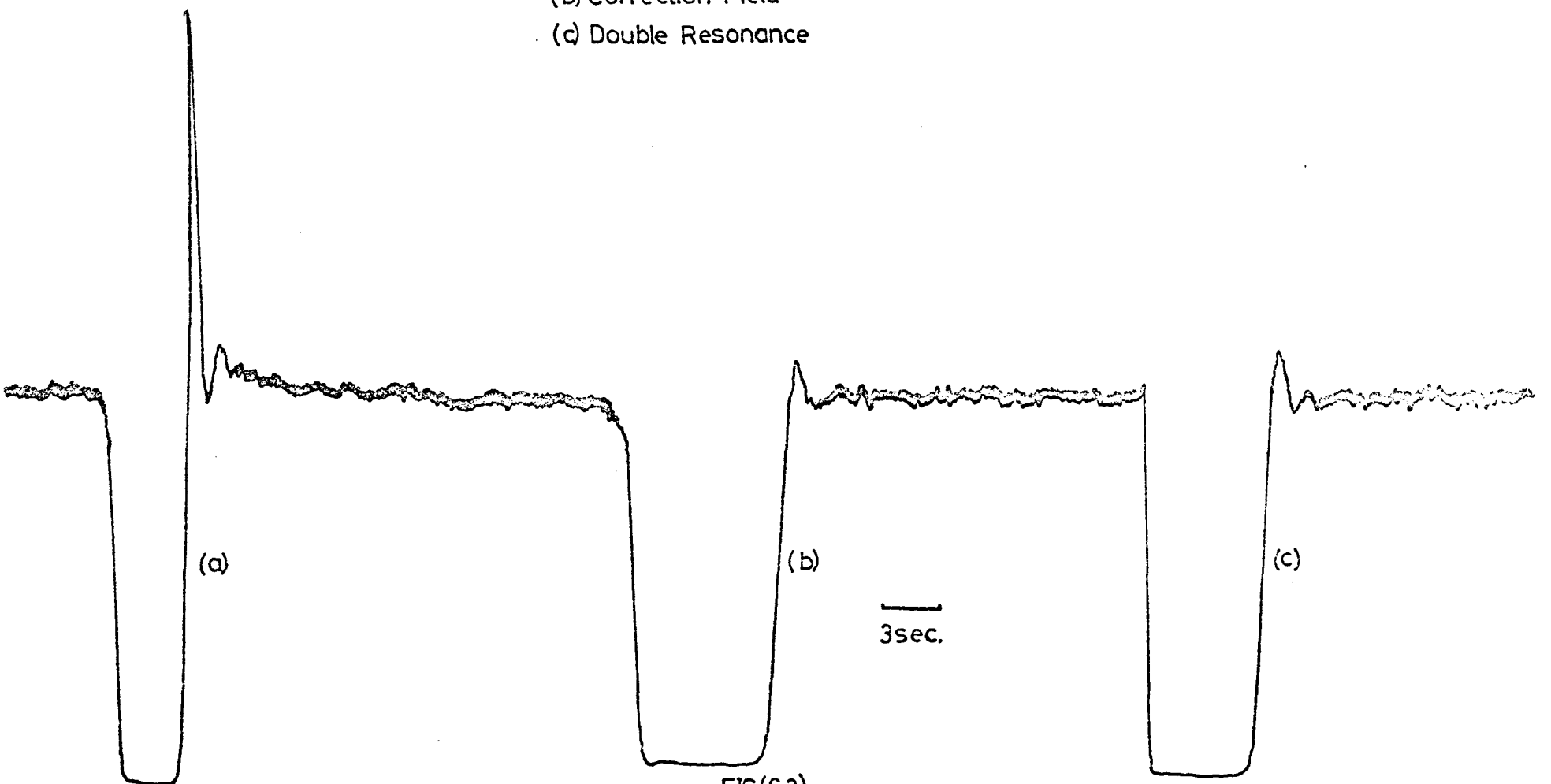

FIG(6·3)

Oscillation Transient Types

Voltage Applied to Coil

(a) 45 V.

(b) 30 V.

(c) 20 V.

(d) 15 V.

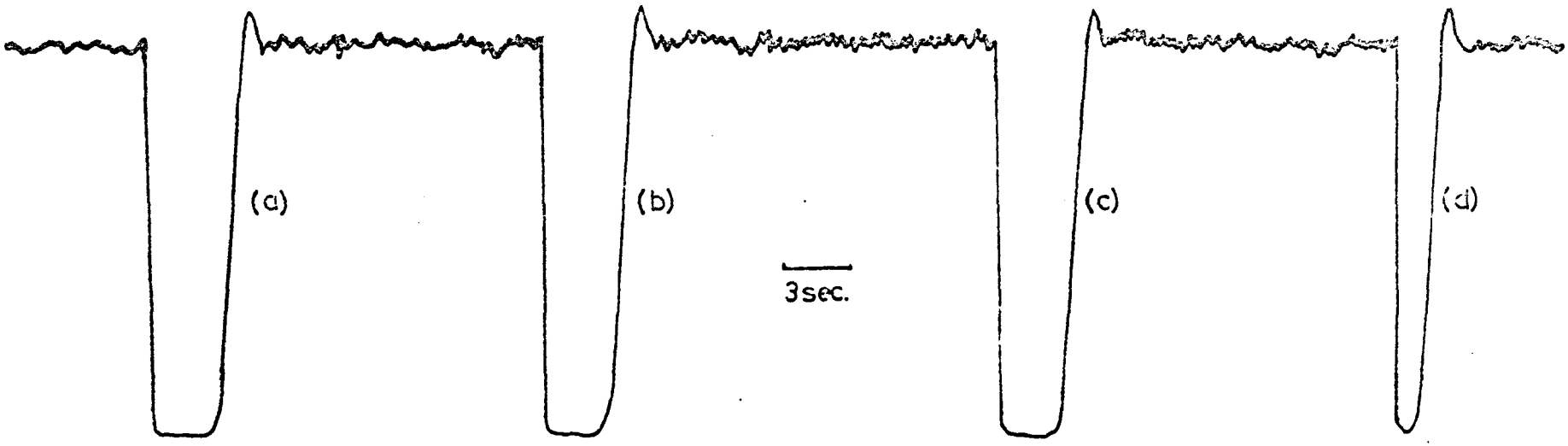

FIG(6-4)
Transients following a voltage pulse applied to the correction coil.

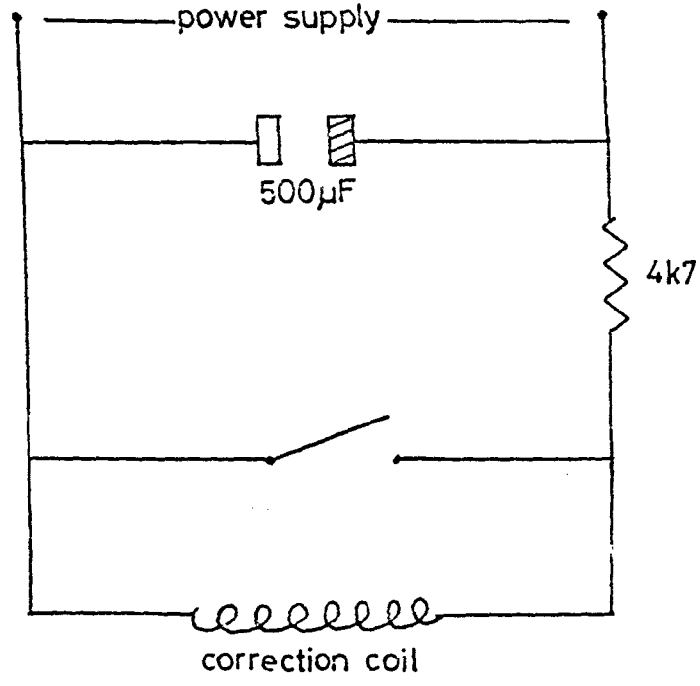

Circuit for application of excess correction field to the cavity region.

FIG.(6·5)

Transients following cavity detuning

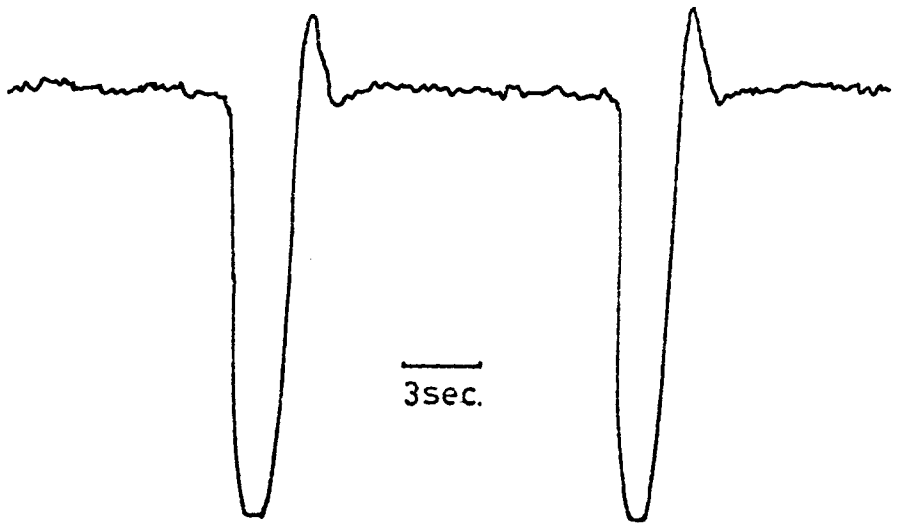

FIG.(6·6)

longer fulfilled. On releasing the tuner and allowing the top plate to fall back to its rest position, oscillation builds up and an amplitude transient is observed. The result is of a similar nature to those obtained using magnetic methods of switching.

The outstanding feature of the results so far, is the distinct difference in strength of the transients produced by switching the discharge on and off in comparison with all other techniques. It was possible that this may have been due to an enhancement of the transient by virtue of changes taking place when the hydrogen discharge was re-ignited, since only this technique effected any change in the atomic beam flux entering the cavity. This possibility was easily checked by comparing the results of the technique with those obtained by switching the beam by deflecting it away from the cavity upon tilting the bellows containing the state separating magnets. The build-up of oscillation, on allowing the bellows to return to their original position was then observed. The amplitude transients obtained using both methods are shown in fig. (6.7). There is no significant difference in the two results and hence the processes involved during the re-ignition of the atomic hydrogen discharge was evidently not the cause of the difference in the initial overshoot of the amplitude transients produced by the different methods.

Having discounted any contribution due to the re-ignition of the atomic hydrogen discharge, the large amplitude transient produced by this method was studied in more detail as a function of the following: (i) the speed of the beam switching (ii) the level of steady state oscillation level by varying the pressure behind the discharge tube.

(i) The results of the experiments carried out are shown in fig (6.8a,b,c,d,e,). The times shown indicate the time from switching of the discharge to re-igniting it. In (a) this is 0.4sec. and oscillation quenching is incomplete thus re-establishment is not from thermal noise in the cavity and the resulting

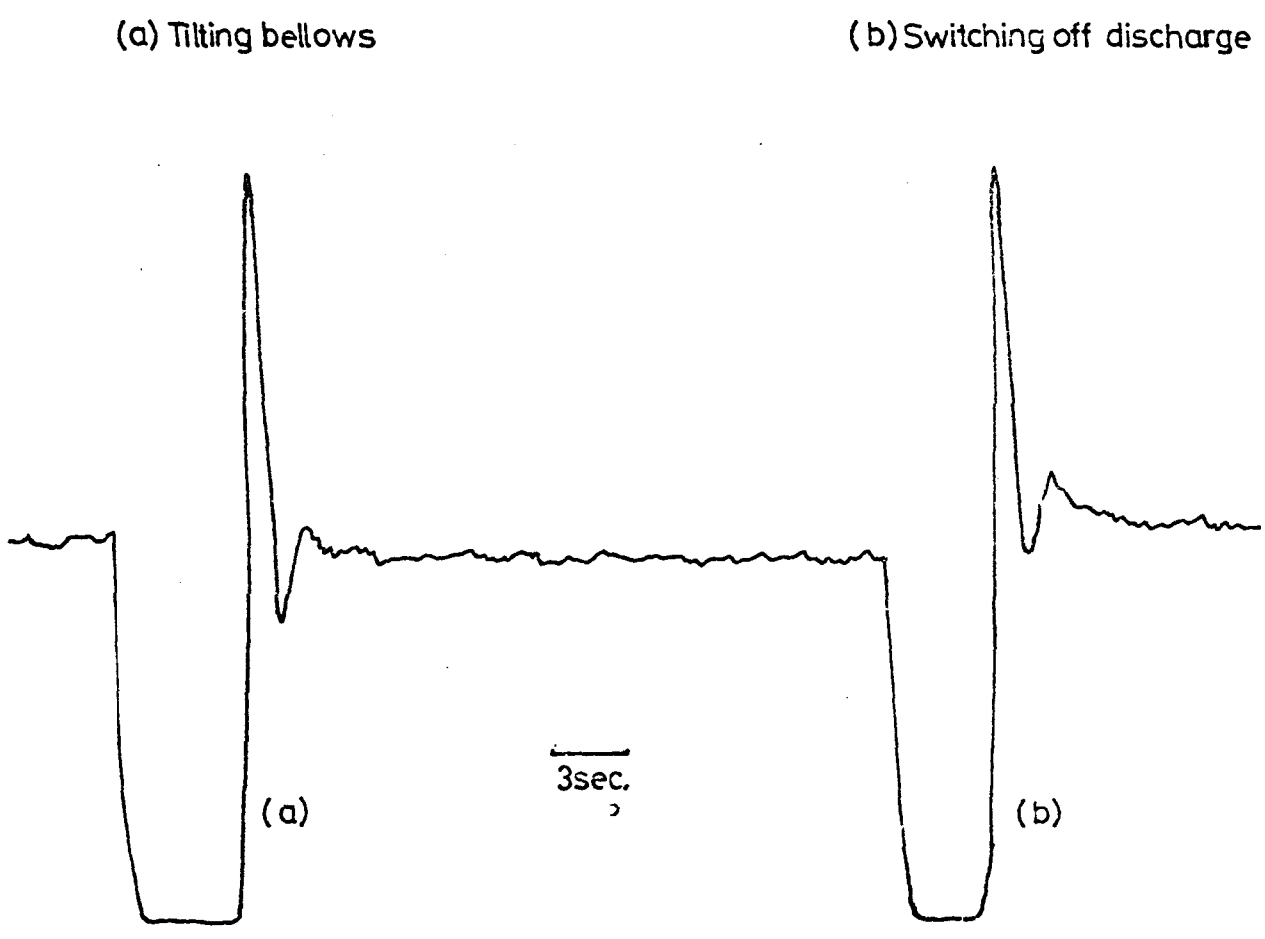

FIG.(6·7)
Transients after quenching by removing atomic hydrogen flux from cavity

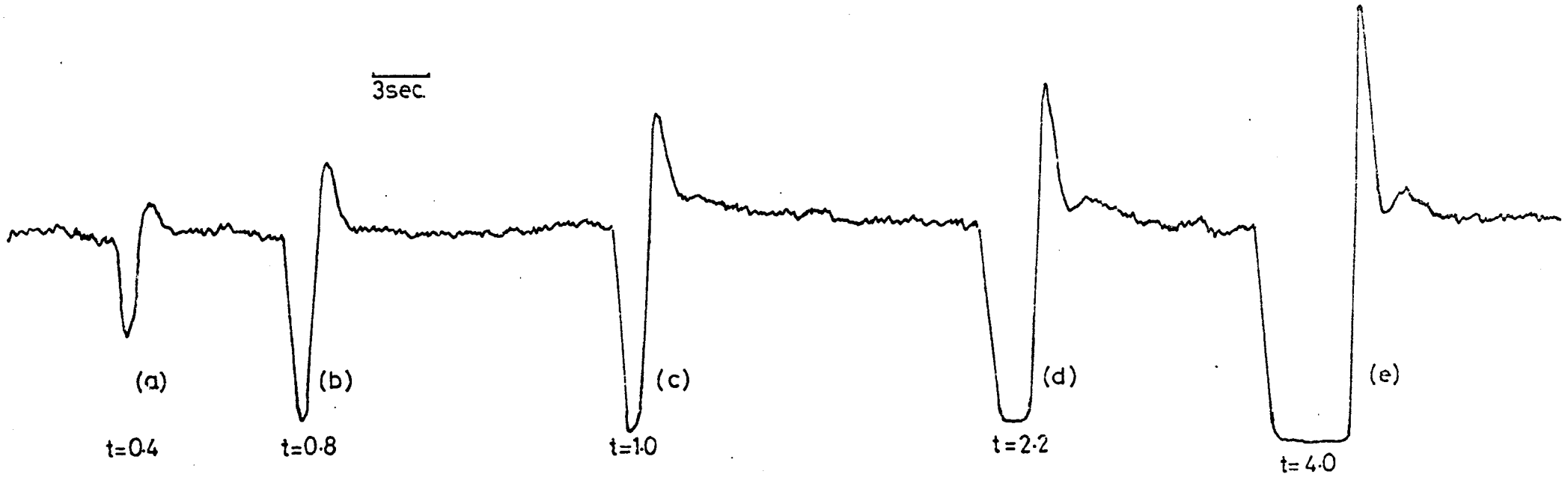

FIG(6·8)

Transient variation with beam switching speed t(sec.)

(t = off/on time)

transient is small. In (b) the time is 0.8sec. and quenching is still not quite complete but the transient produced is stronger. As the 'off time' increases to approximately 1sec. in (c) oscillation buildup starts as the quench is completed and again there is an improvement in the transient overshoot. In (d) the switch back on does not take place for 2.2sec and this produces an amplitude transient which shows signs of a second peak. In (e) the beam is 'off' for 3sec. after complete quenching and in this case the normally observed transient with a second peak is apparent. Increasing the 'off' time further, does not enhance the transient effect.

The 'off time' required with this method to produce the best transient response is dictated by the T_1 time constant for the system. Although the discharge is switched off instantaneously, the number of active atoms remaining in the bulb decays exponentially with a time constant T_1 (i.e. population difference decays with the time constant T_1). Thus, if the discharge is re-ignited in a time $t < T_1$, then a substantial number of upper-state atoms will still be in the storage vessel and the buildup of oscillation is not that of the empty bulb. Since oscillation decays with the time constant T_2 of the system, then if $t < T_2$ the oscillation will be incompletely quenched and the resulting transient will be adversely affected because the oscillation buildup is not from the thermal radiation field in the cavity.

(ii) The effect of the steady state oscillation amplitude on the transients produced by the beam switching technique is shown in fig. (6.9(a),(b),(c)). In (a) the background pressure of hydrogen measured behind the discharge tube is 5torr and this value gives the optimum steady state oscillation amplitude. The transient produced at this hydrogen pressure has the usual characteristics at the present level of oscillation. Increasing the pressure to 10torr (b) resulted in a smaller initial overshoot and also the presence of the second peak becoming less obvious. As the pressure was increased above 10torr (c),

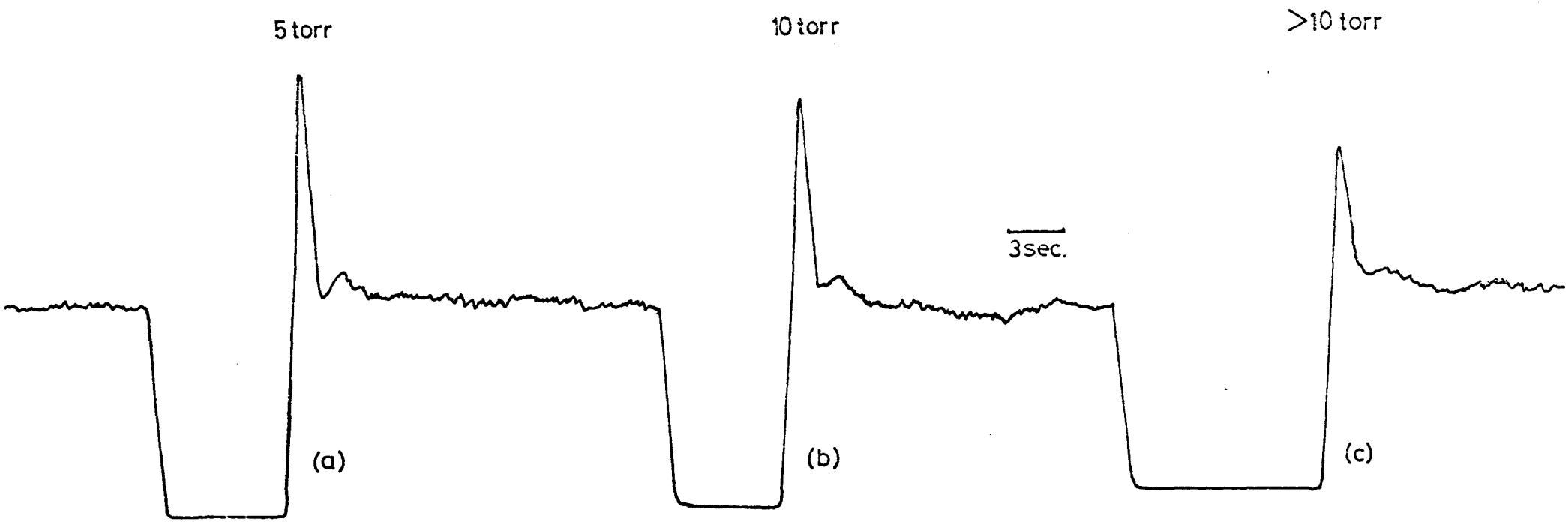

FIG.(6·9)

Transient variation with gas pressure

the initial overshoot in the amplitude continued to decrease and any evidence of a second peak disappeared. A further increase of the pressure reduced the strength of the transient until at a sufficiently low level of steady state oscillation, no transient is produced. If the gas pressure is reduced from the optimum value, the oscillation level falls accordingly and hence the characteristics of any transients observed are degraded as in the case of pressure increse.

The results outlined in (ii) above are directly analogous to results which have been abtained with the ammonia maser (33). This is seen by comparing the ammonia results of fig. (6.10(a)to(f)) with those of fig. (6.9). For ammonia maser the oscillation is quenched using a 'stark probe' to apply an inhomogeneous electric field inside the microwave cavity. This is an effective 'molecular Q-switch' to which the pulsed correction magnetic field switching technique is analogous in the hydrogen maser. The mean level of oscillation for ammonia maser is not altered by varying the backgound pressure of gas behing the effuser, but rather by varying the voltage applied to the state separator. This would be possible in hydrogen masers using an electromagnetic state separator system. Photos. (a) to (f) correspond to results with applied separator voltages of 55, 40, 30, 27.5, 22 and 21 kV respectively. The beam pressure behind the effuser is constant at 2.3torr). The same reduction in the height of the initial overshoot of the re-established oscillation signal and the gradual disappearance of a second peak are clearly seen. The results for hydrogen, (obtained by varying the gas pressure), were limited to three values only, due to difficulties of fine adjustment of the needle valve controlling the flow of hydrogen gas.

With the other techniques of transient production, the responses observed were very weak even at the maximum oscillation level. It was not practicable, therefore, to study separately the behaviour of those types under conditions of varying gas pressure around the optimum value. In addition one might

(a)

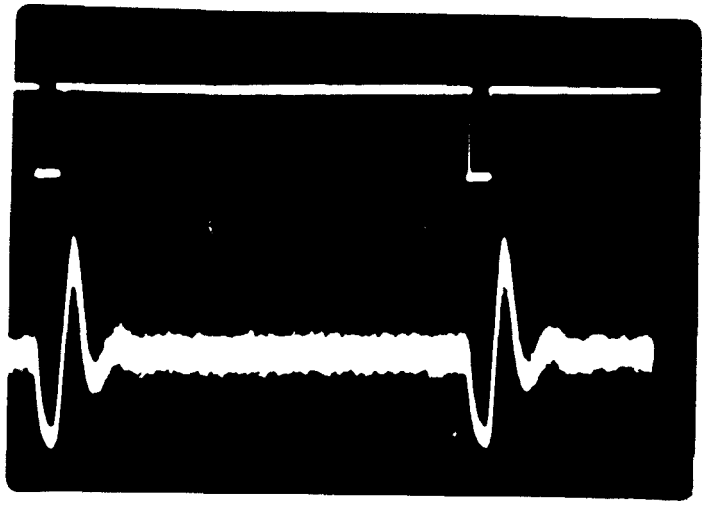

(b)

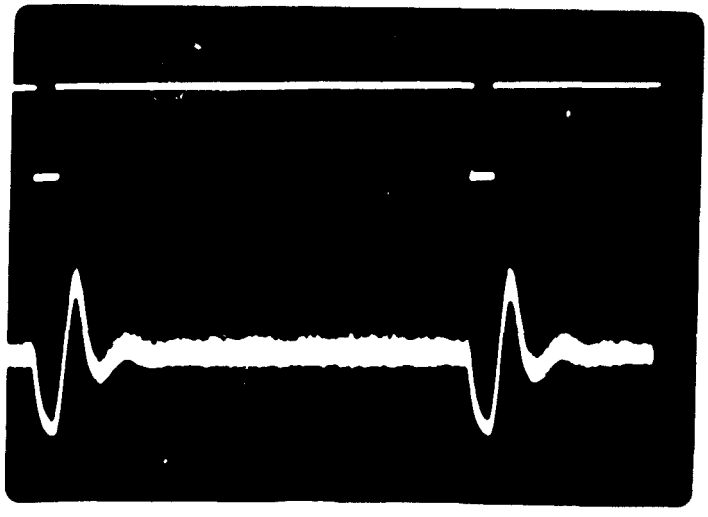

(c)

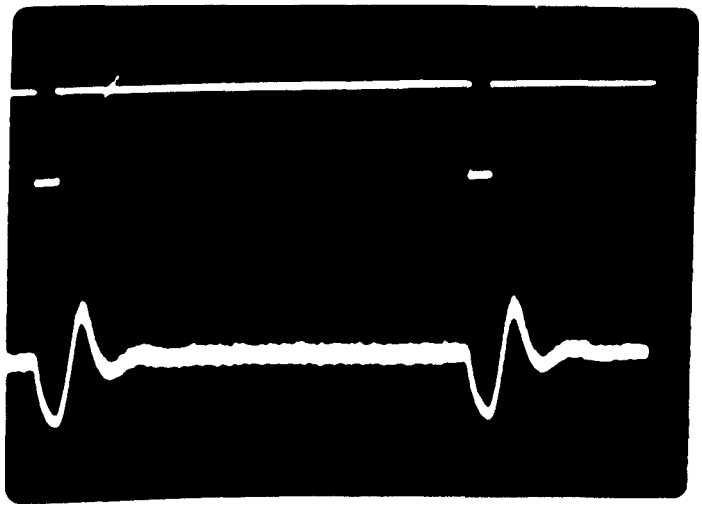

(Scale: Marker Pulse Width = 50μs.)

Fig.(6.10)

(a)

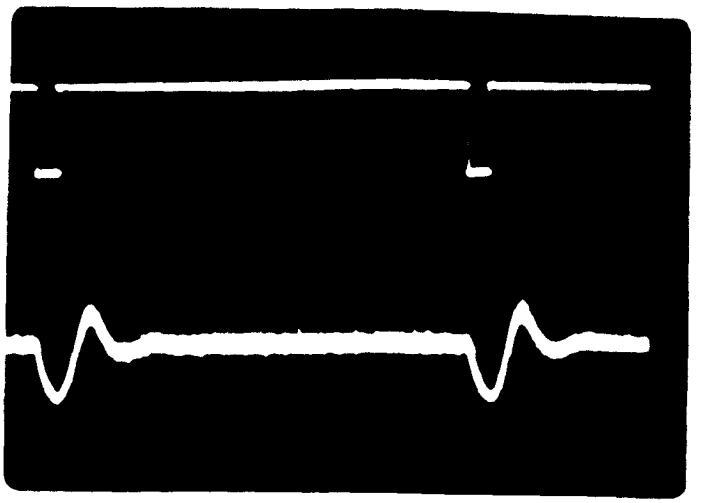

(e)

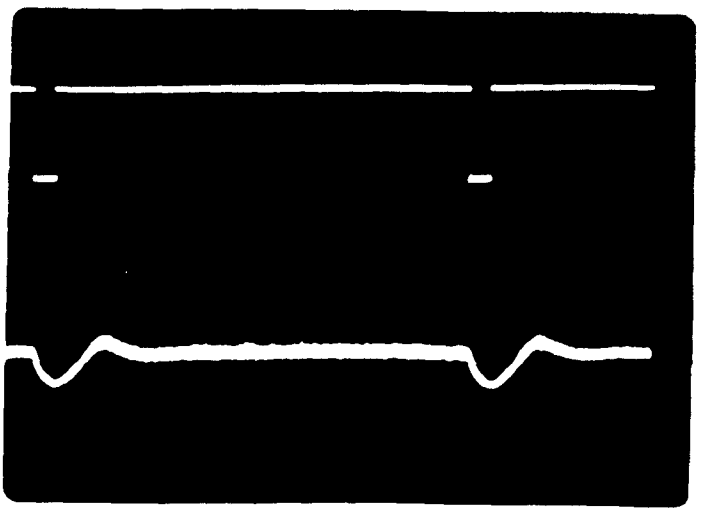

(f)

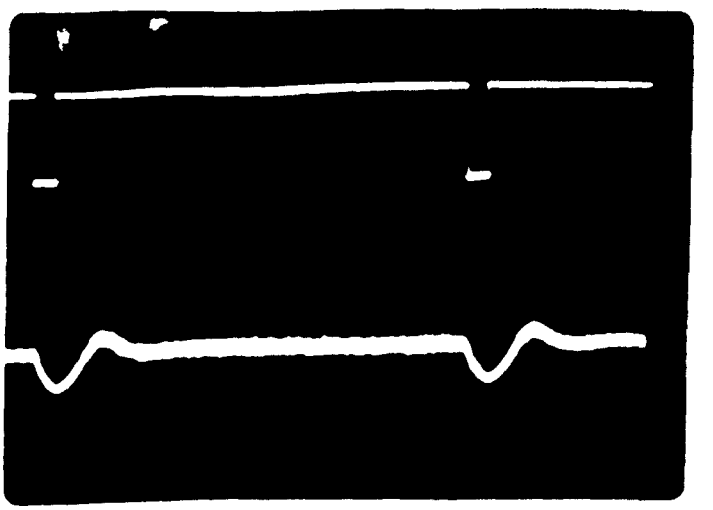

(Scale: Marker Pulse Width = 50μs.)

Fig. (6.10)

expect that their behaviour as a result of the variation of the speed of switching would not be limited by the T_1 time constant for the system, since the atomic beam is not removed, at any time, from the storage vessel. The dependence on the T_2 time is, however, still applicable.

Discussion of Results Thus Far

The results are best compared by considering the photographs taken from the storage oscilloscope, of a typical transient produced under optimum conditions by each of the different methods. These are shown in figs. (6.11) and (6.12).

The main features requiring comment are (i) the form of the oscillation decay upon quenching (ii) the strength and buildup time of the transient from noise on re-establishing oscillation conditions.

(i) Oscillation Quenching Methods

The form of the decay falls into two categories; (a) beam switching and (b) oscillation switching employing double resonance, cavity detuning and magnetic field switching. In (a) the decay is characteristic of the total relaxation time γ^{-1} of the system when the atomic discharge is switched off. (c.f. Chapter 5). An expanded trace of this section is shown in fig. (6.11(b)). From this result it is possible to measure γ^{-1}, which in the present experiment is approximately 0.7sec. For category (b) the rate at which the oscillation signal decays is dependent entirely upon the rate at which the upper working level of the maser is depopulated by the quenching mechanism involved. In the double resonance method, the decay depends on how rapidly the exact quench position, as read from the oscillator frequency range, is set up. For cavity detuning, the rate varies with the speed at which the top plate of the cavity is tilted, again a manual process. In the electrical method based on the sudden application of a current pulse to the correction coil, the quenching rate is a function of the time constant of circuit including the correction coil. These variations in quenching rates are also evident from the chart

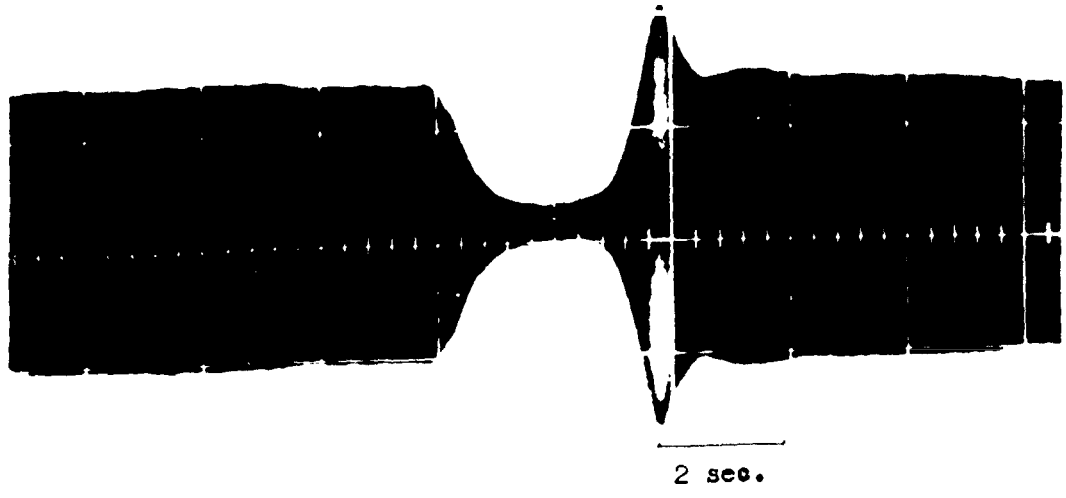

(a) Transient following quench by beam switching

(b) Decay of oscillation on switching off discharge

Fig. (6.11)

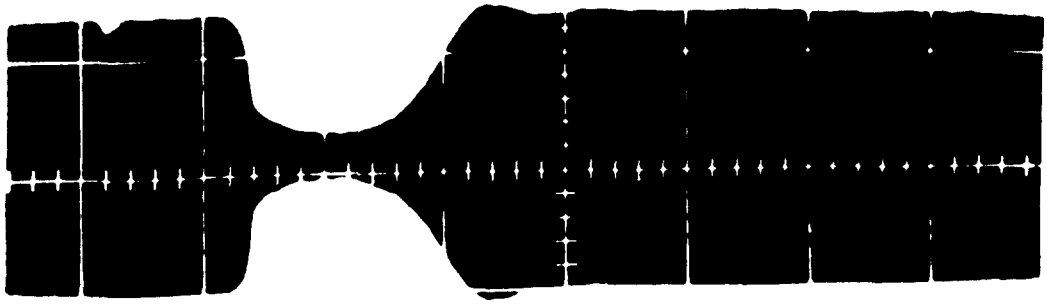

(a) Double Resonance (Quench frequency 580kHz)

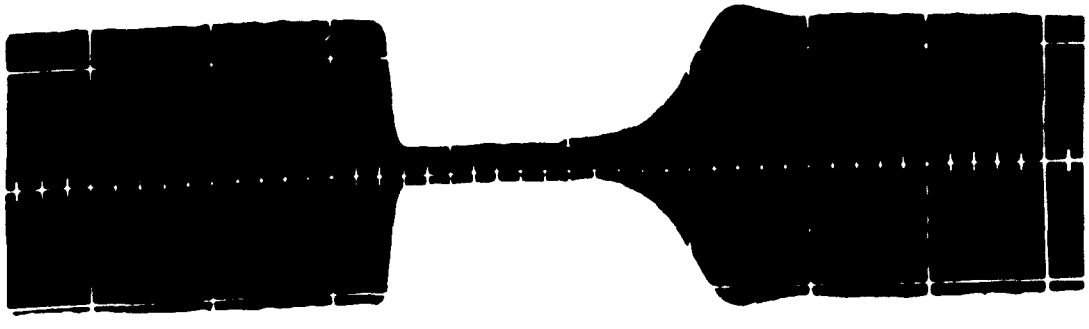

(b) Excess correction field

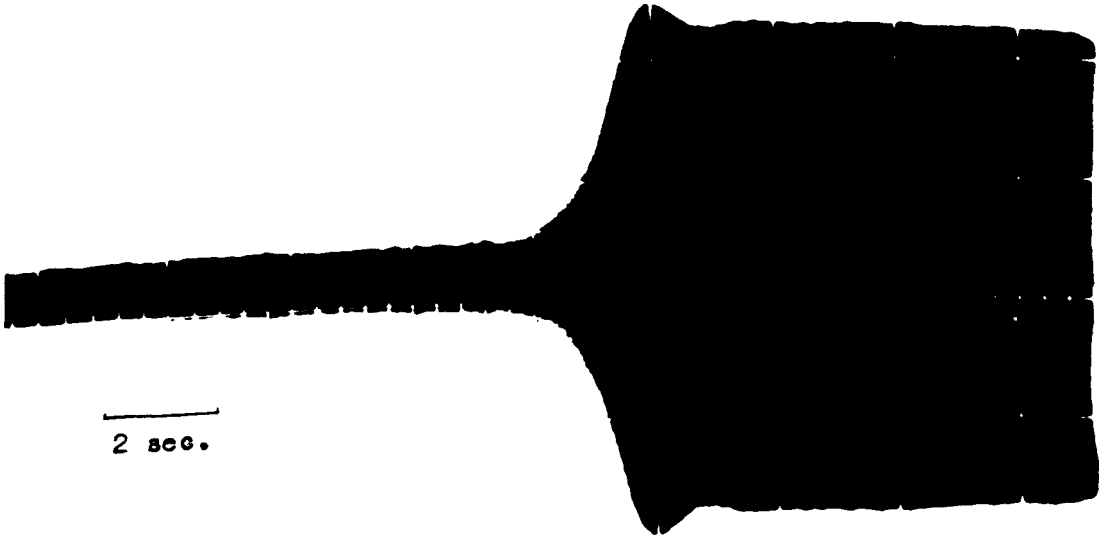

(c) Cavity detune (2dB more I.F. gain)

Transient types

Fig. (6.12)

recording data.

(ii) Strength and Buildup of the Transients:

The result again divides into the two categories (a) and (b) mentioned previously. With beam switching, the time taken for the oscillation to return to the steady state value is shorter than in the other cases, i.e. ~3sec. as opposed to ~4sec.. This time is referred to as 'time of silence' or 'quiescent time' T_q (32).

In accordance with the theory developed for molecular oscillators (34) the quiescent time of an oscillator, T_q, increases with decreasing levels of steady state oscillation. The varaition in the amplitude of oscillation $\mathcal{E}$ during the period of re-establishment of the steady state level varies in time according to (32).

$$\mathcal{E} = \mathcal{E}_0 \exp.\left(-\tfrac{1}{2}\gamma t\right) \cos.\left(\sqrt{\beta - 1{\cdot}25}\,\gamma t + \phi\right)$$

where β is a parameter which characterizes the extent to which the conditions of self excitation of the oscillator are overfulfilled, γ is the relaxation rate of hydrogen atoms in the storage vessel and ϕ is the initial phase of oscillations. The time of quiescence can be expressed in terms of the parameter β and the quantity $\varkappa_n^2/\chi\varkappa_i^2$ - the ratio of the noise power of the receiver $\varkappa_n^2$ to the initial value of the power of oscillations in the resonator $\varkappa_i^2$ multipied by the coupling coefficient χ of the resonator with the receiver (32).

$$T_q = \gamma^{-1}\left(1 + \ln.\frac{\beta}{\beta-1} + \frac{1}{\beta-1}\ln.\frac{\varkappa_n^2}{\chi\varkappa_i^2}\right)$$

Thus, although the level of steady state oscillation is constant for the different techniques, the different values for T_q may be explained by a difference in the parameter β for the two basic transient producing methods.

It has already been observed in this thesis, that improvements in the level of steady state oscillation result in the improvement of any amplitude transient produced by a given technique. In those cases, improvements were

made by changing variousnon-quantifiable parameters such as bulb coatings or discharge tube properties. An excellent example of the direct result of improvement of the steady-state oscillation conditions of a system by varying a single quantifiable parameter is given in fig. (6.13). The results are the work of Audoin et.al. (28). They show the difference in amplitude transients produced when the value of Q_c (loaded cavity Q) is changed from Q_c=350,000 to Q_c=50,700, whilst using the same technique to produce the transient (in this case the application of a large inhomogeneous magnetic field). Under the conditions giving a higher level of steady state oscillation (higher Q), the initial overshoot of the resulting transient increasesand the period of amplitude oscillations decrease as theory predicts.

Our results obtained so far, indicate that improved transient behaviour is observed when using beam switching, as opposed to any of the other technique employed, under the same conditions of steady state oscillation. This may be explained if the overfulfillment of the conditions of steady state oscillation, measured by β, is greater for the case of the beam switching technique. Hence the physical processes involved in the two basic switching methods is now considered.

For the techniques of transient production in which the atomic hydrogen flux remains incident in the storage vessel, the mechanism producing amplitude transient behaviour may be explained as follows.

On removal of the quenching mechanism, the pumping rate of upper state atoms into the storage bulb builds up to a level in excess of that associated with steady state oscillation. This is possible because until the atomic hydrogen flux in the bulb exceeds the threshold value there is no radiation field present in the cavity to bring the population inversion to its steady state value by the process of stimulated emission. Thus oscillation can build up initially to a level in excess of the steady state. Once the flux of

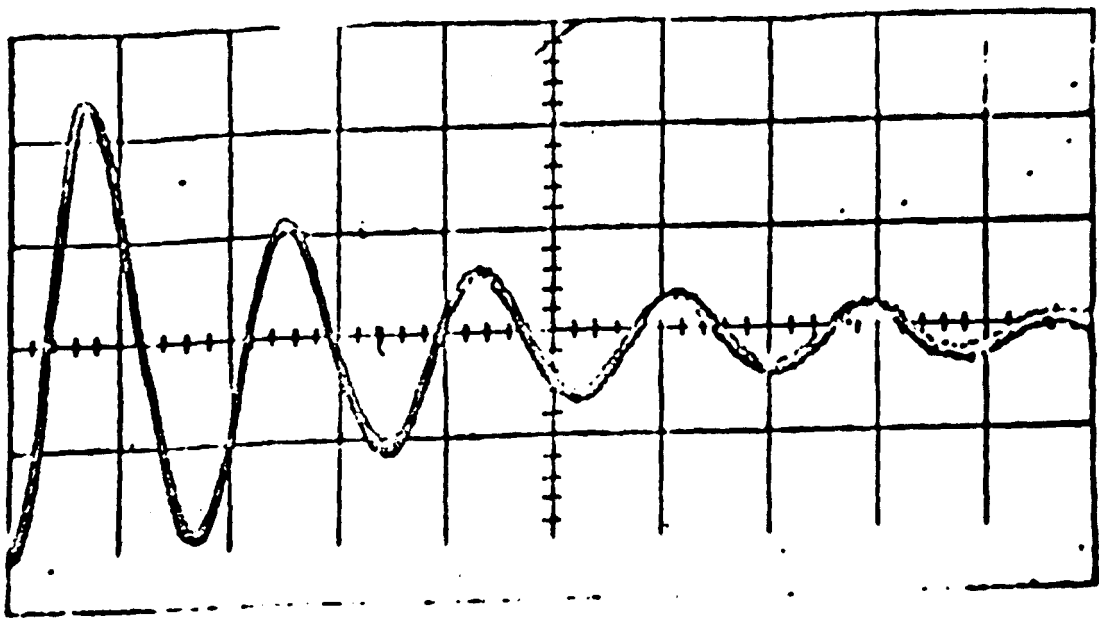

(a) Loaded cavity - Q = 350,000

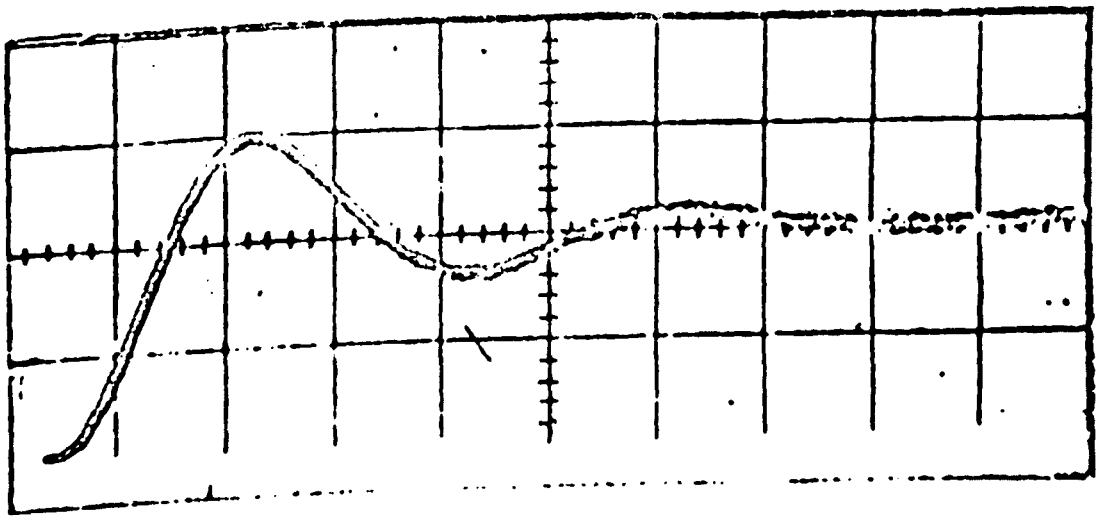

(b) Loaded cavity - Q = 50,700

(Scale: One Full Division = 100ms.)

Transients produced after quenching with inhomogeneous static magnetic field
(After Audoin)

Fig. (6.13)

hydrogen atoms in the bulb reaches the threshold value, oscillation builds up fromthermal noise in the cavity and produces an increasing radiation field density resulting in depopulation of the upper state energy level by stimulated emission. Thus amplitude of oscillation reaches a maximum and then decreases when the upper state is depopulated by the effect of an increased intensity of the radiation field. At this point the radiation field density is higher than the steady state value and the oscillation amplitude is pulled below the steady state level by subsequent reabsorption of radiation. This periodic transfer of energy between the atoms and the radiation field results in a decaying amplitude of oscillations to the steady state level. The amplitude and frequency of these oscillations is dependent on the level of steady state oscillation. The observation of similar results when using the quenching techniques of either double resonance or magnetic field inhomogeneity, or cavity detuning is consistent with the above reasoning.

In the case of the technique of beam switching, or chopping, the atomic flux is removed from the storage vessel during quenching. On re-establishing oscillation conditions the same flux of atomic hydrogen is re-introduced into the bulb. The basic reasoning for the production of transients applies as for the above mentioned methods. However, there is still an additional factor to be considered. As referred to earlier in this chapter, when the atomic beam has been removed fromthe bulb for a time longer than T_1, then the storage vessel is virtually empty of hydrogen atoms. The total pressure in the vessel is hence reduced. On re-introducing the atomic beam into the bulb re-establishes oscillation conditions but at an initially lower total pressure in comparison with other methods. Thus β, the measure of overfulfillment of oscillation conditions, will be higher in this case due to the initially lower pressure in the storage vessel. Theory (32) predicts a larger transient in this case. However, the pressure improvement in the bulb deteriorates with time, eventually reaching a steady state level of pressure equal to that

of the other methods. Thus, any transient produced, is a result of the mechanisms involved in the other methods of production combined with the effect due to the rapidly decaying improvement in total pressure in the storage vessel. The nett result observed is of a larger initial amplitude of the transient as expected from the above reasoning.

A problem arises in the explanation of the reduced period of amplitude oscillations. Theory predicts that this period is dependent only upon the level of steady state oscillation of the maser. In the beam switching technique, the period of the amplitude of oscillations is reduced although there is no improvement in the level of steady state oscillations. The result is consistent with a higher level of steady state oscillation. The initial improvement in total pressure in the bulb, if sustained, would lead to a higher level of steady state oscillation and hence a reduction in the period of oscillations of the amplitude. Any improvement, however, is time varying and returns to an inferior steady state level. Thus the resulting shorter period of the amplitude oscillations is probably a result of an averaged effect of the initial pressure improvement (i.e. lower H-H spin exchange) in the bulb and the value when conditions of steady state oscillation are reached.

As a result of the above, if the value of is calculated from experimental data

$$\beta = \left[1{\cdot}25 + 1/(T_{osc.}\gamma)^2\right]$$

where $T_{osc.}$ is the period of oscillation of the transient. The value obtained is subsequently used to calculate T_q. Thus, for various levels of steady state oscillation, the corresponding value of T_q would not be expected to fit the theoretically predicted curves. In fact, the expt. values of T_q for a given level of oscillation should be smaller than the predicted theoretically. This would only apply in the case of transients produced by beam switching.

In considering the results obtained by Nitikin et.al. (32) which use a beam switching technique, these appear to be in conflict with the aforegoing reasoning. In fact, the anomalous behaviour as a result of the beam switching technique is not commented upon. Other authors (28) studying transient behaviour in hydrogen masers, do not experience or comment on this problem since beam switching techniques are not used.

In conclusion, it would appear that the differences in the techniques of transient production are not commented on since the published literature to the present time does not contain a comparative study of the various transient producing techniques. It is hoped that with the system under investigation, it will be possible to obtain more quantitative data with the beam switching technique in order to compare the theoretical and experimental variation of T_q with the steady state oscillation level. Experimental values of T_q which are lower than the theoretically predicted values would be expected.

Quenching with an Injected Signal - an Analogue with the Ammonia Maser

Reference has already been made with respect to the results of quenching by inhomogeneous magnetic fields in the hydrogen maser, in comparison with the 'stark transients' produced in the ammonia maser (33). In the following, the quenching prior to transient observation is achieved by the injection of a signal, at the resonant frequency, into the microwave cavity. It is an exact analogy with results obtained using an ammonia maser (29). Unlike the other techniques used with the present system, this has not previously been used for transient production in the atomic hydrogen beam maser.

The theory for the dynamic process of buildup of the oscillation in a two-level maser system predicted that the maser oscillation amplitude should approach its steady state value in a damped periodic fashion, at high levels of oscillation. The first experimental evidence of this was reported by Audion (35) and Nitikin (32), for the hydrogen maser. The techniques for

transient production in these cases being by the application of large inhomogeneous static magnetic field and atomic beam switching respectively.

Initial attempts to observe the oscillation transient in ammonia (34) were unsuccessful. This was due to the technique used for the production of the transient, which involved the application of a high voltage pulse to the electrostatic focusser. The failure was probably because of the relatively long time required for the establishment of the active beam of upper state molecules, the subsequent smearing effect due to the velocity distribution and the time required for penetration into the cavity.

The first observation of transient behaviour in ammonia was in 1969 (29) using the technique of injecting a high level signal into the cavity at the resonant frequency. The success of the method was attributable, in large part to the fact that the molecules were perturbed inside the cavity where they are all coupled to a common radiation field, and where the effects of the finite magnitude of the velocity distribution are minimised. The results of the above method are shown in fig. (6.14(a)).

The signal injection method used with the hydrogen maser, based on the ammonia technique was as follows.

Under conditions of self sustained maser oscillation, a high level, frequency modulated signal was injected into the cavity via the second coupling loop. This signal was produced by applying a slow frequency sweep over a range of approximately 5OH_z to the 10MH_z crystal oscillator, which after doubling, is used to mix with the 1400MH_z signal from the phase locked loop and produce a small frequency sweep around 1420MH_z (see fig. (6.15)). In this way, the signal injected into the cavity sweeps through the resonant frequency of the maser transition. Because of the narrowness of the atomic resonance the full sweep was slow taking approximately 20sec. This can be compared with

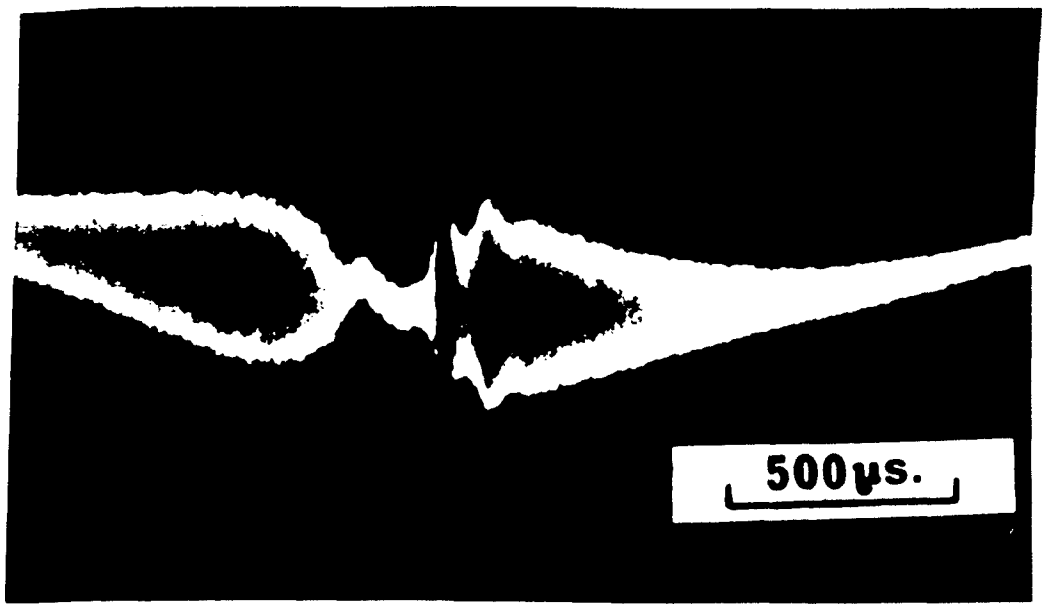

(a) Result with Ammonia Maser
(After Bardo)

(b) Result with Hydrogen Maser

Transients following oscillation quenching by
an injected signal

Fig. (6.14)

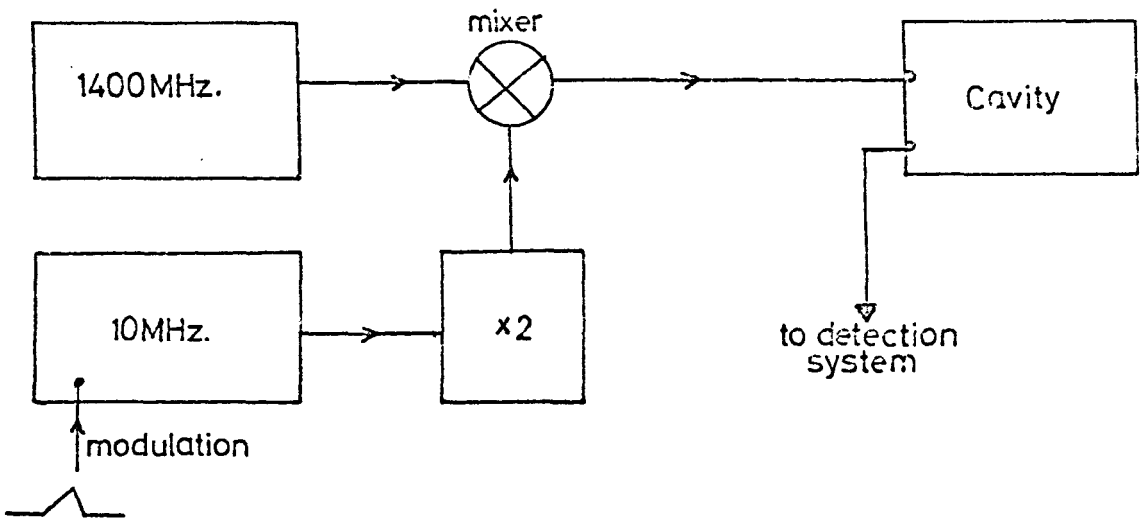

Electronics for injection of frequency modulated signal into the cavity under oscillation conditions.

FIG.(6.15)

the ammonia case where a sweep width of 20kHz in a time of 2ms. was required because of the relatively wide resonance line (~5kHz). The results obtained with the hydrogen maser are shown in fig. (6.14(b)).

As the signal approaches the maser frequency, the detected maser signal is modulated and the beat envelope observed. At the zero beat position, the oscillation is quenched due to saturation of the upper maser level. The injected signal moves through resonance and maser oscillation builds up inside the cavity producing a small oscillation amplitude transient. It can be seen that the transient is of a similar nature to those produced by the other 'non-beam switching' techniques used. The strength of the transient appears to be less, but this is due to the fact that at the zero-beat position, the quenching is incomplete. This, as in other methods, results in a weaker transient being observed since the oscillation does not build up from thermal noise in the cavity. The low level oscillation present produces a radiation field in the cavity and hence on re-establishing oscillation conditions, the overfulfillment of these conditions is reduced and hence the transient observed is smaller.

At the present level of steady state oscillation, the transient observed using this technique may be improved by ensuring that complete quenching of the oscillation at the zero-beat position is achieved. This is possible by adjusting the sweep rate and amplitude of the injected signal into the microwave cavity. Further improvement in the level of steady state oscillation should also result in an improved strength of the observed transient. In this way, recorded transients of the quality of that of fig. (6.11(a)) should be obtainable. The main difference being of course, the beat envelope superimposed with this type of quenching. This would allow a more convincing visual comparison between the results with ammonia and hydrogen masers.

Suggestions for further work:

(i) Production of Oscillation Spiking Behaviour:

The level of steady state maser oscillation may be usefully increased by the following modifications (a) replacement of the Mk.1 magnet in the state separator by a magnet with a reduced gap and increased field between the pole tips. (b) The use of a silver plated quartz cavity giving a higher cavity Q.

An increased level of steady state oscillation should allow the production of transients approaching those hitherto quoted for the ammonia maser. With a sufficiently high level of oscillation, the phenomenon of oscillation spiking may also be studied. This phenomenon has been observed in the ammonia maser (36).

In the case of ammonia, the spiking is produced with the experimental arrangement used for transients but with a relatively narrow frequency sweep such that the beat frequency is $\leqslant$ 10Hz. A series of spikes of oscillation of relatively large amplitude is observed before and after quenching. These may be regarded as the result of a partial quenching of oscillation with a periodic modulation of the maser transition at the beat frequency.

With the hydrogen maser, the very low beat frequencies involved (a few Hz.) should make it possible to produce the required periodic modulation, for example, by electrically switching the discharge or by electro-magnetic chopping of the atomic beam. Any oscillation parameter which may be modulated at the periodic frequency of oscillation amplitude transients should also produce spiking behaviour.

(ii) Magnetic Dipole Echoes:

During the series of experiments leading to self sustained maser oscillation, an effect described as a 'phasing effect' (Chapter 5) was noted. This resulted from the application of consecutive microwave pulses, with a

repetition frequency $\geq 0{\cdot}5$Hz, when maser signal 'ring times' (T_2) of around 3sec. were obtained.

In the production of magnetic dipole echoes, two pulses are applied, separated such that the time interval is less than T_2 for the particular dipole system. One expects at first glance, therefore, that under the above mentioned conditions for the hydrogen maser, echo behaviour would result. However, on closer consideration of the conditions under which echoes are produced (37) it would appear that in the hydrogen maser the averaging effect on the magnetic dipoles of the system, as a result of the large volume storage bulb in a region of relatively high magnetic field homogeneity, would prevent the observation of echoes.

Transient operation of the maser without magnetic shields and with the storage vessel divided into compartments, may produce smaller regions of sufficiently local field inhomogeneity to facilitate the observation of magnetic dipole echoes.

APPENDIX

Cavity Q-Measurements

Two separate methods of Q measurement have been used, resulting in the same value for loaded Q of the microwave cavity.

In the initial measurement an external signal swept over the resonant frequency of the cavity was injected from a tuneable klystron oscillator. The frequency sweep was achieved by applying a suitably potentially divided saw-tooth output froman oscilloscope to the klystron reflector. The response signal from the cavity output was mixed with the harmonic output signal from a transfer oscillator type HP 504B. The resulting cavity response envelope was displayed on the oscilloscope and the zero beat point for the two mixed signals used as a marker pip to measure the position of the half power points of the response curve. The frequency difference of these two positions was measured and the value divided into the measured centre frequency to yield the loaded Q factor for the cavity.

In the other Q measuring technique, the klystron was used in a c.w. mode of operation and the transmitted signal power from the cavity output monitored using a calibrated Saunders r.f. power meter type 6460, whilst the input frequency to the cavity was varied. The maximum output power at resonance was noted together with the corresponding frequency. The klystron was detuned up and down in frequency until a fall in transmitted power of 3dB was noticed in each direction separately. The frequency difference between these upper and lower '3dB points' was measured. This value obtained divided into the resonant frequency gave the loaded Q factor for the cavity.

Before both the above measurements were made, the output power of the klystron oscillator was checked whilst its frequency was varied. The output level was found to be constant over the range of frequency used in determining the Q value for the cavity. The estimated errors of measurement were approximately 10% for the first method and 5% for the second.

REFERENCES

(1) Gordon, Zeiger, Townes. (1954), Phys. Rev. 95, 282.

(2) Basov, Prokhorov. (1954), Sov. Phys. J.E.T.P. 27, 347.

(3) Bernstein. (1950), Bull. Acad. Sci. (URSS) Ser. Phys. 14, 187.

(4) Balquière. (1953), Annal. Radioelec. 36, 153.

(5) Shimoda, Wang, Townes. (1956), Phys. Rev. 102, 1308.

(6) Goldenberg, Kleppner, Ramsey. (1960), Phys. Rev. Lett. 5, 361.

(7) Crampton. (1967), Phys.Rev. 158, 57.

(8) Essen et. al. (1971), Nature, Vol. 229.

(9) Crampton et. al. (1966), Phys. Rev. 141, 1.

(10) Mathur et. al. (1967), Phys. Rev. 158, 1.

(11) Myint et. al. (1966), Phys. Rev. Lett. 17, 405.

(12) Berg H. C. (1965), Phys. Rev. 6, 136

(13) Louiselle W. 'Radiation & Noise in Quantum Electronics'. McGraw-Hill

(14) Kleppner, Goldenberg, Ramsey. (1958) Phys. Rev. Lett. 7, 232.

(15) Fowler, Guggenheim. 'Statistical Thermodynamics'. Camb. Univ. Press CH.2.

(16) Steacie. 'Atomic & Free Radical Reactions'. Reinhold p. 490.

(17) Kleppner, Goldenberg, Ramsey. (1962), Phys. Rev. 126, 1.

(18) Basov et. al. (1965), Trudy 31.

(19) Paul W. (1960), Int. Symp. on Polariz. Helv. Phys. Act. Supp. 6 .

(20) Christensen, Hamilton. (1959), Rev. Sci. Inst. 30, 5.

(21) Berg, Kleppner. (1964), Rev. Sci. Inst. 33, 248.

(22) Ramsey. (1968), Amer. Sci. 4, 56.

(23) Ramsey et. al. (1970), Rev. Sci. Inst. 41.

(24) Ramsey et. al. (1965), Phys. Rev. 4A, 138.

(25) Mungal et. al. (1968), Metrologia. 4, 3.

(26) Nitikin, Strahkovskii. (1968), Izev. VUZ Radiofisika. 12, 4.

(27) Audoin et. al. (1971) R. Acad. des Sci.

(28) Audoin et. al. (1967), R. Acad. Sci. 264, 698.

(29) Lainé, Bardo. (1969), Electronics Lett. 5, 364.

(30) Combrison. 'Quantum Electronics'. Columbia U. Press. p. 167.

(31) Audoin et. al. (1968), Proc. 22nd. Symp. on Frequ. Control. p. 493.

(32) Nitikin, Stradhovskii. (1966), Radio Electron Phys. 11, 1650.

(33) Bardo W. S. (1969), Ph.D. Thesis, Keele.

(34) Grasyuk, Orayevskiy. (1964), Rad. Eng. Electron Phys. 9.

(35) Audoin. (1966), C. R. Acad. Sci. 263, 524.

(36) Lainé, Bardo. (1969), Electronics Lett. 5, 26.

(37) Hahn E.L. (1950), Phys. Rev. 80, 580.